PB-222 340

LOW NOx EMISSION COMBUSTOR FOR AUTOMOBILE GAS TURBINE ENGINES

E. P. Demetri, et al

Northern Research and Engineering Corporation

Prepared for:

Environmental Protection Agency

February 1973

DISTRIBUTED BY:

NTIS

National Technical Information Service
U. S. DEPARTMENT OF COMMERCE
5285 Port Royal Road, Springfield Va. 22151

BIBLIOGRAPHIC DATA SHEET

1. Report No. APTD-1454

2.

3. Recipient's Accession No. PB-222 340

4. Title and Subtitle

Low NOx Emission Combustor for Automobile Gas Turbine Engines (Northern Research and Engineering Corporation)

5. Report Date February 1973

6.

7. Author(s)

E. P. Demetri and R. J. Murad

8. Performing Organization Rept. No.

9. Performing Organization Name and Address

Northern Research and Engineering Corporation
219 Vassar Street
Cambridge, Massachusetts 02139

10. Project/Task/Work Unit No.

11. Contract/Grant No. 68-04-0017

12. Sponsoring Organization Name and Address

U.S. ENVIRONMENTAL PROTECTION AGENCY
Mobile Source Pollution Control Program
Advanced Automotive Power Systems Development Division
Ann Arbor, Michigan 48105

13. Type of Report & Period Covered

14.

15. Supplementary Notes

16. Abstracts Two research combustors were designed and tested, one of which was representative of low pressure-ratio, regenerative gas turbine cycles and the other representative of high pressure-ratio, nonregenerative cycles. The design goal was to achieve emission levels not exceeding one-half of the Federal 1975/76 emission standards. The over-all aim was to develop design guidelines on the basis of detailed experimental data. Extensive modifications were made to conventional combustor configurations, but direct use was made of existing combustor design technology. Both combustors were designed for a lean, well-mixed primary zone over the full range of operating conditions. This required variable geometry to control the combustor air flow distribution to maintain stable and efficient combustion. Both were designed for a relatively high value of pressure-loss factor in order to promote aerodynamic mixing. The diameter was oversized to accomplish the high-pressure loss factor and also to aid in reducing CO and HC emissions. An airblast type of fuel nozzle was used to achieve a reasonably uniform fuel/air mixture in the primary zone. Both were single-can, throughflow configurations. Full-scale models were tested over wide ranges of operating conditions representative of typical driving cycles. Cold-flow tests were made to measure aerodynamic performance and detailed combustion tests were made to measure emission, combustion, and thermal performance. In general the NOx emissions obtained were higher than the goal whereas CO and HC emissions were satisfactory along with the combustion efficiency, stability limits, pressure loss, exit temperature traverse quality, and combustor wall temperature. Both the experimental and analytical results indicated that the high NOx emissions were principally due to inadequate fuel/air mixing in the primary zone. This in turn was due to inadequate distribution of the fuel spray in the nozzle and swirler airstreams and insufficient proportion of the primary-zone air flow through the nozzle/swirler assembly relative to the flow through the secondary holes. The results of additional tests indicated that the NOx emission goals could be met by improving the uniformity of the primary-zone fuel/air distribution via specific modifications of the method of fuel injection.

17. Key Words and Document Analysis. 17a. Descriptors

Air pollution
Nitrogen oxides
Exhaust emissions
Gas turbine engines
Design criteria
Tests
Pressure
Heat transfer
Flow rates
Combustion
Aerodynamics
Carbon monoxide
Hydrocarbons
Temperature
Fuel injectors

17b. Identifiers/Open-Ended Terms

17c. COSATI Field/Group 13B

18. Availability Statement Unlimited

19. Security Class (This Report) UNCLASSIFIED

20. Security Class (This Page UNCLASSIFIED

21. No. of Pages 183

22. Price $11.25 / $1.45

FORM NTIS-35 (REV. 3-72)

THIS FORM MAY BE REPRODUCED

USCOMM-DC 14952-P72

PB 222 340

APTD - 1454

Low NOx Emission Combustor
for Automobile Gas Turbine Engines
(Northern Research and Engineering Corporation)

Prepared By
E. P. Demetri and R. J. Murad
Northern Research and Engineering Corporation
219 Vassar Street
Cambridge, Massachusetts 02139

CONTRACT NUMBER: 68-04-0017

EPA Project Officers
H. F. Butze and Robert B. Schulz

Prepared For
U.S. ENVIRONMENTAL PROTECTION AGENCY
Office of Air and Water Programs
Mobile Source Pollution Control Program
Advanced Automotive Power Systems Development Division
Ann Arbor, Michigan 48105

February 1973

Reproduced by
NATIONAL TECHNICAL
INFORMATION SERVICE
U S Department of Commerce
Springfield VA 22151

182

The APTD (Air Pollution Technical Data) series of report is issued by the Office of Air and Water Programs, U.S. Environmental Protection Agency, to report technical data of interest to a limited number of readers. Copies of APTD reports are available free of charge to Federal employees, current contractors and grantees, and non-profit organizations - as supplies permit - from the Air Pollution Technical Information Center, U.S. Environmental Protection Agency, Research Triangle Park, North Carolina 27711 or may be obtained for a nominal cost, from the National Technical Information Service, U.S. Department of Commerce, 5285 Port Royal Road, Springfield, Virginia 22151.

This report was furnished to the U.S. Environmental Protection Agency by Northern Research and Engineering Corporation, Cambridge, Massachusetts, in fulfillment of Contract Number 68-04-0017. The contents of this report are reproduced herein as received from Northern Research and Engineering Corporation. The opinions, findings, and conclusions expressed are those of the author and not necessarily those of the Environmental Protection Agency.

Office of Air and Water Programs Publication Number APTD - 1454

The program reported here was carried out under the technical direction of Dr. D. M. Dix with Mr. E. P. Demetri assuming project responsibilities. Other participants in the program included Mr. R. J. Murad and Mr. P. R. Smith; Professor A. H. Lefebvre, Professor J. B. Heywood, and Mr. E. R. Norster served in a consulting capacity during the course of the program.

This program was sponsored by the Environmental Protection Agency under Contract No. 68-04-0017. Technical monitoring of the program was conducted by Mr. H. F. Butze of NASA Lewis and Mr. R. B. Schulz of EPA.

TABLE OF CONTENTS

SUMMARY 1

INTRODUCTION 4

Background 4

Problem Definition 4

Method of Attack 6

Report Arrangement 9

DESIGN APPROACH FOR REDUCING EMISSIONS 10

Emission Goals 10

Major Factors in Emissions of NOx 11

Control of NOx Emissions 13

DESIGN OF COMBUSTORS 19

Cycle Conditions 19

Combustor Design Conditions 21

Aerothermodynamic Design 25

Mechanical Design 27

COLD-FLOW TESTS 29

Water-Visualization Tests 29

Air Flow Distribution Tests 31

Nozzle Spray Visualization Tests 32

COMBUSTION TESTS 35

Over-All Approach 35

Discussion of Test Results for Combustor B 37

Discussion of Test Results for Combustor A 42

Analysis of Results 45

Experimental Verification of Analysis 50

Recommended Approaches for Achieving Low Emissions 53

CONCLUSIONS AND RECOMMENDATIONS 57

Conclusions 57

Recommendations 59

REFERENCES 62

TABLES 65
FIGURES 106
NOMENCLATURE 156
APPENDICES 160
    I - DESCRIPTION OF EXPERIMENTAL FACILITIES 161
    II - DATA REDUCTION 167
    III - NOZZLE SPRAY ANALYSIS TESTS 171

LIST OF TABLES

Table I: Federal 1975/76 Emission Goals 66

Table II: Assumed Cycle Operating Conditions for Design of Combustors 67

Table III: Selected Combustor Design Conditions 68

Table IV: Design Distributions of Airflow 69

Table V: Nozzle Design Specifications 70

Table VI: Metering and Bleed Hole Dimensions 71

Table VII: Average Values of Effective Flow Areas Calculated from Results of Cold-Air Tests 72

Table VIII: Summary of Test Conditions Examined with Combustor B 74

Table IX: Results of Combustion Tests for Combustor B with Nozzle B1.1 and "Closed" Variable-Geometry Setting . . 76

Table X: Results of Combustion Tests for Combustor B with Nozzle B1.1 and "Full Open" Variable-Geometry Setting 79

Table XI: Results of Combustion Tests for Combustor B with Nozzle B2.1 and "Closed" Variable-Geometry Setting 82

Table XII: Results of Combustion Tests for Combustor B with Nozzle B2.1 and "Full Open" Variable-Geometry Setting 84

Table XIII: Results of Combustion Tests for Modified Combustor B with Nozzle B2.1 and "Closed" Variable-Geometry Setting 85

Table XIV: Summary of Test Conditions Examined with Combustor A 87

Table XV: Results of Combustion Tests for Combustor A with Nozzle A2.1 and "Closed" Variable-Geometry Setting . . 88

Table XVI: Results of Combustion Tests for Combustor A with Nozzle A2.1 and "Part Open" Variable-Geometry Setting 91

Table XVII: Summary of Test Conditions Examined with Modified Combustor A 94

Table XVIII: Calculated Nozzle and Swirler Air Flows for Modified Combustor A 95

Table XIX: Results of Combustion Tests for Modification No. 1 of Combustor A with Nozzle A2.2 and "Closed" Swirler Setting 96

Table XX: Results of Combustion Tests for Modification No. 1 of Combustor A with Nozzle A2.2 and "Open" Swirler Setting 98

Table XXI: Results of Combustion Tests for Modification No. 2 of Combustor A with Nozzle A2.2 100

Table XXII: Hot-Test Measurements 101

Table XXIII: Radial Coordinates of Exit Temperature Traverse for Each Thermocouple Probe 102

Table XXIV: Specifications of the Emission Instruments 103

Table XXV: Hot Rig Flow Conditions Modeled in Conducting Spray Analysis Tests of Nozzle A2.2 104

Table XXVI: Experimentally Determined Droplet Size Distribution for Nozzle A2.2 105

LIST OF FIGURES

Figure 1: Effects of Fuel Distribution on Predicted NO Emission Rate for Representative Aircraft Gas Turbine Combustor (Ref 2) 107

Figure 2: Combustion Performance Map for Fixed and Variable-Geometry Combustors 108

Figure 3: General Configuration of a Piloted Airblast Nozzle . . . 109

Figure 4: Diagrammatic Representation of Class A and Class B Cycles 110

Figure 5: General Configuration of Combustors 111

Figure 6: Final Design Configurations 112

Figure 7: Radial Swirler Design 113

Figure 8: Airblast Nozzle Configuration 114

Figure 9: Estimated Axial Distributions of Liner Temperature . . . 115

Figure 10: Variable-Geometry Configuration 116

Figure 11: General Flow Pattern Observed in Flow Visualization Tests 117

Figure 12: Variation of Effective Primary-Zone Flow Rate for Combustor A 118

Figure 13: Variation of Effective Primary-Zone Flow Rate for Combustor B 119

Figure 14: Effects of Nozzle Air Pressure Drop on Spray Performance 120

Figure 15: Effects of Axial Position of Nozzle on Spray Performance 121

Figure 16: Summary of NO_x and CO Emissions for Combustor B 122

Figure 17: Summary of Hydrocarbon Emissions (HC) and Combustion Efficiency (η_c) for Combustor B 123

Figure 18: Typical Effect of Residence Time on NOx and CO Emissions for Combustor B 124

Figure 19: Typical Variation of NOx Emissions with Flow Conditions for Combustor B 125

Figure 20: Effect of Nozzle Air/Fuel Ratio on NOx and CO Emissions 126

Figure 21: Comparison of NOx and CO Emissions for Original and Modified Combustor B Configurations 127
Figure 22: Weak Extinction Limit for Combustor B 128
Figure 23: Summary of NOx and CO Emissions for Combustor A 129
Figure 24: Summary of Hydrocarbon Emissions (HC) and Combustion Efficiency (η_c) for Combustor A 130
Figure 25: Typical Variation of NOx Emissions with Flow Conditions for Combustor A 131
Figure 26: Weak Extinction Limit for Combustor A 132
Figure 27: Combustor Flow Pattern Schematic 133
Figure 28: Fuel-Air Distribution in Primary-Zone Inlet Region . . . 134
Figure 29: Calculated Results for Combustor B 135
Figure 30: Calculated Results for Combustor A 136
Figure 31: Modifications of Combustor A Tested 137
Figure 32: Comparison of NOx and CO Emissions for Original and Modified Combustor A 138
Figure 33: Effect of Pressure Drop and Residence Time on NOx Emissions for Modified Combustor A 139
Figure 34: Effect of Fuel Injection on NOx Emissions for Modified Combustor A 140
Figure 35: Flow Schematic of Water Rig 141
Figure 36: Flow Schematic of Cold-Air Test Rig 142
Figure 37: Nozzle Mounting for Fuel Nozzle Tests 143
Figure 38: Air Flow Schematic for Combustion Test Rig 144
Figure 39: Fuel Flow Schematic for Combustion Test Rig 145
Figure 40: Combustion Test Section 146
Figure 41: Thermocouple Probe 147
Figure 42: Spacing of Thermocouple Probes 148
Figure 43: Relative Circumferential Orientation of Thermocouple Probes 149
Figure 44: Spacing of Gas Sampling Rakes 150
Figure 45: Relative Circumferential Orientation of Gas Sampling Probes 151
Figure 46: Design of Gas Sampling Rakes 152
Figure 47: Sampling Train of Existing NREC Engine Exhaust Sampling Facility 153

Figure 48: Experimentally Determined Variation of Mean Droplet Size with Air Pressure Drop for Airblast Portion of Nozzle A2.2 154

Figure 49: Experimentally Determined Radial Distributions of Spray for Airblast Portion of Nozzle A2.2 155

SUMMARY

This report describes a program sponsored by the Environmental Protection Agency under Contract No. 68-04-0017 as part of the continuing research and development effort aimed at demonstrating an automotive gas turbine engine capable of meeting the Federal 1975/76 emission standards. The program consisted of the design and testing of two low-~~emission~~ research combustors for automotive gas turbine applications, one of which was representative of low pressure-ratio, regenerative gas turbine cycles and the other representative of high pressure-ratio, nonregenerative cycles. The goal ~~in~~ the design of the combustors was to achieve emission levels not exceeding one-half of the Federal 1975/76 emission standards. The over-all ~~objective of the~~ program was to develop design guidelines on the basis of detailed experimental data which could be used to design automotive gas turbine combustors capable of achieving the specified emission goals.

The approach adopted for controlling the emissions involved extensive modifications to conventional combustor configurations, but made direct use of existing combustor design technology. The specific approach utilized was selected on the basis of results obtained in previous programs conducted by NREC dealing with the prediction and control of NOx emissions, and consisted of designing both combustors were designed for to operate with a lean, well-mixed primary zone over the full range of operating conditions. The necessity of operating with a lean primary zone required the use ~~of~~ variable geometry to control the combustor air flow distribution ~~so~~ as to maintain stable and efficient combustion over the ~~combustor~~ operating range. Inasmuch as the uniformity of the fuel/air mixture depends on the aerodynamic design of the combustor as well as the manner in which fuel is introduced, both variable-geometry combustors were designed for a relatively high value of pressure-loss factor in order to promote aerodynamic mixing. The diameter ~~of each combustor~~ was somewhat oversized to accomplish the high-pressure loss factor and also to aid in reducing CO and HC emissions. With regard to fuel injection, the approach adopted was to use an airblast type of fuel nozzle which was expected to aid in achieving a reasonably uniform fuel/air mixture

in the primary zone of the combustor.

Using the over-all approach discussed above, each of the two combustors was designed as a single-can, throughflow configurations. Full-scale models of both combustors were fabricated and tested over wide ranges of operating conditions representative of typical driving cycles. Two types of tests were conducted-- cold-flow tests to measure aerodynamic performance and detailed combustion tests to measure emission, combustion, and thermal performance.

The test results showed that in general the NOx emissions obtained were higher than the goal whereas CO and HC emissions were satisfactory along with the ~~measured values of the~~ more conventional combustor performance parameters such as combustion efficiency, stability limits, pressure loss, exit temperature traverse quality, and combustor wall temperature. A critical analysis of the test data was performed to determine the effects of the major parameters on emission performance and to identify specifically the causes of the high NOx emissions. This analysis included use of the analytical model previously developed by NREC for predicting the formation and emission of NOx in gas turbine combustors. Both the experimental and analytical results indicated that the high NOx emissions were principally due to inadequate fuel/air mixing in the primary zone. This in turn was due to inadequate distribution of the fuel spray in the nozzle and swirler airstreams and insufficient proportion of the primary-zone air flow through the nozzle/swirler assembly relative to the flow through the secondary holes. These conclusions were verified experimentally by conducting an additional series of tests with modified combustor configurations. The results of this test series indicated that the NOx emission goals could be met by improving the uniformity of the primary-zone fuel/air distribution. Specific modifications of the method of fuel injection were identified which if implemented should result in achieving the emission goals with the existing combustor configurations.

Despite the fact that not all of the emission goals were met, the experimental evidence obtained in the program demonstrates that the variable-geometry concept utilized has the potential of producing the necessary reductions in emission levels. The major conclusion reached on the basis of the program results is that the specified emission goals can be achieved with modifications of essentially conventional combustor configurations utilizing the approaches identified in the program, and that further development of this concept is warranted.

INTRODUCTION

Background

The motor vehicle is the greatest single contributor to the increasingly serious health hazard of air pollution, producing some 60 per cent of the pollutants released into the atmosphere in the United States. In recognition of this fact and in accordance with the requirements of the Clean Air Act of 1970, the Environmental Protection Agency has prescribed standards regulating the emissions of nitrogen oxides, carbon monoxide, and hydrocarbons from new motor vehicles effective with the 1975/76 model years. Although research, development, and legislation are resulting in significant reductions in pollutant emissions from conventional internal combustion engines, it is possible that in the long term these may be replaced by alternative power units. The gas turbine engine represents an attractive alternative as a source of power for automotive applications because of its inherently low level of pollutant emissions. For this reason, the Environmental Protection Agency is sponsoring a number of programs representing a concerted research and development effort aimed at demonstrating a practical automotive gas turbine engine which meets the Federal 1975/76 emission goals. Since the combustor is the critical factor with regard to emissions, most of this effort has been directed towards establishing a combustor design concept capable of achieving the specified emission goals. The program described in this report was sponsored by EPA under Contract No. 68-04-0017 as part of this effort and consisted of the design and testing of two low-emission research combustors for automotive gas turbine applications.

Problem Definition

Two types of gas turbine cycles having potentially different emission characteristics are the primary candidates for use in automotive applications-- the regenerative cycle and the simple or nonregenerative cycle. In both cases, the combustor is the major component from the standpoint of emissions. The most practical and direct approach to the control of all pollutant species is to design the combustor itself properly rather than attempt to treat the exhaust products. A major problem in designing for a low over-all level of emissions is the fact that operating conditions leading to a reduction in some pollutant species favor the formation of others. For example, decreasing the temperature of the primary zone reduces the production of nitric oxide, the major pollutant problem in gas turbine engines, but may tend to increase the emissions of carbon monoxide and unburned hydrocarbons. An additional complicating factor is that a gas turbine engine for automotive applications does not have a single operating point, but must function efficiently over a wide range of conditions. The combustor has a major effect on cycle performance and fuel economy over the entire operating range and therefore has to be designed to satisfy both pollution and performance requirements. Unfortunately, all of these requirements are by no means mutually compatible, and an effective compromise among them must be achieved.

The gas turbine combustor has been studied quite extensively in the past, particularly with regard to its application in aircraft engines. Consequently, a great deal of information on the design and development of conventional combustors is available, and the technology is fairly well-established. However, until recently, a relatively small proportion of the effort expended on combustors has been devoted to investigating their emission performance and determining the major factors governing the formation and emission of the pollutant species of concern. The program described in this report was oriented towards bridging this gap in the state-of-the-art by providing information which could be applied directly to the future design and development of low-emission combustors. This program involved the design and development of two combustors suitable for automotive gas turbines with the objective of achieving emission levels not exceeding one-half of the Federal 1975/76 emission goals.

The program consisted of three major tasks. The first task consisted of the design of the two research combustors, one of which (designated as Combustor A) was representative of low pressure ratio, regenerative gas turbine cycles, and the other (designated as Combustor B) representative of high pressure ratio, nonregenerative cycles.

The primary goal in the design of these combustors was to obtain configurations which would be capable of meeting the specified emission standards. The second task involved fabricating full-scale models of the selected configurations and preparation of facilities for their testing. The final task consisted of detailed testing of the two configurations and critical evaluation of the results obtained.

Method of Attack

Objectives

The major objective of the program conducted by NREC was to develop design data and guidelines which could be used to design automotive gas turbine combustors capable of achieving the specified emission goals. Thus, an approach was adopted which involved extensive modifications to conventional combustor configurations, but which made direct use of present technology; similarly, the program consisted of designing the two combustors with the goal of meeting the emission standards insofar as possible and evaluating the potential of the selected approach by testing the combustors over operating conditions representative of automotive gas turbine engines.

It was recognized from the outset that, while considerable reductions in over-all emission levels could be achieved with this approach, there could be no guarantee that the specified standards could be met during the course of the program-- the program was not directed toward the investigation of any novel concepts, representing radical departures from current practice, which ultimately might have been required to satisfy the specified emission goals. It was felt strongly that the latter approach would require development costs and time beyond the scope of the desired effort, and that in any case the recommended program was an essential step for the practical solution of the problem of achieving acceptable emission levels in automotive gas turbine engines. The major purpose of the program was then to obtain experimental information which would identify specifically the steps required to achieve acceptably low emission levels and provide a firm basis for the subsequent design of practical gas turbine combustors which can meet the specified emission goals.

Design

The major problem in the design of the two combustors was to arrive at configurations which were capable of achieving low emission levels of nitrogen oxides (NOx). Evidence obtained by NREC in previous studies (Refs 1, 2, and 3) of this problem showed that NOx emission is a function of three major factors which can be controlled by the combustor designer: primary-zone equivalence ratio, uniformity of the primary-zone fuel/air mixture, and residence time. Emissions of NOx decrease as the primary-zone equivalence ratio departs from unity, the fuel/air mixture is made more uniform, and the residence time is reduced. The first two of these factors have a significantly greater effect than residence time. Therefore, the approach selected for reducing emissions was to design for a lean, well-mixed primary zone at all operating conditions.

The necessity of operating with a lean primary zone required the use of variable geometry both to control the combustor air flow distribution and to maintain low carbon monoxide (CO) and hydrocarbon (HC) emissions, as well as stable combustion, over the required combustor operating range. Inasmuch as the uniformity of the fuel/air mixture depends on the aerodynamic design of the combustor as well as the manner in which the fuel is introduced, both variable-geometry combustors were designed for a relatively high value of pressure-loss factor (defined as the ratio of the pressure drop to the reference dynamic head), in order to promote aerodynamic mixing.

With regard to fuel injection, the ideal situation would be to premix the fuel with air prior to entering the combustor. The actual approach adopted was to use an airblast type of fuel nozzle which was expected to aid in achieving a reasonably uniform fuel/air mixture in the primary zone of the combustor. Since this type of nozzle is still in the development stage, it was not possible to specify the required design characteristics exactly. Therefore, six nozzles (two for Combustor A and four for

Combustor B) differing primarily in the amount of nozzle air flow were fabricated for testing. As will be shown in a subsequent section of this report, experimental results have indicated that this fuel injection system is the major deficiency in the over-all approach and requires improvement.

Testing and Evaluation

Using the over-all approach discussed above, each of the two combustors was designed as a single-can, throughflow configuration. Full-scale models of both combustors were fabricated and tested over a wide range of operating conditions representative of typical driving cycles. Two types of tests were conducted-- cold-flow tests to measure aerodynamic performance and detailed combustion tests to measure emission, combustion, and thermal performance. The cold-flow tests consisted of flow visualization tests of the combustors and nozzles with water as the flow medium and pressure loss and flow distribution tests with air. The combustion tests consisted of taking complete performance measurements for independent variations of combustor geometry, fuel nozzle, fuel flow rate, air flow rate, and combustor inlet temperature and pressure. The performance variables measured included air and fuel inlet conditions and flow rates, exhaust concentrations of the major pollutant species, pressure loss, liner temperature, and exhaust gas temperature distribution.

The experimental evaluation of both combustors provided detailed information on the variations of combustor performance with geometry and operating conditions. The results obtained were analyzed in detail to determine the effects on performance (particularly emissions) of independent variations in the major test parameters. This analysis included the use of the NOx prediction model previously developed by NREC (Refs 1, 2, and 3) to isolate the major factors contributing to the formation and emission of NOx. On the basis of the conclusions reached in this analysis, the original Combustor A configuration was modified for the purpose of reducing NOx emissions. These conclusions were then verified experimentally by conducting an additional series of tests with the modified configuration. The critical evaluation of all of the test results obtained in the experimental program identified specifically the measures which must be taken to achieve the emission goals with a practical combustor configuration.

Report Arrangement

The design approach selected for achieving reduced emissions is presented in the next section of this report. This is followed by a section which describes in detail the design procedures employed and the resulting configurations of the two combustors. The cold-flow tests and combustion tests are discussed separately in the next two sections. Each of these two sections contains a description of the tests conducted, a complete presentation of the results obtained, and a detailed discussion of the analysis of these results. The final section contains the major conclusions reached on the basis of the program results and recommendations regarding the application of these results to future efforts in the design of low-emission gas turbine combustors. The details of the experimental rigs, methods of data analysis, and results of nozzle spray tests are presented in three appendices.

DESIGN APPROACH FOR REDUCING EMISSIONS

Emission Goals

The major pollutant species of concern with regard to emissions from gas turbine engines are nitrogen oxides (NOx), carbon monoxide (CO), hydrocarbons (HC), and particulates. The general factors leading to the emissions of these species are discussed below.

Nitrogen-oxide emissions from gas turbines arise from the reaction of nitrogen and oxygen in the high-temperature flame region in the combustors. Nitric oxide, NO, is usually the predominant species formed in the combustor. This is oxidized outside the engine to produce nitrogen dioxide which is the form that plays a large part in the photochemical oxidation of hydrocarbons to produce photochemical smog. Nitric oxide is formed through the Zeldovich chain reaction mechanism and the amount produced is kinetically controlled. The formation of nitric oxide is increased by high oxygen content in the burned gas and long residence time at high temperature. In terms of the design variables, nitric oxide formation is increased in various degrees by high combustor air inlet temperature, high combustor pressure, primary-zone fuel/air ratio near stoichiometric, and long primary-zone residence time. The rate of quenching in the dilution zone is important when the primary-zone mixture is stoichiometric or richer than stoichiometric.

Carbon monoxide emissions are usually due to the too rapid quenching of the burned gases. The oxidation of carbon monoxide to carbon dioxide is the last and slowest step in the kinetic chain of hydrocarbon combustion, and sufficient time must be available for these reactions to come to equilibrium before quenching with dilution air begins. At the high burned gas temperatures corresponding to near-stoichiometric combustion in the primary zone, chemical equilibrium is attained quite rapidly. However, significant amounts of carbon monoxide are present even when equilibrium is established. The initial rate of dilution then should be sufficiently slow so that the carbon monoxide has time to maintain pace with the equilibrium shift caused by the addition of air to the combustion gases. When lean primary zones are used, the amount of carbon monoxide at equilibrium is relatively small. However, at the lower burned gas temperatures corresponding to the lean conditions, the carbon monoxide oxidation rate is low. Therefore, the slow carbon monoxide oxidation in the hydrocarbon reaction chain is the dominant factor for lean primary zones.

Unburned hydrocarbons are usually caused by local fuel-rich regions or by fuel droplets which impinge on the liner walls or are entrained in the film-cooling air stream and pass through the hot reaction zone. Combustion of this fuel does not occur and the fuel is carried through the combustor without reacting. Some unburned hydrocarbons arise from the quenching of the hydrocarbon reactions before they have reached completion.

Particulate emissions from gas turbines are principally in the form of soot particles (smoke). Soot is usually formed in the fuel-rich regions near the fuel nozzle in designs with rich primary-zone equivalence ratios. A large proportion of the soot formed in this region is usually consumed in the dilution zone of the combustor. Smoke emissions can be controlled by correct attention to eliminating fuel-rich areas in the combustor primary zone.

The Federal 1975/76 Emission Standards (Ref 4) prescribe maximum allowable exhaust levels of NOx, CO, and HC based on a specified representative driving cycle. The goals in terms of the emissions from the combustor are given in Table I. For the program described in this report, the emission goals in the design of the combustors were to achieve exhaust levels not exceeding one-half the Federal 1975/76 emission standards. Although standards for the emissions of particulates have not been specified as yet, efforts are proceeding to define such standards. Therefore, it was considered necessary to attempt to reduce particulate emissions as well as the other species in the design of the combustors.

Major Factors in Emissions of NOx

As noted previously, the achievement of low emission levels of nitrogen oxides is the most difficult problem with regard to the controlling of emissions. This then dictated the conceptual design of the combustors. NREC has conducted a number of programs (Refs 1, 2, and 3) dealing with this problem. The most relevant of these is one sponsored by the Federal Aviation Administration and the Environmental Protection Agency which involved the development of improved techniques of predicting and controlling the formation of NOx in gas turbine combustors (Refs 1 and 2). This program has consisted of developing an analytical model of the kinetic processes by which NO is generated in a combustor and verifying the model experimentally by conducting emission performance tests of two representative combustors. The model treats the primary zone as a partially stirred reactor with a Gaussian distribution of fuel/air ratios. The uniformity of this distribution is characterized by a mixedness parameter[*] (S_0) defined as the ratio of the standard deviation of the distribution to the mean value of the fuel/air ratio. In accordance with this definition, decreasing the value of S_0 corresponds to improving the uniformity of the fuel/air distribution; a value of $S_0 = 0$ representing a perfectly mixed system. The evidence obtained by NREC in the previous studies of NOx has shown that NOx emission is a function of three major factors which can be controlled by the combustor designer:

1. Primary-zone equivalence ratio (ϕ_p , defined as fuel/air ratio divided by stoichiometric fuel/air ratio).
2. Uniformity of primary-zone mixture (degree of "mixedness" as characterized by the value of S_0).
3. Primary zone residence time.

Emission of NOx is also strongly dependent on the combustor inlet temperature. However, this quantity is usually fixed by the cycle conditions and cannot be altered significantly without compromising cycle efficiency.

Emissions of NOx decrease as the primary-zone equivalence ratio departs from unity, the fuel/air mixture is made more uniform, and the residence time is reduced. It has been found that primary-zone equivalence ratio and degree of mixing have significantly greater effects on NOx emissions than residence time. The variation of NOx emissions with residence time is at most linear. The combined effects of primary-zone equivalence ratio and degree of mixing are illustrated by Figure 1 which is taken from Reference 2. The results given in the figure were obtained using the analytical model previously developed by NREC and show the predicted variations of NO emissions with degree of mixedness at selected values of primary-zone equivalence ratio for a representative aircraft gas turbine combustor operating at full-power conditions. At low values of S_o (well-mixed primary zone), the emission rate decreases rapidly as the mean primary zone equivalence ratio is decreased from the stoichiometric value ($\phi_p = 1$); a similar but less rapid decrease in emissions is observed for values of ϕ_p above unity. At the higher values of S_o corresponding to a poorly-mixed primary zone, the effect of equivalence ratio on emissions is significantly lessened and all but very lean mixtures would appear to have roughly the same emission level.

---

[*] See NOMENCLATURE following main body of report.

Control of NOx Emissions

Potential Approaches

Before describing the methods selected for controlling NOx emissions, it is worthwhile to discuss alternative methods which were considered and discarded for a variety of reasons. In general, low NOx emissions can be achieved by reducing oxygen concentrations in the primary zone, insuring that the combustion reactions are carried out at low temperature, attaining very short residence times, or combinations of these approaches. The only practical way to limit oxygen concentrations would be to operate with a fuel-rich primary zone. With this approach, the fuel/air ratio would pass through the stoichiometric value at some point in the combustor, and it is doubtful whether this transition could be accomplished quickly enough to avoid generating excessive amounts of NOx; in addition, the use of a fuel-rich primary zone would create a problem with respect to smoke emissions. It is estimated that combustion temperatures must be limited to about 3400 deg F or lower if the NOx goals are to be met. Possible methods of accomplishing this are by burning only very weak mixtures, by abstracting heat from the combustion zone by convection, conduction, or radiation, or by admixing with a heat-absorbing inert fluid. Continous combustion at mixture strength below the lean flammability limit can only be achieved by passing the mixture through a catalyst matrix or by continuously admixing it with the high-temperature products from a pilot flame. Such techniques are used in the control of combustible emissions from industrial processes by the use of so-called "afterburners" (Ref 5). The use of a catalyst matrix in a gas turbine combustion system is precluded by volume and cost considerations. Control of combustion temperatures by radiation is not feasible due to the large amount of heat that needs to be removed. Heat removed by convection would presumably require the use of a large amount of convective surface in the combustion zone. This would rapidly become fouled by coke formation, if a fuel spray injection system is used. Fuel pre-vaporization would be required and the convective surface would need to be internally cooled by what is conventionally dilution air. The resulting system would become overwhelmingly complex. Heat removal by conduction could be achieved by the use of an air-cooled porous plug burner, but this would need to be excessively large. Exhaust gas recirculation is not a feasible system for automotive gas turbines as the exhaust gases would have to be cooled and recompressed if flame temperatures are to be kept sufficiently low. Water injection into the flame zone would be a feasible system, but since the water flow rate required would be of the order of the fuel flow rate, this would correspond to a significant penalty on the vehicle. Appropriately large reductions in effective residence time do not appear to be feasible due to the time required to evaporate and mix the fuel and allow completion of the hydrocarbon reactions. A multiple swirl-can combustor concept (Ref 6) was considered by NREC, but was eliminated on the grounds that low NOx emissions could only be achieved by programming the fuel to individual swirl cans which would operate with an equivalence ratio of near 0.7. Such programming would require continual ignition and extinction of the individual cans leading to excessive hydrocarbon emissions. A particularly promising concept considered by NREC consisted of employing a pre-vaporization chamber which evaporates and intimately mixes most of the design fuel flow and injects the resulting very lean mixture at high velocity into the exhaust of a pilot burner (Ref 7). It was felt that this concept stood the best chance of success in ultimately achieving the emission goals. However, since this approach would have represented a radical departure from conventional combustor designs, it was felt that the amount of development time and effort required for its successful application would be beyond the scope of the program.

Selected Approach

The method adopted for achieving low emissions was selected on the basis of the considerations discussed above and the evidence obtained by NREC in previous programs. In general terms, the selected approach consisted of designing each of the two combustors to operate with a lean, well-mixed primary zone over the full range of operating conditions.

The problem with designing a standard combustor for lean primary-zone operation is illustrated schematically in Figure 2 which shows a typical plot of blow-out limits including contours of constant combustion efficiency versus primary-zone equivalence ratio and combustor loading parameter ($1/\theta$). With fixed combustor geometry, the air flow split is essentially independent of the operating conditions and so the primary-zone air/fuel ratio is proportional to the over-all air/fuel ratio. This latter may increase by as much as a factor of four from design point to idle conditions. The slope of the operating line for a standard fixed-geometry combustor is then fixed by the cycle conditions. For this reason, a standard combustor is usually designed to have an approximately stoichiometric primary-zone fuel/air ratio ($\phi_p = 1$)at the full-power condition in order to achieve an acceptable stability margin. A higher design-point value of ϕ_p is usually precluded by the necessity of avoiding smoke at high power. Under these conditions, the idle point often falls fairly close to the lean blow-out limit in a region of low combustion efficiency. Typically, NOx emissions are high at the design point (full power) and low at idle, while hydrocarbon and carbon monoxide emissions are low at full power and high at idle. If a standard combustor were designed to operate lean at the full-power point, the operating range would be unacceptably narrow, since most of the operating points would fall below the lean blow-out limit. In addition, the low-power points would be in the region of low combustion efficiency resulting in excessive HC and CO emissions. In order to achieve efficient lean primary-zone operation at all conditions, it is necessary to resort to variable geometry to control the distribution of air flow in the combustor. The use of variable geometry provides an additional degree of freedom allowing the slope of the combustor operating line to be made independent of the cycle conditions as indicated in Figure 2. With this approach, the operating conditions of the combustor can be controlled so as to minimize over-all emissions while maintaining an acceptable operating range.

The uniformity of the fuel/air mixture in the primary zone depends mainly on the aerodynamic design of the combustor and the manner in which the fuel is introduced. From the standpoint of aerodynamic design, the degree of mixing (hence, the uniformity of the primary zone) improves with increasing values of the pressure-loss factor defined as the ratio of the combustor pressure loss (ΔP) to the dynamic head based on the reference flow area of the combustor (q_{ref}). For a given set of inlet conditions and flow rate,

$$\frac{\Delta P}{q_{ref}} \propto \Delta P \cdot D_{ref}^4 .$$

where D_{ref} is the reference diameter. Increasing the combustor pressure loss improves mixing by increasing the energy of the air jets entering the combustor liner which serve the function of "stirring" the main flow. Increasing the reference diameter has the effect of reducing the through-flow velocity in the combustor; within reasonable limits, this improves mixing by allowing the entering air jets to penetrate more easily into the main flow stream. The combustor pressure loss has a significant effect on over-all cycle efficiency. Therefore, attaining significant improvements in mixing by increasing the design value of combustor pressure loss would not appear to be a practical solution. Since $\Delta P/q_{ref}$ varies as D_{ref}^4 , it was felt that an acceptable mixing performance could be achieved most effectively by a moderate increase in the combustor diameter. The approach adopted for obtaining good mixing then was to design for a value of pressure loss typical of automotive gas turbine applications and somewhat oversize the diameter to achieve a relatively high value of $\Delta P / q_{ref}$. A consequence of increasing the combustor diameter is to increase the primary-zone residence time. This would tend to increase NOx emissions and reduce HC and CO emissions. However, as mentioned previously, achieving a lean, well-mixed primary zone has a significantly greater effect in reducing NOx emissions than residence time. Therefore, a moderate increase in residence time was considered acceptable for the sake of obtaining good mixing, particularly since it would aid in reducing HC and CO emissions.

With regard to fuel injection, the ideal situation would be to pre-vaporize the fuel and pre-mix it with air prior to entering the combustor. The actual approach adopted consisted of using an airblast type of fuel nozzle which was expected to aid in achieving a reasonably uniform fuel/air mixture in the primary zone of the combustor. The airblast fuel nozzle differs from conventional air-assisted nozzles primarily in that it operates with the available pressure drop across the combustor liner and does not require an external source of high-pressure air. The principle of operation of the airblast nozzle is indicated by the sketch shown in Figure 3 which illustrates the general design features of this type of nozzle. The airblast nozzle is usually designed to operate in conjunction with the main combustor swirler. The main fuel is introduced downstream of the nozzle swirler forming a film along the inside wall of the nozzle. The angles of the main combustor swirler and the nozzle swirler are chosen such that the air streams through these components are counter-rotating as they enter the combustor. The fuel film enters the combustor in the resulting high-shear region between the two swirler flow streams. Break-up of the fuel film into droplets occurs just downstream of the nozzle exit with the atomization energy being supplied by the dynamic pressure of the two swirler streams. The mean droplet size obtained with this type of atomization is characteristically very small, on the order of one-half of the values typical of a conventional fuel-pressure atomizer. Consequently, the airblast nozzle has relatively narrow stability limits. The stability performance can be improved by the use of a conventional single-orifice pilot atomizer as shown in Figure 3.

Effects on Emissions of Other Species

Although the design approach utilized was dictated by the requirements for reducing NOx emissions, it was necessary to insure that in so doing the emissions of the other pollutant species were not increased beyond acceptable limits. The use of a lean primary zone was expected to eliminate smoke formation provided that care was taken to avoid local fuel-rich regions. Burning lean mixtures would tend to increase the emissions of CO and HC by virtue of the reduced flame temperatures. However, it was expected that the increased residence time resulting from the use of an oversized combustor diameter would be sufficient to counteract the effect of reduced temperature. In general, it was felt that the selected approach was capable of achieving acceptable emission levels of all pollutant species of concern.

DESIGN OF COMBUSTORS

The methods utilized in designing the two combustors are described in this section. In general, these methods are fairly standard and are based on information documented in a two-volume handbook (Refs 8 and 9) on the technology of combustor design. This handbook was produced by NREC and is widely used in the gas turbine industry by those organizations who have sponsored its compilation. The selection of the design conditions is discussed first. This is followed by a description of the aerothermodynamic and mechanical design of the two combustors. Although the elements of the design process are discussed separately below, the actual design process involved an iterative approach to determine the relative trade-offs and arrive at the necessary compromises among the various performance requirements.

Cycle Conditions

As mentioned previously, the combustors were designed so as to be representative of two different automotive gas turbine cycles-- a low-pressure-ratio, regenerative cycle (designated as Class A) and a high-pressure ratio, nonregenerative cycle (Class B). These two cycles are shown schematically in Figure 4. The cycle operating conditions relevant to the design of the combustors were selected on the basis of an engine power rating of 150 hp for both cycles. The estimated nominal values of these conditions are given in Table II.

The main purpose of defining the cycle performance was to provide a nominal set of operating conditions on which to base the design and subsequent testing of the combustors. In so doing, the primary requirement was to insure that the combustor designs and measured performance were representative of the two types of gas turbine cycles considered. The combustors were not intended for use in any specific engine, but instead were to be capable of being tested over wide ranges of operating conditions. In addition, the design approaches to be utilized represented moderate but significant advances in combustion technology which were as yet untried in terms of their measured effects upon performance. Therefore, the use of sophisticated analysis procedures to determine the cycle operating conditions to any great degree of accuracy was not warranted.

The values of the combustor inlet temperature and pressure and exit temperature at the design point (full-power operation) were selected in accordance with the criteria specified in the contract. The design-point values of the other operating conditions were estimated on the basis of approximate cycle calculations using assumed typical values of component efficiencies which might be achievable for the given pressure ratios. These calculations were simplified by ignoring entrance, exit, duct, and mechanical losses. Although this approximation results in optimistic values of fuel flow rate, it had little effect on the sizing of the combustors, since specific power (hence air flow rate) is relatively insensitive to these losses (Ref 10). For both cycles, a 3 per cent pressure drop and 100 per cent combustion efficiency were assumed for the combustor. The calculations for the regenerative cycle assumed a compressor and turbine isentropic efficiency of 85 per cent, a regenerator effectiveness of 89 per cent, and regenerator pressure losses of 1 per cent on the cold side and 4 per cent on the hot side; for the nonregenerative cycle, the compressor and turbine isentropic efficiency was assumed to be 80 per cent. The off-design cycle conditions given in Table II were estimated by approximately scaling data available in the literature (Refs 11 through 17) for existing gas turbine engines of the regenerative and nonregenerative type and data obtained in previous programs by NREC. This approach consisted of normalizing the available data on off-design conditions with respect to the values at design point and assuming that the operating conditions for the two cycles of concern followed the same general trends.

Combustor Design Conditions

General Configuration

Both combustors were designed as single-can, throughflow configurations, since this type is suitable for most simple cycle and regenerative engines and is simpler to fabricate and test than alternative arrangements. The general configuration of both combustors is depicted in Figure 5, and, as can be seen, is typical of conventional gas turbine combustors. The major components consist of a casing, liner, dome, and radial-inflow swirler. Fuel is injected by means of an airblast nozzle. The ignition source consists of a standard high-voltage gas turbine spark plug. Essentially all of the combustion occurs in the primary zone, a highly turbulent region with a recirculating mean flow path and a low mean axial velocity. The recirculating flow pattern is established by the swirler air and reinforced by the secondary jets. The intermediate zone provides a region of relatively high temperature for the completion of the combustion reactions and the recombination of any dissociated products of combustion. The bulk of the remaining air enters the liner through the dilution holes and mixes with the combustion gases as the flow passes through the dilution zone thus lowering the temperature to the required turbine inlet value and achieving the desired exit temperature profile. Cooling of the flametube liner and dome is accomplished by four film-cooling slots, one for the dome and one for each of the three major zones of the combustor; additional cooling of the downstream portion of the liner is accomplished by allowing some flow to bleed through keyhole-shaped holes in the piece joining the liner to the casing at the exit of the combustor.

Most of the air participating in the combustion process occurring in the primary zone is supplied by airflow through the fuel nozzle and swirler ($\dot{m}_{FN}$ and $\dot{m}_{SW}$) and part of the air entering through the secondary holes ($\dot{m}_{sy,p}$). The combustors are variable-geometry configurations by virtue of the fact that the airflow through the swirler and secondary holes (hence, the primary-zone equivalence ratio) is controlled by adjusting the flow areas of these components. For the secondary holes, this area adjustment is accomplished by means of a movable sleeve fitting around the liner. The flow area of the radial-inflow swirler is adjusted by an annular cup which fits over the swirler and fuel nozzle. These variable-geometry devices are described in more detail in the subsequent discussion of the mechanical design of the combustors given in this section of the report.

Selected Values of Design Parameters

The values of the pertinent design conditions selected for the combustors are given in Table III, and the design distributions of air flow are given in Table IV. The inlet flow conditions, temperature rise, and heating rate follow directly from the cycle design-point conditions. The values of the other design parameters were selected on the basis of the considerations discussed below.

The exit temperature traverse quality is defined as the difference between the maximum and mean values of the exit gas temperature profile divided by the temperature rise in the combustor. The selected value for both combustors is typical of the design goal for standard gas turbine combustors. The maximum allowable wall temperature was selected to provide acceptable durability with reasonable construction materials. As discussed in the previous section, it did not appear justified to design for a large pressure loss in order to achieve good mixing; instead, the selected approach consisted of moderately oversizing the combustor diameter. Therefore, the selected pressure loss is also a value typical of automotive gas turbine combustors.

The pressure-loss factor ($\Delta P/q_{ref}$) is usually on the order of thirty for standard combustors. The approach adopted for obtaining good mixing consisted of choosing a larger than standard design value of the pressure-loss factor. Ideally, this choice should involve a trade-off between the opposing effects of mixing and residence time on NOx emissions. The effect of residence time was examined with the aid of an approximate NOx emission model previously developed by NREC (Ref 18) which assumes perfect mixing. However, no information was available on the quantitative effect of $\Delta P/q_{ref}$ on the degree of mixedness. The final design value for both combustors then was chosen somewhat arbitrarily to be about three times larger than the standard value. This design value was felt to be high enough to achieve acceptable mixing without increasing the residence time excessively. The pressure-loss factor also affects combustion efficiency (hence, CO and HC emissions) in that it fixes the size (diameter) of the combustor. Within the accuracy of the available correlations of combustion efficiency (Refs 8 and 9), the size of each combustor dictated by the selected design value of $\Delta P/q_{ref}$ was considered sufficient to achieve the combustion efficiency goals.

The principal consideration in choosing the primary-zone equivalence ratio was the requirement of minimizing NOx emissions. From this standpoint, it was desirable to select as low a value of ϕ_p as possible. In order to obtain acceptable ignition performance and flame stability, ϕ_p should not be lower than about 0.5. This is the value that was chosen for Combustor A. With the lower air/fuel ratio of Combustor B, less air was available for dilution and cooling. Therefore, a higher value of ϕ_p was required in order to achieve adequate dilution and cooling performance.

The values of air flow through the nozzle, swirler, and secondary holes listed in Table IV were chosen to provide the required amount of primary-zone air flow for the selected values of ϕ_p. This was done assuming that the primary-zone air flow participating in the combustion process ($\dot{m}_{p,eff}$) consisted of the total air entering through the nozzle, swirler, and dome film-cooling slot and 50 per cent of the air entering through the secondary holes and primary-zone film-cooling slot. The proportion of the air entering the primary zone through the swirler was selected in accordance with conventional design practice (Refs 8 and 9) to be on the order of 30 per cent of the primary-zone combustion air. The remainder of the air not required by the primary zone was divided so as to achieve an acceptable compromise between dilution and cooling performance.

Fuel Nozzle Design Specifications

As mentioned previously, one aspect of the selected approach to obtaining good mixing consisted of using a piloted airblast type of fuel nozzle. The major design parameters for the airblast nozzle are the nozzle air/fuel ratio, spray cone angle, flow number, and spray characteristics (mean droplet diameter, droplet size distribution, and spray distribution). Since this type of nozzle is still under development, it was not possible to specify the required characteristics exactly. Instead, six different nozzles (two for Combustor A and four for Combustor B) were obtained from the Parker-Hannifin Corporation and investigated experimentally in the testing phase of the program. From the standpoint of controlling emissions, the principal nozzle variables were expected to be the spray characteristics, the amount of air flow surrounding the fuel (nozzle air/fuel ratio), and the weak extinction performance. With the airblast nozzle, the general spray characteristics (particularly mean droplet diameter, SMD) are principally dependent on the available dynamic head of the air which is proportional to the combustor pressure loss. In addition, the effect of spray characteristics on emissions is known only in a qualitative sense. Therefore, it was felt that specifying nozzle designs with significant variations in spray characteristics was not warranted. The desired spray characteristics of all the nozzles were then specified in terms of achieving a well-developed fuel spray at all operating conditions with a mean droplet diameter (SMD) of less than sixty microns; the droplet sizes achieved from the nozzles for the two combustors were estimated to be on the order of 45-68 microns for Combustor A and 12-42 microns for Combustor B assuming negligible wetting of the combustor dome. The six nozzles specified then consisted of piloted and unpiloted configurations having different design values of nozzle air/fuel ratio.

The desired specifications for the nozzles are given in Table V. The values of air/fuel ratio were chosen to be 2-4 times higher than conventional airblast nozzles in order to aid in achieving a low mean equivalence ratio; it was felt that still higher values would aggravate the stability problems inherent in this type of nozzle. The spray cone angles were selected essentially on the basis of conventional design practice. A wide main spray angle would be beneficial from the standpoint of allowing sufficient time for the fuel and air to mix before combustion. However, too high an angle can result in an excessive amount of fuel impinging on the internal surfaces of the combustor and increasing the emissions of unburned hydrocarbons. A 90 degree angle is generally considered to represent a reasonable compromise. A relatively narrow pilot spray cone angle is desirable to provide a small local fuel-rich region for the purpose of improving flame stability. The flow number of the pressure atomizing pilot was selected to be as small as practicable in order to achieve acceptable atomization at low fuel flow rates. The flow number of the main airblast portion of the nozzle was unspecified, since this factor has virtually no effect on atomization quality.

Aerothermodynamic Design

Final Configurations

The final configurations and dimensions for Combustors A and B resulting from the design specifications discussed above are shown schematically in Figure 6. The dimensions of the radial-inflow swirler used in both combustors are given in Figure 7. In each combustor, the dome is cooled by a combination of impingement and film cooling. The dome film-cooling slot is fed by a number of circular metering holes spaced so as to provide uniform impingement cooling. The liner film-cooling slots are also fed by circular metering holes spaced uniformly around the circumference of the liner. Additional cooling of the downstream end of the liner is provided by allowing air to flow through a number of keyhole-shaped bleed holes located in the annulus at the combustor exit. The numbers and dimensions of these holes are given in Table VI.

As mentioned previously, six airblast nozzles were designed and supplied by Parker-Hannifin Corporation. All of the nozzles were designed to have the same external space envelope so that they could be tested in either of the combustors. The general nozzle configuration and external dimensions are presented in Figure 8. The nozzle length was made larger than would be conventional in order to accommodate the required travel distance of the device used to control the flow through the radial-inflow swirler.

Sizing

The casing (reference) diameter for each combustor was calculated from the selected design values of pressure loss and pressure-loss factor using the definition of $\Delta P/q_{ref}$. The flametube liner diameter was selected to provide a reasonable amount of convective cooling of the liner by the annulus airflow without seriously compromising jet penetration. The total combustor length is the sum of the lengths of the primary, intermediate, and dilution zones. A primary-zone length equal to one-half the liner diameter was selected to provide a recirculating flow pattern in the primary zone corresponding to a toroid of zero inner diameter. The major function of the intermediate zone is to allow sufficient time for the reaction of carbon monoxide to reach completion before quenching with dilution air. In accordance with general design practice, an intermediate-zone length of approximately one-half the liner diameter was selected as being sufficient for this purpose. The length of the dilution zone was chosen to provide the selected design value of exit temperature traverse quality using standard correlations of traverse quality versus pressure-loss factor and length given in References 8 and 9.

The various openings in the combustor were sized to provide the selected air-flow distributions and pressure drop. In performing these calculations, the standard equation for flow through a row of holes was used along with discharge coefficients obtained from available correlations and data for different hole types and flow configurations (Refs 8, 9, and 19). The secondary holes were designed as plunged slots to provide good penetration and to simplify the means of varying their flow area. Both the swirler and secondary holes were oversized in order to allow sufficient flexibility in obtaining variations in primary-zone flow rate during testing. The dilution holes were designed using the approach described in Reference 20 to provide as close to optimum penetration of the dilution jets as possible with the available dilution air.

Thermal Analysis

A thermal analysis involving calculations of the temperature distributions of the combustor surfaces was performed for the final configuration and air-flow distribution of each combustor. Standard correlations (Refs 8, 9, and 19) were used in determining the values of heat-transfer coefficients, flame radiation properties, and film-cooling effectiveness. The calculated axial distributions of liner temperature for both combustors are plotted in Figure 9 for both a nonluminous and a luminous flame. With the airblast nozzle, it was expected that a relatively nonluminous flame would be obtained. As can be seen, the estimated maximum temperatures were lower than the selected maximum allowable value (1700 deg F). It was decided not to reduce the amount of cooling any further and to remain with a somewhat conservative cooling approach. The results described here were obtained for the design point which corresponds to a relatively lean primary zone. During testing of the two combustors, it was planned to examine primary-zone equivalence ratios higher than the design values which would result in higher flame temperatures. Therefore, being somewhat conservative in terms of cooling at the design point allowed greater latitude in the conditions which could be examined safely during testing.

Mechanical Design

The major task in the mechanical design of the combustors consisted of selecting the method to be used in controlling the flow areas of the swirler and secondary holes. The variable-geometry configuration used for both combustors is illustrated in the sketch of part of the primary-zone region given in Figure 10. The device for controlling the flow through the swirler (swirler flow throttle) consists of an annular cup which fits over the swirler and fuel nozzle as shown in Figure 10. This piece contains blades which fit into the slots of the swirler and is supported and adjusted by means of four rods which pass through a spider mounting attached to the casing. A seal is provided to minimize leakage through the clearance between the throttle and the nozzle. The combustor dome is also supported by a spider attached to the casing. The device for controlling the flow through the secondary holes (secondary flow throttle) consists of a movable sleeve around the liner. The diameter of the sleeve is large enough to maintain a positive clearance between the sleeve and the liner. The sleeve is supported on the liner by four spring clips; the axial position of the sleeve is maintained by four adjustable straps attached by lockscrews to the upstream end of the liner. In the design of the variable-geometry elements, it was not intended to achieve a mechanized, operational system for use in the program. However, the specific devices utilized for controlling the swirler and secondary flow streams were selected so as to represent a realistic approach which ultimately could be mechanized in a fairly straightforward manner.

As mentioned previously, the swirler throttle and combustor dome are supported by spiders attached to the casing. The downstream end of the liner is supported by the conical-shaped piece containing the bleed holes which is attached to the casing by screws. A sealing ring is attached to the upstream end of the liner. In assembling the combustor, this ring fits over and rests on the dome. This mounting arrangement allows for relative axial growth of the liner and dome, since they are not rigidly attached to each other. The liner, upstream sealing ring, dome, and secondary flow throttle are fabricated of Hastelloy. The remaining components are fabricated of 310 stainless steel.

COLD-FLOW TESTS

In addition to detailed combustion experiments, four different series of tests were conducted under nonburning conditions. These were primarily of a diagnostic nature and provided information which aided in determining what modifications to the combustor configurations were required and interpreting the results obtained in the subsequent combustion tests. The specific purpose of these cold-flow tests was to measure the aerodynamic performance of both combustors and examine the spray performance of the airblast nozzles. The four types of tests conducted were:

1. Flow visualization tests with water as the flow medium.
2. Pressure loss and flow distribution tests with nominally ambient air as the flow medium.
3. Qualitative spray performance tests with air supplying the atomization energy and water as the nozzle test fluid.
4. Spray analysis tests providing quantitative information on droplet size and spray distribution.

The tests conducted and results obtained in each of the first three series are discussed in this section, and the experimental rig and instrumentation utilized are described in Appendix I. The spray analysis tests are described in Appendix III.

Water-Visualization Tests

The objective of these tests was to determine the jet penetration and mixing in the combustion and dilution zones by observing the flow patterns in each of the two combustors for different flow rates and variable geometry settings (ℓ_{sw} and ℓ_{sy} as shown in Fig 10). All of these tests were conducted with full-scale transparent models of the two combustors which were as close in detail as possible to the actual combustors. The flow conditions were chosen so as to simulate Reynolds number approximately. The effects of variable-geometry settings were investigated systematically by observing the flow patterns obtained for variations in the secondary-hole setting (ℓ_{sy}) at each of a number of different swirler settings (ℓ_{sw}). In each test, electrically generated hydrogen bubbles were used as the flow tracers. The flow patterns and jet penetration were observed by illuminating flow planes in the combustor containing the axis and the center lines of diametrically opposite pairs of secondary holes and dilution holes. Observations were also made by illuminating planes normal to the combustor axis at different axial positions along the length of the combustor.

The results of the water tests were essentially qualitative in nature and consisted of observations regarding the flow patterns and degree of mixing achieved in the various regions (particularly the primary zone) of the combustor. The initial tests indicated that a modification of the swirler assembly was required in order to achieve a strong recirculatory flow pattern in the primary zone. The final swirler configuration described previously is the result of the modifications made on the basis of the water tests. In addition, the early tests indicated that the clearance between the liner and the sleeve used to control the secondary-hole flow was too large. This resulted in excessive leakage and reduced the effectiveness of the control, a fact confirmed by the cold-air tests. In all subsequent tests, this leakage was reduced to an acceptable value by inserting 0.015 inch thick shim stock between the sleeve and the liner.

The general flow pattern observed in the flow-visualization tests is shown in Figure 11. As can be seen, this corresponds to the classic flow pattern for a well-designed gas turbine combustor. In general, the results indicated that vigorous mixing in the primary zone and good penetration of the dilution jets was achieved for the final configurations of both combustors. This appeared to be true for all variable-geometry settings except those in which the secondary sleeve was nearly closed; that is, when the secondary sleeve was in a position such that the shape of the secondary holes was virtually circular. For these closed settings, the secondary jets were diverted more strongly by the upstream flow. Therefore, the jets entered the liner at a shallower angle and did not penetrate to the combustor center line. As a result, the amount of flow recirculating back into the primary zone was reduced along with the degree of mixing achieved in this region. For a given variable-geometry setting, the flow rate (hence, pressure drop) seemed to have no discernible effect on the general flow patterns observed. However, as would be expected, increasing the flow rate increased the apparent strength of the mixing by virtue of the higher velocity levels in the combustor. The general conclusions reached on the basis of the flow-visualization tests were that the degree of mixing and general flow patterns achieved in both combustor configurations appeared to be satisfactory for virtually all variable-geometry settings.

Air Flow Distribution Tests

The principal objective of these tests was to obtain experimental information which could be used to determine the distribution of air flow in each of the two combustors for any given flow condition and variable-geometry setting. Basically, this required measuring the variation of effective flow area (defined in general here as the product of discharge coefficient and actual flow area) for each set of openings into the combustor liners. Determining the effective flow areas involved measuring the flow rate through and pressure drop across each set of openings. The approach selected for accomplishing this consisted of testing each set of openings independently. All of these tests were performed with the actual combustors. In each test, all of the openings were blocked off except the set being tested. The air flow rate into the combustor was then varied over a predetermined range and the combustor pressure loss measured at a number of different values of flow rate. This approach is somewhat inaccurate, since the discharge coefficient (hence, effective flow area) depends to some extent on the conditions into which the flow through the holes is discharging. However, information given in References 8 and 9 indicates that the inaccuracy due to this effect is at most on the order of ten per cent. The magnitude of this effect was estimated to be negligible by conducting some tests with various combinations of openings. An additional approximation involved in this approach is that the static pressure in the liner is constant and equal to the exit value. This corresponds to assuming that the pressure changes due to combustion and frictional losses in the liner flow are negligible in comparison to the pressure drop across the openings in the liner. Estimates of the relative magnitudes of these losses showed that the accuracy of this assumption was acceptable for both combustors.

The air flow and pressure-drop data obtained in these tests were used to compute the values of effective flow area ($A_{h,eff}$) for each set of openings. In general, the results showed that the effective area did not vary significantly with flow rate and an average value for each set of openings was sufficiently accurate for calculation purposes. The average values of effective flow area are listed in Table VII. These values were used to calculate the anticipated distributions of air flow in both combustor configurations as functions of the variable-geometry settings of the swirler (ℓ_{sw}) and secondary holes (ℓ_{sy}). The results of these calculations showed that the values of flow rate obtained for each set of openings were reasonably close to the selected design values.

As mentioned previously, it was assumed in the design of the two combustors that the portion of the primary-zone flow which participates in the combustion process ($\dot{m}_{p,eff}$) consists of the air flow entering through the nozzle, swirler, and dome cooling-film slot and 50 per cent of the flow entering through the secondary holes and the primary-zone (film-cooling) slot. The results of the water flow-visualization tests and preliminary combustion tests indicated that a more reasonable estimate of the effective primary-zone flow would be

$$\dot{m}_{p,eff} = \dot{m}_{FN} + \dot{m}_{sw} + 0.4\,\dot{m}_{sy}$$

The values of $\dot{m}_{p,eff}$ were calculated on this basis and are plotted versus variable-geometry setting in Figures 12 and 13 for the two combustors. As can be seen, the variable-geometry approach utilized provides a variation in effective primary-zone flow (hence, ϕ_p) of a factor of about 3.3 for Combustor A and 2.1 for Combustor B. Examination of the estimated cycle conditions given in Table II shows that the values of over-all air/fuel ratio vary by factors of approximately 2.7 for Combustor A and 2.0 for Combustor B. Therefore, in order to maintain a constant primary-zone equivalence ratio, the variable-geometry should provide corresponding variations in the effective primary-zone flow of about the same order. The selected variable-geometry approach appears to be capable of providing adequate control of the primary-zone equivalence ratio.

Nozzle Spray Visualization Tests

The objective of these tests was to examine qualitatively the general spray performance of the airblast nozzle configuration. The nozzle and radial-inflow swirler assembly were mounted in a test fixture connected to an air supply as described in Appendix I. Initial tests were conducted for two different nozzles. However, no difference in performance was observed. Consequently the bulk of the tests were performed for one nozzle (A2.1). Each test consisted of varying the air and water flow rate for a given configuration. A high-intensity light source provided the necessary illumination for observation of the spray; photographic records of the spray patterns obtained were made for a number of selected tests. The effects on atomization quality of nozzle air pressure-drop and air/fuel ratio, swirler setting, and axial position of the nozzle were examined in this series of tests.

As for most of the cold-flow tests, the spray visualization results obtained are primarily qualitative consisting of observations of the spray cone angle, mean droplet size, and spray distribution. As would be expected, the variable having the major effect on spray performance was the air pressure drop. The effect of pressure drop is illustrated in Figure 14 which contains photographs of the spray obtained for three different pressure drops. At low values of ΔP, the spray is not well-developed and consists principally of individual streams of large droplets. As ΔP is increased, the mean droplet size decreases rapidly and the spray becomes more uniform. In all cases, the observed spray cone angle was approximately equal to the design value of 90 degrees. The effect of nozzle air/fuel ratio on atomization quality was similar to that of pressure drop. Increasing the nozzle air/fuel ratio decreased the mean droplet size and improved the uniformity of the spray. Increasing the amount of air flow through the radial-inflow swirler by opening the swirler setting (ℓ_{SW}) had a similar but less noticeable effect on the spray.

A number of tests were conducted to examine the effects of the relative axial position of the nozzle. In the design position, the exit of the nozzle coincides with the inlet of the swirler air to the primary zone of the combustor as shown in Figure 6. The results of moving the nozzle axially approximately 0.1 inch in either the upstream or the downstream direction are shown in Figure 15. As can be seen, moving the nozzle in a downstream direction does not appear to have any significant effects on the spray. However, moving the nozzle in the upstream direction results in a marked reduction in spray cone angle. This indicates that in order to achieve the desired spray characteristics, care must be taken to insure that the relative position of the nozzle does not change significantly during operation of the combustor.

In all cases, including those at high values of ΔP, the fuel film leaving the nozzle lip persisted for a significant distance into the combustor as indicated by the photographs in Figures 14 and 15. This results in a high fuel/air ratio and nonuniform distribution in the vicinity of the nozzle exit. Appreciable burning can occur in this region resulting in significant increases in the amounts of NOx produced. This conclusion is borne out by the results of the detailed combustion tests discussed in the next section of this report.

COMBUSTION TESTS

This section of the report describes the detailed combustion tests performed with the final configurations of both combustors. The general approach used in conducting the experimental program is discussed first. This is followed by a presentation of the experimental results obtained from each combustor and observations regarding performance made on the basis of these results; the results for Combustor B are discussed first, since this was chronologically the first of the two combustors tested. Next, a critical analysis of the results is presented, and a series of tests conducted to confirm the conclusions reached on the basis of this analysis is discussed. Finally, the recommended approaches for achieving low emissions developed on the basis of the results of the experimental program are presented. The experimental rigs and instrumentation utilized in conducting the combustion tests and the relations used in reducing the data are described in Appendices I and II.

Over-All Approach

The major objectives of the experimental program were to obtain detailed experimental data which could be used in determining the effects on combustor performance (particularly emissions) of the principal design and operating variables, and to demonstrate the potential effectiveness of the selected design approach in ultimately achieving the Federal 1975/76 emission goals. This involved testing variations of the final configurations of both combustors over wide ranges of flow conditions representative of the anticipated operating conditions of the two gas turbine cycles on the basis of which the combustors were designed. As mentioned previously, the major factors with regard to NOx emissions are the combustor inlet temperature, primary-zone residence time, mean primary-zone equivalence ratio, and degree of mixing. The principal variables with regard to these parameters are the combustor size (diameter and length), air flow inlet conditions ($\dot{m}_a$, T_{03}, and P_{03}), fuel flow rate, variable-geometry setting (ℓ_{sw} and ℓ_{sy}), and the fuel nozzle. The combustor diameter and length have a major effect on residence time.

However, in the program described in this report, variations in diameter or length were not investigated for either of the two combustors. The combustor air flow rate primarily affects residence time and liner pressure drop. The inlet pressure and temperature affect not only residence time and pressure drop, but also the kinetics and chemical equilibrium of the combustion reactions occurring in the combustor. The major effect of fuel flow rate is to govern the mean primary-zone equivalence ratio for a given configuration and set of inlet conditions. The variable-geometry setting affects the degree of mixing by altering the pressure-loss characteristics of the combustor and the mean primary-zone equivalence ratio and residence time by controlling the amount of air flow into the primary zone. The characteristics of the fuel nozzle utilized affect primarily the degree of mixing achieved in the primary zone by virtue of their effects on the preparation of the fuel/air mixture entering the combustor.

On the basis of the considerations discussed above, the general approach selected for conducting the combustion tests consisted of measuring performance for independent variations in each of the inlet flow conditions ($\dot{m}_a$, T_{03}, and P_{03}), the primary-zone equivalence ratio, and the combustor configuration (variable-geometry setting and fuel nozzle). The general procedure employed was as follows. With the combustor inlet conditions, the variable-geometry setting, and fuel nozzle fixed, the combustor performance was measured at a number of different fuel flow rates starting from the minimum value capable of sustaining combustion. This was repeated at a number of different sets of inlet conditions covering the desired testing range for a number of different variable-geometry settings and fuel nozzles. Each test consisted of taking complete performance measurements of a given combustor geometry and fuel nozzle for single values of fuel flow rate, air flow rate, and combustor inlet temperature and pressure. The variables measured in each test included air and fuel inlet conditions and flow rate, combustor pressure drop, exhaust gas temperature distribution, and exhaust gas concentrations of CO_2, CO, HC, NO, and NOx. Detailed measurements of the exhaust gas temperature distributions were made only at the highest value of fuel flow rate tested for each run (defined as a single set of inlet conditions); in all other cases, a four-point measurement was made. Smoke emissions were measured for a selected number of tests and found to be negligible as expected with the selected design approach. Therefore, further detailed smoke measurements did not seem to be warranted. The liner surface temperature was measured using thermal paints; the liner was examined at the conclusion of each series of runs for a given combination of variable-geometry setting and fuel nozzle. The test results obtained are discussed separately below for each of the two combustors.

Discussion of Test Results for Combustor B

Description of Tests

A total of thirty-six runs consisting of approximately 175 detailed tests were conducted with Combustor B. These tests covered the following nominal ranges of flow conditions:

Pressure level	53 - 88 psia
Inlet temperature	510 - 900 deg F
Air flow rate	0.30 - 0.84 lbm per sec
Over-all air/fuel ratio	56 - 212

Additional tests at higher pressures were planned originally, but were eliminated per direction of EPA. The tests were performed for two different variable-geometry settings ("closed", corresponding to what would be approximately an idle setting, and "full open", corresponding to a 100 per cent power setting) and two fuel nozzles (B1.1 and B2.1 differing in nozzle air/fuel ratio). The approach adopted in selecting the combinations of flow conditions was to test at a number of different constant values of the standard combustion efficiency parameter (θ). The nominal test conditions examined in each run are listed in Table VIII; the results obtained in each test are given in Tables IX-XIII.

Emission Performance

The pertinent results are summarized in Figures 16 and 17 which show plots of emissions (NOx, CO, and HC) and combustion efficiency versus over-all air/fuel ratio. As can be seen, the NOx emissions are higher than the goal in all cases, ranging from a maximum emission index of about 12 mg per gm fuel to a minimum of about 3 mg per gm fuel. At the same time, the carbon monoxide and hydrocarbon emissions are relatively low, most of the data falling below the goals. The combustion efficiency is correspondingly high-- very close to 100 per cent for most conditions. The data presented in the figures illustrates the effect of variable-geometry setting on emissions. As the swirler and secondary holes are opened allowing more air into the primary zone, NOx emissions decrease somewhat and CO and HC emissions increase. This effect is most noticeable with regard to CO, as seen in Figure 16.

The general trends of the data are as would be expected, NOx emissions increasing as the residence time and inlet temperature and pressure are increased and decreasing as the combustor pressure drop and over-all air/fuel ratio are increased; basically, variations in these quantities have an opposite effect on CO and HC emissions. The major variations in emissions of CO and HC are observed near the weak extinction limit where the emissions of these species rise sharply with increasing air/fuel ratio. The general effect of residence time is shown in Figure 18. As can be seen, varying the residence time while maintaining the pressure drop constant has a somewhat less than linear effect on NOx emissions, but a strong effect on CO emissions. Although part of the difference in CO levels shown in Figure 18 can be attributable to the differences in inlet temperature, it would seem apparent that the major factor is residence time. The typical effects of variations in the other parameters on NOx emissions are illustrated in Figure 19; the variations of CO emissions with these parameters are difficult to determine from the data obtained with Combustor B due to the observed, strong effect of residence time. The combined effect of pressure drop and residence time on NOx emissions at approximately constant inlet temperature and pressure can be seen by comparing the results for Run 23 with the base curve (Run 30). As can be seen, decreasing the air flow rate so as to decrease the pressure drop and increase the residence time produces an increase in NOx emissions. Although it is difficult to separate the effects of residence time and pressure drop, it would appear from the data that these two factors have about the same order-of-magnitude effect on NOx emissions. The curve for the higher temperature (Run 26 on Fig 19) exhibits a higher NOx level than the base curve, illustrating that NOx emissions increase with inlet temperature. The curve for the higher pressure (Run 27) also shows a higher NOx level than the base curve. Part of the observed increase in NOx emissions for the higher pressure can be attributed to the fact that the values of inlet temperature and residence time were also somewhat higher than for the base curve. However, taking into account the effects of inlet temperature and residence time, it would appear that the net effect of increasing inlet pressure is to increase NOx emissions. The data obtained for Combustor A discussed subsequently exhibit the effects of inlet temperature and pressure more clearly.

An additional parameter investigated was the relative amount of air flow surrounding the fuel as it is injected into the primary zone. Increasing this quantity by increasing the relative amount of air flow through the nozzle and/or swirler would be expected to reduce NOx emissions by shielding the fuel sheet from the flame and reducing the amount of fuel burned at high values of equivalence ratio. This parameter was examined by testing two nozzles having different air/fuel ratios. The effects of nozzle air/fuel ratio are illustrated in Figure 20 which contains plots of NOx and CO emissions for the two nozzles at comparable flow conditions. The results show that increasing the nozzle air flow produces an increase in CO emissions. The effect on NOx is not very noticeable; however, it would appear that a slight decrease in NOx emissions was obtained. Since relatively small variations in the amount of nozzle air flow were investigated, the observed magnitude of this effect is not very large.

A series of tests was conducted to examine further the effects of pressure drop on emissions. For this purpose, Combustor B was modified so as to increase the pressure drop for a given set of inlet conditions. The modification consisted of blocking off one-third of the metering holes for each of the film-cooling slots in the primary and intermediate zones and decreasing the diameter of the dilution holes to 0.25 inches. The effects of this modification were to increase the pressure drop by a factor of about two and increase the total primary-zone flow rate (decrease the primary-zone residence time) as calculated from the cold flow data by a factor of about 1.3. The modified configuration was then tested at the same conditions previously examined with the original configuration. The results obtained with the modified configuration are given in Table XIII; the results obtained with the original configuration at the same conditions are those listed in Table XI. The NOx and CO emissions obtained with the original and modified configurations of Combustor B are presented for comparison in Figure 21. As shown previously (Fig 18), residence time has a somewhat less than linear effect on NOx emissions. Therefore, the results given in Figure 21 would seem to indicate that the significant reduction in NOx emissions observed is primarily due to the effect of increasing the pressure drop. The apparent strong effect of pressure drop is not confirmed, however, by the data obtained in other tests. A possible explanation for these results lies in the effect of the modification on the discharge coefficient of the secondary holes. The primary-zone flow for the modified configuration was calculated assuming this discharge coefficient remained constant. In the modified configuration, the amount of dilution flow was significantly reduced, thereby decreasing the annulus air flow at the secondary holes and increasing the local value of $\Delta P/q_{annulus}$. In general, the discharge coefficient for a row of holes increases with $\Delta P/q$ at the point of injection. It would seem then that the actual value of secondary flow and the relative proportion recirculating back into the primary zone were higher than those calculated assuming a constant discharge coefficient. Consequently, the data for the modified configuration were obtained at significantly lower values of ϕ_p than assumed which would account for the discrepancy with regard to the effect of pressure drop.

Other Performance Parameters

Although the emission performance of the combustor is of primary concern, the values of the other more conventional combustor performance parameters must also be acceptable in terms of their effect on over-all engine performance, This is necessary in order to insure that the emission goals are met with a practical combustor configuration which could be utilized directly in an automotive gas-turbine engine. In this regard, the major performance parameters are combustion efficiency, stability limits, pressure loss, exit temperature traverse quality, and combustor wall temperature. In general, the experimentally determined values of these quantities show that the design goals set at the outset of the program have been achieved.

As indicated previously (Fig 17), the combustion efficiency was acceptably high at virtually all conditions investigated. The stability performance of Combustor B is shown in Figure 22, which consists of a plot of the blow-out values of primary-zone equivalence ratio versus combustor loading defined as the inverse of the combustion-efficiency parameter, θ . Also indicated on the figure is the variation in combustor loading over the operating range of the cycle. The relatively large amount of scatter in the data is primarily due to the inherent difficulty in obtaining an accurate determination of blow-out conditions. In the design of the combustor, one of the requirements was that it be capable of operating stably at a mean primary-zone equivalence ratio of 0.65 over the desired range of operating conditions. As can be seen, this requirement was met.

Combustor B was designed to give a 3 per cent pressure drop at full-power conditions. The actual value of pressure drop achieved, of course, depends on the variable-geometry setting. At the "full open" setting corresponding to what would be typical of the setting for design-point operation, the measured values show that the pressure drop which would be obtained at the design-point flow conditions would be around 2.7 per cent, approximately 90 per cent of the design value. The dilution zone of the combustor was designed to provide an exit temperature traverse quality of 0.2. The data given in Tables IX-XIII show that the experimentally determined traverse quality ranged between 0.10-0.26 with most values falling below the design goal. Therefore, the dilution performance achieved was quite satisfactory. The design objective with regard to cooling performance was to maintain the combustor surface temperature below 1700 degrees F. The liner temperature was measured using thermal paints. Inspection of the liner showed that a maximum metal temperature of about 1900 degrees F was reached in the dilution zone; in the primary and intermediate zones the maximum metal temperature observed was on the order of 1700 degrees F, the design goal. Examination of the test results shows that an appreciable number of tests were conducted at primary-zone equivalence ratios close to or greater than 1. In these tests, the gas temperature in the dilution zone would be expected to be significantly higher than would be encountered in normal operation. This would account for the relatively high metal temperatures observed in the dilution zone. In any event, the cooling performance achieved is quite reasonable for an initial design and could be corrected if necessary with a relatively minor expenditure of development effort.

Discussion of Test Results for Combustor A

A total of sixteen runs consisting of approximately 110 detailed tests of Combustor A were conducted. These tests covered the following nominal ranges of flow conditions:

Pressure level	24 - 88 psia
Inlet temperature	700 - 1200 deg F
Air flow rate	0.32 - 1.39 lbm per sec
Over-all air/fuel ratio	60 - 480

The tests were performed for two different variable-geometry settings ("closed", corresponding to what would be an approximately idle setting, and "part open", corresponding to approximately a 50 per cent power setting) and one fuel nozzle (A2.1). It had been planned to conduct additional tests at a "full-open" setting. However, the initial results indicated that this would not add significantly to the understanding of the emission problem. Instead, then, a number of tests were conducted with various modifications of the original combustor configuration which proved quite fruitful as described subsequently in this section of the report. The results obtained with Combustor B showed that emissions varied more significantly with combustor pressure loss and residence time than with the standard combustion-efficiency parameter originally selected as the major correlating parameter. Therefore, the approach adopted in selecting the combinations of flow conditions for Combustor A was to test at a number of different approximately constant values of absolute pressure loss and residence time. The nominal test conditions examined in each run are listed in Table XIV, the results obtained in each test are given in Tables XV and XVI.

Emission Performance

The pertinent results are summarized in Figures 23 and 24 which show plots of emissions (NOx, CO, and HC) and combustion efficiency versus over-all air/fuel ratio. The level of NOx emissions for Combustor A is significantly higher than that obtained for Combustor B primarily due to the higher temperatures at which the tests were conducted. As can be seen, the NOx emissions are higher than the goal in all cases, ranging from a maximum emission index of about 25 mg per gm fuel to a minimum of around 5 mg per gm fuel. The carbon monoxide and hydrocarbon emissions are significantly lower than those obtained with Combustor B, almost all of the points falling well below the goals. The combustion efficiency is essentially 100 per cent at virtually all conditions investigated.

The general trends of the data are again as would be predicted; increasing residence time, temperature, and pressure and decreasing pressure drop and over-all air/fuel ratio produce increases in NOx emissions and have the opposite effect on CO and HC emissions. The effect of residence time on NOx emissions is essentially the same as observed for Combustor B; that is, the variation with residence time is somewhat less than linear. The typical effects of inlet temperature and pressure and combustor pressure drop on NOx emissions for Combustor A are illustrated by the curves shown in Figure 25. Although increasing pressure or temperature increases the over-all level of NOx emissions, it also widens the stability margin considerably allowing operation at much higher values of air/fuel ratio (lower values of ϕ_p). Consequently, the minimum value of NOx achievable using variable geometry to control the primary-zone equivalence ratio is relatively independent of pressure or temperature. As the pressure drop is increased, the mixing in the combustor improves resulting in a more uniform fuel/air distribution. Although it is difficult to isolate the effect of residence time, some indication of the effect of improved mixing can be obtained by comparing the curves for Runs 61 and 60 shown in Figure 25. As can be seen, improving the mixing tends to produce a steeper slope of NOx versus air/fuel ratio. As a result, achieving a more uniform distribution tends to produce an increase in NOx at low values of air/fuel ratio and a decrease at higher values.

Other Performance Parameters

As in the case of Combustor B, the major performance parameters of concern other than emissions are combustion efficiency, stability limits, pressure loss, exit temperature traverse quality, and combustor wall temperature. In general, the experimentally measured values of these parameters either matched or surpassed the selected design goals.

A combustion efficiency of essentially 100 per cent was observed in all cases. The stability performance of Combustor A is shown by the plot of blow-out values of primary-zone equivalence ratio versus combustor loading given in Figure 26. The design goal in terms of stability was that the combustor be capable of operation at a mean primary-zone equivalence ratio of 0.5 over the range in loading parameter indicated in Figure 26. As can be seen, this requirement was satisfied by the final combustor configuration.

In terms of pressure-loss characteristics, the design goal for the combustor was a 3 per cent pressure drop at full-power conditions. Although the combustor was not tested at a variable-geometry setting corresponding to the design point, the data obtained at the "closed" (idle) and "part open" (50 per cent power) settings can be extrapolated to determine the value of ΔP which would be achieved at the design point. The data obtained show that the pressure drop at full-power conditions would be quite close to the design goal.

The results given in Tables XV and XVI show that the measured values of exit traverse quality ranged between 0.06 and 0.26. Most of these values fall well below the design goal of 0.2 indicating that the dilution zone performance was quite satisfactory and that more than enough dilution air was available for achieving the desired exit temperature profile. Thermal-paint measurements indicated that the liner temperature was approximately 200 degrees F higher than the design goal of 1700 degrees F in the primary zone and about equal to the design goal in the intermediate zone. The liner temperature in the dilution zone was significantly lower, on the order of 1500-1600 degrees F. This trend is not surprising in view of the somewhat more conservative cooling approach used in the dilution zone (see Fig 9). The relatively high values of liner temperature observed in the primary zone are most likely due to the fact that a significant number of tests were conducted at primary-zone equivalence ratios near stoichiometric resulting in higher flame temperatures than would normally be encountered. In any case, this situation could be alleviated easily if necessary by using some of the excess dilution air available to increase the amount of film cooling in the primary and intermediate zones.

Analysis of Results

The experimental results clearly show that the singularly unsatisfactory feature of the existing combustor configurations is their excessive NOx emission-- other combustor performance parameters, including other emissions, can be considered satisfactory and in fact the variable-geometry concept can also be judged successful from the standpoint that all emissions can be made relatively independent of power level. Thus, the primary questions to be resolved in the critical analysis of the data concerned the source of the present NOx emissions, and the elimination of this source.

Potential Causes of High NOx Emissions

Fundamentally, there are four possible causes of excessive NO formation in these combustors (see Fig 27).

1. Insufficient Primary Zone Air Flow - If the air flow which participates in the primary-zone combustion process (primarily $\dot{m}_{FN}$, $\dot{m}_{SW}$, and $\dot{m}_{sy,p}$) is inadequate, the mean primary-zone equivalence ratio will be too high to suppress NO formation.
2. Excessive Residence Time - If in conjunction with a fuel/air ratio distribution which produces an appreciable fraction of the primary-zone mixture with an equivalence

ratio in excess of approximately 0.7, the residence time in the primary zone is too long, substantial quantities of NO will be formed. This residence time can be characterized by the transit time of a mixture element along the streamline S-SY in Figure 27.

3. Improper Fuel Atomization - Inadequate atomization, alone, could reduce NO production in the primary zone due to decreased fuel vaporization and hence leaner mixtures. If, however, inadequate atomization is accompanied by a decrease in effective cone angle of the fuel spray such that fuel is injected directly into the recirculation zone, the resulting higher equivalence ratios will result in greater NO production.
4. Inadequate Fuel/Air Mixing - If the fuel is inadequately mixed with the primary-zone air, then local regions in the primary zone will be at relatively high equivalence ratios, and substantial NO will be produced. In the present combustors, the quality of mixing is best displayed by the fuel/air ratio profile across the section A-A in Figure 27. As shown in Figure 28, a poorly mixed profile can provide a substantial maximum in local fuel/air ratio.

The experimental data obtained, in conjunction with an analytical examination of the NOx emissions from the combustors, permit some conclusions with respect to the relative importance of these possible sources.

Experimental Observations

Considering the four possible causes in order, the experimental data obtained permit the following interpretations:

1. Insufficient Primary-Zone Air Flow - The behavior of the NOx emissions as a function of over-all air/fuel ratio (Z) indicates that this is not a major cause of excessive NO formation for these combustors. For example, for the data point shown in Figure 23 for Combustor A at an over-all

air/fuel ratio of 479, the most pessimistic (that is, lowest) estimate of primary-zone air flow would yield a mean primary-zone equivalence ratio of 0.3; given a reasonable distribution of fuel/air ratio in the primary zone, virtually no NO should be produced.

2. Excessive Residence Time - Although the experimental data do indicate the expected effect of increasing NO production with increasing residence time, the effect does not appear to be very substantial (see Fig 18). Further, referring again to the Ƶ = 479 point in Figure 23, given a reasonable fuel/air distribution, virtually no NO should be produced regardless of residence time. It is also clear that to satisfy the NOx emission objectives, a reduction of as much as a factor of ten is required; this obviously could not be accomplished by merely reducing the primary-zone residence time.
3. Improper Fuel Atomization - As mentioned previously, poor fuel atomization, alone, would not seem to account for excessive NO production. However, poor fuel atomization in conjunction with a smaller effective cone angle is a likely cause; unfortunately, there is no direct experimental evidence which sheds light on the importance of the cause. Characteristics of airblast atomizers are such that the effective cone angle is relatively constant, and the spray visualization tests described previously indicate that the cone angle is satisfactory except at very low pressure differentials across the nozzle. The fact that Combustor A sustains combustion at very high values of over-all air/fuel ratio is however an indication of a possible reduction in effective spray angle.
4. Inadequate Fuel/Air Mixing - From the preceding discussion, it can be inferred that the fuel/air mixture in the primary zone is highly nonuniform-- this is virtually the only possible explanation. Unfortunately, there is again little

direct experimental evidence that this is the case. For example, it would be expected that the pressure loss at which the combustors were operated would have an appreciable influence on NOx emission; although the experimental data exhibit some influence of pressure drop, there is no clear trend in this regard. The absence of such a trend does indicate, however, that if inadequate mixing is a problem, it most likely occurs in the immediate vicinity of the nozzle. This view is also supported by both the basic characteristics of the airblast nozzle, which relies on the swirler and fuel nozzle air to distribute the fuel, and the fact that in the present combustors the ratio of the fuel flow to the sum of nozzle and swirler air is well above the stoichiometric value. Additional confirmation of this view is provided by the results of the spray analysis tests described in Appendix III which show that a relatively nonuniform fuel/air distribution is obtained from the nozzle.

Thus, on the basis of the experimental data obtained, it can be concluded that the excessive NOx levels are due to either inadequate fuel/air mixing in the vicinity of the nozzle or possibly due to an insufficient fuel spray angle.

Results of Analytical Modelling

In order to clarify further the possible sources of NOx emissions in the two combustors, the analytical model previously developed by NREC (Refs 1 and 2) for predicting NOx emissions from gas-turbine combustors was used to obtain analytical estimates of NO production in the two combustors. As described earlier in this report, the model is based on the concept of a primary zone which behaves as a partially stirred reactor, in which combustion occurs over a specified Gaussian distribution of fuel/air ratios. The parameter governing the fuel/air ratio distribution is the mixedness parameter, S_o , which defines the distribution of fuel/air ratios about the mean fuel/air ratio in the primary zone. The larger the parameter S_0, the poorer is the mixing in the primary zone.

The analytical results for Combustor B, for two values of the mixedness parameter, are compared with the experimental data in Figure 29. On the basis of the slope of the analytical results as compared to the data, it can be concluded that the empirical value of S_0 for Combustor B is somewhat greater than unity. This represents a poorly mixed primary zone (values of S_0 for typical aircraft combustors have been found to be in the range of 0.3 to 0.7). To appreciate further the significance of the value of S_0, the results obtained from the analytical model can be approximately related to the percentage of the mixture in the primary zone which burns at equivalence ratios greater than 0.8. Although previous experience with the analytical model has indicated that it somewhat underpredicts NO formation at lower inlet temperatures (a fact also indicated by the discrepancy between predicted and measured results here), it nevertheless seems certain from the combination of analytical and experimental data that a substantial fraction of the injected fuel is burning at equivalence ratios greater than 0.8.

Similar results are presented for Combustor A in Figure 30. Here a value of S_0 slightly less than unity is indicated, and it can be deduced from the results of the model that approximately 30 per cent of the injected fuel burns at equivalence ratios greater than 0.8 for all air/fuel ratios.

Although the analytical model is undoubtedly subject to some uncertainty, the nature of the results clearly indicates that in the two combustors a substantial fraction of the injected fuel burns at equivalence ratios greater than 0.8, even though the mean primary-zone equivalence ratio may be less than 0.4.

Major Conclusions

The preponderance of the evidence indicates that the source of excessive NOx emissions in the present combustors is inadequate fuel/air mixing in the primary zone. This in turn is due both to inadequate distribution of the fuel spray in the swirler and nozzle air streams, and to an inadequate proportion of air to the nozzle and swirler relative to the flow through the secondary holes.

Experimental Verification of Analysis

Description of Tests

A number of tests were conducted with modifications of the original Combustor A configuration in order to confirm the conclusions discussed above regarding the source of the high NOx emissions. The previous experimental and analytical results indicated that the amount of air flow in the vicinity of the fuel spray must be increased and the mixing of the fuel with the air prior to burning must be improved to achieve the required reductions in emissions. The simplest method of accomplishing this effect without excessive alterations to the original configuration was to increase the amount of air flow and pressure drop through the nozzle and the swirler. This was done by placing a perforated plate with an open area of about 1.9 square inches across the combustor flow annulus to redistribute the flow and pressure drop as desired. Essentially two modifications as shown schematically in Figure 31 were investigated:

1. Placing the perforated plate at an axial position just downstream of the nozzle inlet to increase the amount of air flow and pressure drop through the nozzle only (Fig 31a).
2. Placing the plate at an axial position just downstream of the swirler inlet to increase the air flow and pressure drop through both the nozzle and swirler (Fig 31b).

In addition, the diameter of the dilution holes was reduced to 0.625 inches. Nevertheless the pressure drop across the portion of the combustor downstream of the plate was nominally the same as would be obtained with the original configuration.

A total of 15 runs consisting of approximately 80 tests were performed. All of the tests were conducted with the piloted version of the Combustor A nozzle (A2.2), with a fixed setting of the secondary-flow control sleeve (about half open), and at a nominal inlet temperature of 900 degrees F. The tests were performed with a number of values of air flow rate at each of two different pressure levels. An additional parameter investigated was the relative proportion of fuel flow through the pilot and main airblast portion of the nozzle. The nominal test conditions examined in each run are listed in Table XVII; the calculated values of nozzle, swirler, and primary-zone air flow for the variable-geometry settings examined are given in Table XVIII for each of the two modifications. The results obtained in each test are given in Tables XIX-XXI.

Discussion of Results

The pertinent results obtained in these tests are presented in Figure 32 which shows NOx and CO emissions plotted versus over-all air/fuel ratio for the two pressure levels investigated. Also included in the figure are the results obtained previously with the original Combustor A at comparable flow conditions. As can be seen, the NOx emissions have been reduced quite dramatically by a factor ranging between 4 and 8. The minimum value of NOx emission index achieved with the modified configuration falls close to or below the goal for both pressure levels investigated. The CO emissions have also been reduced somewhat over a major portion of the range of conditions examined. However, with the modified configuration lean blowout occurs at lower values of air/fuel ratio, thus reducing the stability limits.

Several important observations can be made on the basis of a detailed examination of the test results obtained with the modified configuration. In all cases, increasing the amount of air flow in the vicinity of the fuel spray led to significant reductions in NOx emissions without seriously compromising CO emissions. The effect of increasing the nozzle air flow is to reduce the local fuel/air ratio (see Fig 28) near the flame thus decreasing the relative proportion of fuel burned at high equivalence ratios. Increasing the air flow and pressure drop through the swirler increases the relative velocity and shear between the counterrotating swirler and nozzle streams thus improving the local mixing achievable for a given pressure loss. This effect is indicated by the results obtained for an increased swirler flow (Table XXI) where approximately the same emission level was achieved at a significantly lower pressure loss.

Although increasing the air flow and pressure drop through the nozzle/swirler assembly reduced emissions, increasing the pressure drop and decreasing the residence time by increasing the total air flow rate did not seem to have any significant effect on emissions. This is shown by the results plotted in Figure 33 for two different values of total air flow rate. As can be seen, increasing the pressure drop by about 50 per cent and decreasing the residence time by approximately 25 per cent had no discernible effect on the emissions. This indicates that the amount of mixing which can be achieved by purely aerodynamic means (that is, increasing pressure loss for a given configuration by increasing air flow rate with a corresponding increase in fuel flow rate) is limited. These results also support the conclusion previously reached that reducing residence time is not a practical method of controlling NOx emissions.

The NOx emission curves for the modified configuration shown in Figure 32 exhibit a reduction in slope at the high values of air/fuel ratio. For the tests conducted at these values of air/fuel ratio a major portion or all of the fuel was injected through the pilot in order to maintain stable combustion; in addition, the total fuel flow was comparatively low. A characteristic of the pilot, which is a pressure atomizer, is that the spray cone angle decreases as the fuel flow is reduced leading to a local increase in the equivalence ratio in the vicinity of the nozzle. This effect of a deterioration in the uniformity of the fuel/air distribution would explain the observed behavior of the curves.

The relative effects of the main airblast and pilot portions of the nozzle are illustrated by the results presented in Figure 34 which shows the NOx emissions obtained for three different types of fuel injection: main airblast operating alone, pilot operating alone, and the main operating in conjunction with the pilot. In the latter case, the fuel-flow rate through the pilot was maintained constant at approximately 12 lbm per hour. At a given value of air/fuel ratio, the NOx emissions achieved with the main airblast portion of the nozzle are considerably lower than with the pilot; however, flame blow-out occurred at relatively low values of over-all air/fuel ratio ($\mathbf{Z}$). As can be seen, introducing a small amount of fuel through the pilot has the desired effect of extending the range of air/fuel ratio over which stable combustion can be maintained. At low values of Z where the ratio of pilot to main fuel flow is relatively small, the NOx emissions achieved with the main/pilot combination are approximately the same as with the airblast portion alone. The emission performance of the combination approaches that of the pilot at higher values of Z where proportionately more fuel flows through the pilot. It would seem apparent from these results that there is some optimum combination of main and pilot fuel flow rates which would extend the operating range of the nozzle and achieve an improvement in NOx emissions.

All of the experimental evidence obtained in these tests showed that improving the uniformity of the primary-zone fuel/air distribution by increasing the mixing and eliminating insofar as possible local fuel-rich regions produced the desired effect on emissions. In summary, the test results confirm the conclusions previously reached regarding the most effective means of achieving the necessary reductions in emissions.

Recommended Approaches for Achieving Low Emissions

Although not all of the emission goals were achieved in the present program, the results obtained were sufficiently promising to demonstrate that the concept originally selected has the ultimate potential of producing reduced emission levels which will meet the Federal 1975/76 emission goals. Initial considerations of the problem of NOx control had suggested that novel concepts representing radical departures from conventional design practice would be required. However, on the basis of the test results and a critical analysis of the data, it is now felt that the emission goals can be achieved with modifications of essentially conventional combustor configurations. Therefore, the general guidelines for controlling emissions presented here are discussed in terms of this type of approach.

Control of Primary-Zone Equivalence Ratio

By far the most important factor with regard to NOx emissions has been shown to be the mean value of primary-zone equivalence ratio and the distribution about this mean value. In order to achieve the specified NOx emission level, most of the fuel injected into the primary zone must burn at a uniformly lean value of equivalence ratio. In fact it would appear that the primary zone of the combustor must operate at equivalence ratios very near the weak extinction limit over the full range of cycle conditions. There is little doubt that in order to accomplish this the operating conditions in the primary zone of the combustor must be capable of being controlled independently of the cycle conditions. The approach investigated in this program of using variable geometry has been shown to be an effective means of providing the necessary additional degree of freedom. An alternative to variable geometry would be some form of staged injection. However, since this concept was not examined, no conclusions regarding its applicability can be made.

The test results also showed that increasing the combustor inlet temperature and pressure has a major effect on increasing NOx emissions for a given primary-zone equivalence ratio. However, the minimum achievable values of NOx emissions appeared to be relatively insensitive to the inlet pressure and temperature due to the fact that increasing P_{03} and T_{03} allows operation at considerably lower values of primary-zone equivalence ratio. In fact, there is some evidence to indicate that these parameters have a greater effect on flame stability than on emissions. Therefore, the emissions can be made virtually independent of combustor inlet conditions by using variable geometry to control the primary-zone equivalence ratio as required by the operating conditions of the specific cycle being considered.

In choosing the variable-geometry method to be used for any particular configuration, it should be noted that simply controlling the mean value of primary-zone equivalence ratio is not sufficient to achieve the necessary reductions in emissions. It has been found that it is most important to control the air flow in the immediate vicinity of the fuel as it is introduced into the combustor. Therefore, the variable-geometry approach utilized should be coordinated with the selected method of fuel injection to insure that its primary function is accomplished effectively.

Reduction of CO and HC Emissions

The necessity of burning at a lean primary-zone equivalence ratio aggravates the problem of achieving low levels of CO and HC emissions (that is, high combustion efficiency). The results have shown that residence time has a significantly greater effect on the emissions of these species than on the emissions of NOx. The approach for controlling CO and HC adopted in the design of the two combustors was based on this effect and consisted of oversizing the combustor diameter so as to increase the residence time. This approach appears to have been successful in that low emissions of these species were achieved. It would seem worthwhile to augment the specific approach utilized by lengthening the intermediate zone (moving the dilution holes further downstream).

Mixing

As mentioned above, it is necessary to achieve a uniform fuel/air distribution in the primary zone in order to reduce NOx emissions to the specified level. This requires that most of the fuel be mixed sufficiently well with the primary-zone air participating in the combustion process prior to combustion. The results of the program show that simply increasing the pressure drop to achieve the desired degree of mixing by purely aerodynamic means is not an efficient or practical approach. Excessively high values of pressure drop would be required which would represent an unacceptable penalty on cycle performance. The selected approach which consisted of oversizing the combustor diameter to achieve a relatively high pressure-loss factor at reasonable values of pressure drop did appear to provide an adequate over-all degree of mixing as determined by the results of flow visualization tests conducted. However, it seems apparent that improving the over-all level of mixing in the primary zone is insufficient unless care is also taken to eliminate localized regions of high fuel/air ratio such as exist at the point of fuel injection. The ultimate solution to the problem of achieving an acceptably uniform fuel/air mixture lies in the method of introducing the fuel into the combustor.

Fuel Injection System

One of the major conclusions reached on the basis of the test results is that the fuel injection system is the critical factor in determining the uniformity of the fuel/air distribution which can be achieved for a given configuration. An ideal solution to the problem of attaining a uniform distribution remains pre-mixing the fuel with a sufficient quantity of air prior to entering the combustor. This pre-mixing can be accomplished in a variety of ways; for example, injecting the fuel at multiple points, using a mixing chamber of sufficient length to achieve the desired degree of uniformity, mechanically distributing the fuel over the flow cross-section of the airstream, or combinations of these approaches. An alternative to pre-mixing is to use the more conventional approach adopted in the program of preparing and introducing the fuel in such a form that it will mix with sufficient air within the primary zone prior to undergoing combustion. In doing so, test results have demonstrated clearly the necessity of eliminating extensive regions of high fuel concentration. However, it has also been found that a small proportion of the fuel must be introduced at relatively high values of equivalence ratio in order to maintain stable combustion at the lean primary-zone conditions needed to achieve low NOx emissions. This then requires some form of piloting in which a part of the fuel is injected directly into the recirculation zone. Unfortunately, the information available is insufficient to establish the proportion of main/pilot fuel flow required to achieve the optimum compromise between emission performance and combustion stability.

All of the results obtained indicate, at least reasonably conclusively, that the NOx emissions from the existing combustor can be substantially reduced by improving the fuel/air mixing in the primary zone in the immediate vicinity of the exit of the fuel nozzle. The only effective way to accomplish this is to modify or replace the existing fuel injector in an appropriate manner. It is felt that the implementation of this recommendation will demonstrate the full emission reduction potential of the variable-geometry concept and will show that the emission goals can be satisfied with the existing combustors.

CONCLUSIONS AND RECOMMENDATIONS

Conclusions

A design approach for achieving low emissions in gas turbine combustors has been selected and applied in the design of two combustors for automotive gas turbine applications. Basically, the approach utilized has consisted of designing both combustors to operate with a lean, well-mixed primary zone over the full operating range. The relevant features of the approach included the use of variable geometry for controlling the air flow distributions in the combustors so as to maintain efficient and stable combustion at all operating conditions, a relatively large combustor diameter to achieve a high combustion efficiency and to promote aerodynamic mixing, and an airblast fuel nozzle to improve the uniformity of the fuel/air distribution in the primary zone. An experimental program involving both cold-flow and combustion tests has been conducted to determine the detailed performance of the final configurations of both combustors. The principal conclusions reached on the basis of a critical analysis of the program results are given below:

1. The aerodynamic performance of both combustors as determined from the results of the cold-flow tests was satisfactory. The flow patterns observed in the flow visualization tests showed good penetration of the secondary and dilution jets and a vigorous over-all level of mixing in the primary zone at all conditions. The ambient air tests indicated that the flow distributions achieved were essentially as desired and that the variable-geometry approach utilized was capable of providing sufficient control of the effective primary-zone air flow rate.
2. Qualitative spray tests of the airblast nozzles consisting of visual observations of the spray indicated that the spray cone angle obtained with this type of nozzle does not depend significantly on flow conditions. However, the cone angle is quite sensitive to the axial position of the nozzle with respect to the inlet of the primary zone. For all flow conditions examined, the fuel film

leaving the nozzle persisted a significant distance into the primary zone resulting in a localized region of relatively high fuel concentration near the nozzle lip. The results of quantitative spray analysis tests (see Appendix III) confirm that the fuel/air distribution provided by the nozzle is relatively nonuniform.

3. In general, the over-all levels of NOx emissions for both combustors were significantly higher than the specified goal. The emissions of CO and HC were generally below the specified goals except at conditions very near the weak extinction limit where the emissions of these species rose sharply with increasing air/fuel ratio. The measured values of the other major performance parameters (combustion efficiency, stability limits, pressure loss, exit temperature traverse quality, and combustor wall temperature) were quite satisfactory and essentially equal to the selected design goals.
4. The general effects of combustor inlet temperature and pressure on emissions are as would be expected, NOx emissions increasing and CO and HC emissions decreasing as temperature and pressure are increased at a constant value of air/fuel ratio. However, at high values of combustor inlet temperature and pressure, the stability limits are greatly extended allowing operation at significantly lower values of primary-zone equivalence ratio. The use of variable geometry to control the primary-zone equivalence ratio as required has been found to be an effective means of making the emissions relatively independent of combustor inlet conditions.
5. Residence time has a somewhat less than linear effect on NOx emissions but a strong effect on CO and HC emissions. Therefore, reducing residence time does not represent a practical means of reducing NOx emissions to the level required.
6. The most important factors with regard to NOx emissions are the mean primary-zone equivalence ratio and the distribution

about this mean value. An extremely uniform fuel/air distribution is required in order to meet the NOx emission goals. Although a reasonable value of combustor pressure drop is necessary to obtain adequate mixing, the use of an excessively high value of ΔP in itself is not a practical or effective approach to attaining the uniform primary-zone fuel/air distribution required. The solution to the problem of achieving an acceptably uniform fuel/air distribution lies in the design of the fuel injection system. The high values of NOx emissions observed in the two combustors have been demonstrated to be due to inadequate fuel/air mixing in the primary zone. The test results have indicated that this is primarily due to the method of fuel injection used and to an insufficient proportion of the primary-zone air introduced in the vicinity of the fuel spray.

Despite the fact that not all of the emission goals were achieved, the experimental evidence obtained in the program has demonstrated that the variable-geometry concept selected and utilized in the design of the two combustors has the potential of producing the necessary reductions in emission levels. A major conclusion on the basis of the program results then is that the specified emission goals can be achieved with modifications of essentially conventional combustor configurations utilizing the approaches described in this report.

Recommendations

A number of general recommendations regarding design approaches for achieving low emissions were presented in the previous section of this report. These are summarized below:

1. In order to achieve the necessary reductions in NOx emissions, most of the fuel must be burned at low values of equivalence ratio. Variable geometry is the approach recommended for attaining stable and efficient combustion at these conditions over the full operating range of the combustor. The use of

staged injection offers a potentially attractive alternative to variable geometry, and it is recommended that some development effort be devoted to investigating the feasibility of this concept.

2. Since NOx emissions appear to be less sensitive to residence time than CO or HC emissions, designing for a relatively high residence time is suggested as the most practical method of achieving the necessary control of CO and HC emissions.
3. The uniformity of the primary-zone fuel/air distribution is the major factor in controlling NOx emissions. The key to obtaining necessary uniformity in the fuel/air distribution is in the proper design of the method of introducing the fuel into the combustor. In general, the major requirement of the fuel injection system is that the fuel be mixed uniformly with a sufficient amount of air prior to combustion. In doing so, care must be taken to avoid producing localized regions of relatively high fuel concentration. The ideal solution to the problem of achieving a uniform distribution is to pre-mix the fuel and air before entering the combustor. An alternative to pre-mixing is to use essentially conventional injector configurations modified to achieve a more rapid dispersal of the fuel in the primary-zone air prior to combustion.

The program results have indicated that the variable-geometry concept utilized has the ultimate potential of achieving emission levels which will meet the Federal 1975/76 emission goals. Analysis of these results has pointed out specific areas in which further development effort is required in order to obtain the necessary reductions in emissions. With regard to the configurations investigated in the program, the major aspect requiring improvement is the method of fuel injection. It is felt that the replacement or modification of the existing fuel injector to achieve a more uniform fuel/air distribution in the primary zone should result in achieving the emission goals. The ability to meet the emission standards in what is essentially a conventional combustor configuration with a single point of fuel injection and most likely a single variable-geometry element has an obvious advantage. Subsequent designs could rely heavily on the extensive background and experience available on the design technology of conventional combustor configurations. For these reasons, it is strongly recommended that development of the emission-control approach utilized in the design of the two combustors be continued to demonstrate fully the capability of this concept in meeting the emission goals.

REFERENCES

1. Fletcher, R. S. and Heywood, J. B., A Model for Nitric Oxide Emissions from Aircraft Gas Turbine Engines (AIAA Paper No. 71-123), American Institute of Aeronautics and Astronautics, New York, 1971.

2. Fletcher, R. S., Siegel, R. D., and Bastress, E. K., The Control of Oxides of Nitrogen Emissions from Aircraft Gas Turbine Engines, Volume I: Program Description and Results (NREC Report No. 1162-1), Northern Research and Engineering Corporation, Cambridge, Mass., December, 1971.

3. Bastress, E. K., et al, Control of Nitrogen Oxide Emissions from Diesel Engines: A Theoretical Analysis (NREC Report No. 1160-1), Northern Research and Engineering Corporation, Cambridge, Mass., June 8, 1971.

4. "Exhaust Emission Standards and Test Procedures", Federal Register, Washington, D. C., vol. 36, no. 128, July, 1971.

5. Control Techniques for Particulate Air Pollutants (NAPCA Publication No. AP-51) National Air Pollution Control Administration, Department of Health, Education, and Welfare, January, 1969.

6. Butze, H. E. Trout, A. M., and Moyer, H. M., Performance of Swirl-Can Turbojet Combustors at Simulated Supersonic Combustor-Inlet Conditions (NASA TN D-4996) National Aeronautics and Space Administration, Washington, D. C., January, 1969.

7. Low NO_x Emission Combustor for Automobile Gas Turbine Engines (NREC Report No. 959-111), Northern Research and Engineering Corporation, Cambridge, Mass., January 25, 1971.

8. The Design and Performance Analysis of Gas-Turbine Combustion Chambers, Volume I: Theory and Practice of Design (NREC Report No. 1082-1), Northern Research and Engineering Corporation, Cambridge, Mass., December, 1964.

9. The Design and Performance Analysis of Gas-Turbine Combustion Chambers, Volume II: Design Methods and Development Techniques (NREC Report No. 1082-2), Northern Research and Engineering Corporation, Cambridge, Mass., December, 1964.

10. Investigation of Gas-Turbine Engine Components, Part I: Over-all Cycle and System Studies, (NREC Report No. 1099-1), Northern Research and Engineering Corporation, Cambridge, Mass., July 15, 1966.

11. Cornelius, W., Stivender, D. L., and Sullivan, R. E., A Combustion System for a Vehicular Regenerative Gas Turbine Featuring Low Air Pollutant Emissions (SAE Paper No. 670936) Society of Automotive Engineers, Inc., 1967.

12. Montgomery, J. E., Furst, D. G., and Schelp, H. R., *200-300 HP Gas Turbine Engine Family for the U. S. Army* (SAE Paper No. 795A) Society of Automotive Engineers, Inc., 1964.

13. Kahle, G. W., *The Turbine Powered Vehicle -- Promises or Profit* (SAE Paper No. 660171) Society of Automotive Engineers, 1965.

14. Haasis, J. M., *Development of the Combustion System for the AiResearch TPE331 Turboprop Engine* (ASME Paper No. 67-GT-25) The American Society of Mechanical Engineers, 1967.

15. Collet, P. J., *A 3-Shaft Versus a 2-Shaft Cycle in Automotive Gas Turbines* (SAE Paper No. 670955) Society of Automotive Engineers, 1967.

16. Bell, L. E., *Design Requirements of Small High-Temperature Rise Combustors* (SAE Paper No. 680447) Society of Automotive Engineers, 1968.

17. Wright, E. S., *The Potential of the Gas-Turbine Vehicle in Alleviating Air Pollution* (ASME Paper No. 70-WA/GT-8) The American Society of Mechanical Engineers, 1970.

18. *A Rapid Estimation Method for Nitric Oxide Emissions from Gas Turbine Combustors* (NREC Internal Technical Memorandum), Northern Research and Engineering Corporation, Cambridge, Mass., January 4, 1971.

19. *Computer Program for the Analysis of Annular Combustors* (NREC Report No. 1111), Northern Research and Engineering Corporation, Cambridge, Mass., Sponsored by NASA Lewis Research Center under Contract No. NAS3-9402, January 29, 1968.

20. Lefebvre, A. H. and Norster, E., R., "The Design of Tubular Gas Turbine Combustion Chambers for Optimum Mixing Performance", *Proceedings of the Institution of Mechanical Engineers*, vol. 183, part 3N, 1968-69.

21. *Instruments and Apparatus: Chapter 4 Flow Measurement, Part 5 - Measurement of Quantity of Materials* (Supplement of ASME Paper No. PTC 19.5; 4) The American Society of Mechanical Engineers, 1959.

22. *Aircraft Gas Turbine Engine Exhaust Smoke Measurement* (SAE Paper No. ARP 1179) Society of Automotive Engineers, 1970.

23. Findl, E., Brande, H., and Edwards, H., *Study of Physiochemical Properties of Selected Military Fuels*, (AD 274623) Armed Services Technical Information Agency, 1960.

24. Hougen, O. A., Ragatz, R. A., and Watson, K. M., *Chemical Process Principles, Part I: Material and Energy Balances*, 1954.

25. Simmons, Harold C. and Lapera, Dominic J., A High-Speed Spray Analyzer for Gas Turbine Fuel Nozzles, Presented at Session 26 of ASME Gas Turbine Conference, Cleveland, Ohio, March 12, 1969.

26. Engineering Design Report for Droplet Size Measurement and Analysis (EDR 6720182), Parker Hannifin, Cleveland, Ohio, September, 1972.

TABLES

TABLE I

FEDERAL 1975/76 EMISSION GOALS

	Vehicle Emission Goals (grams/mile)	Combustor Emission Goals* (mg/g fuel)
Hydrocarbons (HC)**	0.41	1.42
Carbon Monoxide (CO)	3.4	11.8
Oxides of Nitrogen (NOx)***	0.40	1.38

---

* For 10.0 miles/gal fuel economy and JP-4 jet fuel (S. G. = .763)

** Total hydrocarbons plus total aldehydes

*** NOx computed as NO2

TABLE II

ASSUMED CYCLE OPERATING CONDITIONS FOR DESIGN OF COMBUSTORS

	Net Power Output, Per Cent of Design	$\dot{m}_a$ (lbm/sec)	$\dot{m}_F$ (lbm/hr)	Z	P_{03} (atm)	T_{03} (deg F)	T_{04} (deg F)
			Combustor A				
Design	100	1.56	51.1	110	4.00	1100	1700
	75	1.25	37.8	119	3.31	1160	1700
	50	1.03	27.6	134.5	2.69	1200	1690
	25	.845	17.1	178	2.11	1200	1670
Idle	0	.765	9.2	299	1.60	1200	1420
			Combustor B				
Design	100	1.43	89.6	57.5	12.0	760	1900
	75	1.17	68.1	62.0	9.60	565	1625
	50	.915	46.6	70.7	8.15	540	1475
	25	.658	26.9	88.0	7.31	527	1280
Idle	0	.400	12.6	115.0	5.28	442	1019

TABLE III

SELECTED COMBUSTOR DESIGN CONDITIONS

	Combustor A	Combustor B
Inlet Temperature, deg F	1100	760
Inlet Pressure, atm	4	12
Air Flow Rate, lbm per sec	1.56	1.43
Temperature Rise, deg F	600	1140
Heating Rate, Btu per hr	0.96×10^6	1.68×10^6
Exit Temperature Traverse Quality	.2	.2
Maximum Combustor Wall Temperature, deg F	1700	1700
Pressure Drop, per cent of inlet pressure	3	3
Pressure-Loss Factor ($\Delta P/q_{ref}$)	90	90
Combustion Efficiency, per cent	99.8	99.8
Primary-Zone Equivalence Ratio (ϕ_p)	.5	.65

TABLE IV

DESIGN DISTRIBUTIONS OF AIRFLOW*

	Flow Rates, Per Cent of Total	
	Combustor A	Combustor B
Secondary Holes, $\dot{m}_{sy}$	24.2	35.6
Dilution Holes, $\dot{m}_{dil}$	40.0	26.1
Swirler, $\dot{m}_{sw}$	6.2**	10.3**
Fuel Nozzle, $\dot{m}_{FN}$	3.6**	7.0**
Dome Film-Cooling Slot, $\dot{m}_{cf,d}$	2.0	2.0
Primary-Zone Film-Cooling Slot, $\dot{m}_{cf,p}$	6.0	5.0
Intermediate-Zone Film-Cooling Slot, $\dot{m}_{cf,i}$	6.0	5.0
Dilution-Zone Film-Cooling Slot, $\dot{m}_{cf,dil}$	8.0	5.0
Spark Plug Cooling, $\dot{m}_{sp}$	.5	.5
Bleed Flow, $\dot{m}_{bleed}$	3.5	3.5

---

*See Figure 5 for definition of flow streams.

**These values are for a nozzle air/fuel ratio of 4.

TABLE V

NOZZLE DESIGN SPECIFICATIONS

Nozzle Designation	Description	Design Nozzle Air/Fuel Ratio	Design Nozzle Air Flow, Per Cent of Total
A2.1	No pilot nozzle	4	3.6
A2.2	With pilot nozzle	4	3.6
B1.1	No pilot nozzle	2	3.5
B1.2	With pilot nozzle	2	3.5
B2.1	No pilot nozzle	4	7.0
B2.2	With pilot nozzle	4	7.0

Notes:

1. The "A" nozzles were designed for Combustor A and the "B" nozzles for Combustor B. However, nozzles B2.1 and B2.2 were capable of being tested in both combustors.

2. For all nozzles:

Main spray cone angle = 90 degrees
Pilot spray cone angle = 70 degrees
Pilot flow number = 0.42 gal per hr per psi $^{0.5}$

TABLE VI

METERING AND BLEED HOLE DIMENSIONS

Metering Holes

Cooling Slot Location	Combustor A		Combustor B	
	No. of Holes	Hole Diameter, in	No. of Holes	Hole Diameter, in
Dome	54	.065	30	.0455
Primary Zone	40	.133	40	.0628
Intermediate Zone	40	.133	30	.0725
Dilution Zone	40	.154	30	.0725

Bleed Holes

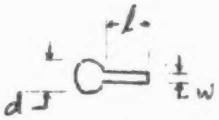

	No. of Holes	d in	ℓ in	w in
Combustor A	24	.063	.320	.032
Combustor B	24	.052	.312	.025

TABLE VII

AVERAGE VALUES OF EFFECTIVE FLOW AREAS

CALCULATED FROM RESULTS OF COLD-AIR TESTS

Combustor A

Flow Element	$A_{h,eff}$ sq ft x 10^{-3}
Dome Slot	1.03
Primary Zone Slot	2.71
Intermediate Zone Slot	2.75
Dilution Zone Slot	3 70
Dilution Holes	16.52
Bleed Holes	1.03
Spark Plug	.35
Nozzle: A2.i, A2.2	1.25
Swirler: l_{sw} = .0	.18
.2	.79
.4	1.42
.6	2.03
.8	2.50
Secondary Holes: l_{sy} = .0	1.00
.3	4.17
.6	7.31
.9	10.46
1.2	12 61

TABLE VII (CONTINUED)

AVERAGE VALUES OF EFFECTIVE FLOW AREAS

CALCULATED FROM RESULTS OF COLD-AIR TESTS

Combustor B

Flow Element	$A_{h,eff}$, sq ft x 10^{-3}
Dome Slot	.211
Primary Zone Slot	.665
Intermediate Zone Slot	.713
Dilution Zone Slot	.661
Dilution Holes	2.83
Bleed Holes	.551
Spark Plug	.300
Nozzle: B1.1, B1.2	.358
B2.1, B2.2	.763
Swirler: l_{sw} = .0	.151
.05	.738
.15	.552
.25	.798
.35	1.095
Secondary Holes: l_{sy} = .0	.350
.20	1.56
.40	2.79
.60	4.00
.75	4.92

TABLE VIII

SUMMARY OF TEST CONDITIONS EXAMINED WITH COMBUSTOR B

Run No.	Nozzle	l_{sw} in	l_{sy} in	P_{o3} psia	T_{o3} deg F	$\dot{m}_a$ lbm per sec	ΔP per cent of inlet pressure	$\bar{\tau}_p$ msec
13	B1.1	.1	.3	68	515	.305	1.1	22
14	↓	↓	↓	↓	725	.375	2.1	14
15	↓	↓	↓	↓	735	.425	2.6	13
16	↓	↓	↓	↓	735	.480	3.4	11
17	↓	↓	↓	↓	705	.545	4.3	10
18	↓	↓	↓	↓	890	.840	9.1	5
19	↓	↓	↓	88	730	.770	5.4	9
20	↓	↓	↓	53	730	.320	2.5	13
29	↓	↓	↓	78	530	.390	1.3	19
21	B1.1	.35	.75	68	520	.305	.5	16
22	↓	↓	↓	↓	700	.390	1.1	11
23	↓	↓	↓	↓	710	.420	1.4	10
24	↓	↓	↓	↓	695	.485	1.8	9
25	↓	↓	↓	↓	690	.545	2.2	8
26	↓	↓	↓	↓	875	.840	6.3	4
27	↓	↓	↓	88	710	.775	2.8	7
28	↓	↓	↓	53	700	.320	1.3	10
30	↓	↓	↓	68	695	.850	5.6	5
31	↓	↓	↓	78	510	.390	.7	15
37	B2.1	.1	.3	68	700	.390	1.9	13
38	↓	↓	↓	↓	700	.430	2.3	12
39	↓	↓	↓	↓	690	.545	3.8	9
40	↓	↓	↓	78	515	.390	1.2	18
41	↓	↓	↓	68	890	.840	10.8	5
42	↓	↓	↓	88	705	.785	4.7	8
32	B2.1	.35	.75	68	700	.385	1.0	10
33	↓	↓	↓		705	.435	1.2	9
34	↓	↓	↓		690	.590	2.2	7
35	↓	↓	↓	78	520	.385	.6	14
36	↓	↓	↓	88	705	.780	2.6	6

TABLE VIII (CONTINUED)

SUMMARY OF TEST CONDITIONS EXAMINED WITH COMBUSTOR B

Run No.	Nozzle	l_{sw} in	l_{sy} in	P_{03} psia	T_{03} deg F	$\dot{m}_a$ lbm per sec	ΔP per cent of inlet pressure	$\bar{\tau}_p$ msec
43*	B2.1	.1	.3	67	695	.385	4.0	10
44	↓	↓	↓	68	695	.430	4.9	9
45	↓	↓	↓	68	715	.540	8.1	7
46	↓	↓	↓	77	515	.390	2.6	14
47	↓	↓	↓	68	900	.660	13.8	4
48	↓	↓	↓	87	680	.625	6.1	8

*Runs 43-48 were for modified configuration in which one third of the metering holes for the primary and intermediate cooling slots were blocked off and the diameter of the dilution holes was reduced to 0.25 in.

TABLE IX

RESULTS OF COMBUSTION TESTS FOR COMBUSTOR B WITH NOZZLE B1.1 AND "CLOSED" VARIABLE-GEOMETRY SETTING

Design Nozzle Air/Fuel Ratio = 2:1
Swirler Setting, ℓ_{sw} = .1 in
Secondary-Hole Setting, ℓ_{sy} = .3 in
Estimated Effective Primary-Zone Flow Rate = 18.3 per cent

Run No.	P_{03} psia	T_{03} deg F	$\dot{m}_a$ lbm per sec	$\dot{m}_{fu}$ lbm per hr	Z	ϕ_p	EI_{NO} mg per gm fuel	EI_{NO_2} mg per gm fuel	EI_{CO} mg per gm fuel	EI_{HC} mg per gm fuel	ΔP per cent	$1-\eta_c$ per cent	TQ
13	67.8	507	.292	18.5	60.1	1.35	4.11	7.08	2.07	.00	.99	.048	.14
	67.9	510	.303	15.9	74.8	1.08	3.84	6.50	2.78	.12	1.08	.076	
	67.9	518	.313	14.7	78.3	1.03	3.86	6.54	2.76	.16	1.10	.079	
	67.9	520	.312	12.2	94.4	.86	4.15	7.27	2.76	.07	1.06	.071	
	67.9	523	.301	9.0	120.0	.67	3.26	6.14	4.44	.26	1.15	.128	
14	68.2	722	.348	14.5	86.7	.93	6.90	11.27	2.2	.00	2.04	.051	
	67.4	721	.390	16.0	87.7	.92	6.98	10.70	2.74	.57	2.20	.118	.15
	68.0	726	.347	12.1	103.1	.78	6.68	11.23	2.21	.00	2.10	.051	
	67.9	730	.406	11.3	129.4	.63	6.48	10.76	2.14	.00	2.21	.050	
	68.2	729	.381	9.7	142.0	.57	5.92	9.87	1.93	.00	1.97	.045	
15	67.6	733	.423	20.1	75.8	1.07	6.84	11.33	2.52	1.13	2.76	.167	.12
	67.6	734	.414	18.5	80.4	1.01	7.08	12.14	2.36	.35	2.51	.088	
	67.5	736	.431	16.4	94.4	.86	6.71	11.51	2.30	.29	2.65	.081	
	67.5	736	.422	13.9	109.0	.74	6.49	10.82	2.18	.20	2.61	.070	
	67.2	733	.430	12.5	123.7	.65	5.55	9.4	1.93	.19	2.69	.063	
	67.7	733	.423	8.2	186.0	.44	4.26	7.12	2.35	.23	2.54	.076	
16	67.7	737	.473	22.7	75.0	1.08	6.53	11.22	2.79	.17	3.36	.081	.10
	67.7	739	.479	20.1	85.6	.95	6.90	11.68	3.10	.09	3.45	.081	
	67.7	737	.479	18.3	94.3	.86	6.51	11.04	3.04	.09	3.54	.079	
	67.7	736	.479	16.5	104.6	.77	6.34	10.89	3.11	.16	3.36	.088	
	67.7	738	.479	12.6	137.3	.59	5.15	9.0	2.34	.32	3.34	.084	
	67.9	735	.480	9.2	187.6	.43	4.39	6.73	3.01	.66	3.18	.133	

TABLE IX (CONTINUED)

RESULTS OF COMBUSTION TESTS FOR COMBUSTOR B WITH NOZZLE BI.1 AND "CLOSED" VARIABLE-GEOMETRY SETTING

Design Nozzle Air/Fuel Ratio = 2:1
Swirler Setting, ℓ_{sw} = .1 in
Secondary-Hole Setting, ℓ_{sy} = .3 in
Estimated Effective Primary-Zone Flow Rate = 18.3 per cent

Run No.	P_{03} psia	T_{03} deg F	$\dot{m}_a$ lbm per sec	$\dot{m}_{fu}$ lbm per hr	Z	Φ_p	EI_{NO} mg per gm fuel	EI_{NO_x} mg per gm fuel	EI_{CO} mg per gm fuel	EI_{HC} mg per gm fuel	ΔP per cent	$1-\eta_c$ per cent	TQ
17	68.1	699	.542	26.3	74.2	1.09	4.98	8.36	3.34	-	4.32	.078	.11
	68.0	702	.548	24.2	81.6	.99	5.05	8.52	3.59	-	4.40	.083	
	67.8	705	.547	22.0	89.6	.90	5.15	8.62	3.32	-	4.28	.077	
	67.8	709	.546	19.5	100.6	.80	4.94	8.39	3.14	-	4.30	.073	
	67.8	711	.538	15.8	122.9	.66	4.36	7.28	2.51	-	4.15	.058	
	67.8	711	.538	12.1	160.5	.50	3.51	5.89	1.87	-	4.08	.043	
18	67.8	888	.840	31.6	95.5	.85	5.09	8.42	5.97	-	9.06	.138	.16
	67.8	892	.836	28.6	105.0	.77	5.05	8.41	5.33	-	9.06	.124	
	68.0	888	.842	27.9	108.8	.74	4.55	7.32	4.88	-	9.08	.113	
	67.8	891	.840	25.2	120.0	.67	4.38	7.11	4.56	-	9.08	.106	
	68.1	892	.837	23.3	129.6	.62	4.06	6.63	4.29	-	9.11	.100	
19	88.8	721	.764	31.2	88.1	.92	5.26	9.19	2.50	-	5.29	.058	.10
	87.7	731	.770	30.3	91.5	.88	5.17	9.10	2.59	-	5.43	.060	
	87.8	729	.771	28.2	98.3	.82	5.14	9.14	2.40	-	5.39	.056	
	87.4	728	.779	25.9	108.4	.75	5.10	8.86	2.22	-	5.40	.051	
	87.8	729	.771	24.3	114.3	.71	4.65	8.23	1.89	-	5.28	.044	
20	52.8	722	.308	15.9	69.6	1.16	5.41	8.97	3.07	-	2.63	.071	.17
	52.8	733	.322	14.5	80.1	1.01	5.46	9.01	3.37	-	2.56	.078	
	53.2	731	.318	11.8	97.4	.86	5.8	9.52	3.33	-	2.47	.077	
	53.0	731	.323	10.9	106.7	.76	5.57	9.23	3.23	-	2.54	.075	
	52.8	730	.322	9.2	126.6	.64	4.36	7.29	2.47	-	2.56	.057	

TABLE IX (CONTINUED)

RESULTS OF COMBUSTION TESTS FOR COMBUSTOR B WITH NOZZLE BI.1 AND "CLOSED" VARIABLE-GEOMETRY SETTING

Design Nozzle Air/Fuel Ratio = 2:1
Swirler Setting, ℓ_{sw} = .1 in
Secondary-Hole Setting, ℓ_{sy} = .3 in
Estimated Effective Primary-Zone Flow Rate = 18.3 per cent

Run No.	P_{03} psia	T_{03} deg F	$\dot{m}_a$ lbm per sec	$\dot{m}_{fu}$ lbm per hr	Z	ϕ_p	EI_{NO} mg per gm fuel	EI_{NO_x} mg per gm fuel	EI_{CO} mg per gm fuel	EI_{HC} mg per gm fuel	ΔP per cent	$1-\eta_c$ per cent	TQ
29	77.9	529	.388	18.8	74.4	1.09	4.13	7.18	2.62	2.24	1.34	.275	.11
	77.9	531	.396	16.5	86.6	.93	4.08	7.23	2.79	.06	1.39	.070	
	77.9	531	.388	14.9	93.9	.86	4.23	7.38	2.80	.08	1.30	.073	
	77.9	531	.388	12.8	108.9	.74	3.98	7.15	2.97	.09	1.33	.077	
	78.1	531	.378	12.5	108.9	.74	3.75	6.80	3.45	.10	1.24	.090	

TABLE X

RESULTS OF COMBUSTION TESTS FOR COMBUSTOR B WITH NOZZLE B1.1 AND "FULL OPEN" VARIABLE-GEOMETRY SETTING

Design Nozzle Air/Fuel Ratio = 2:1
Swirler Setting, ℓ_{sw} = .35 in
Secondary-Hole Setting, ℓ_{sy} = .75 in
Estimated Effective Primary-Zone Flow Rate = 27.7 per cent

Run No.	P_{03} psia	T_{03} deg F	$\dot{m}_a$ lbm per sec	$\dot{m}_{fu}$ lbm per hr	Z	ϕ_p	EI_{NO} mg per gm fuel	EI_{NO_2} mg per gm fuel	EI_{CO} mg per gm fuel	EI_{HC} mg per gm fuel	ΔP per cent	$1-\eta_c$ per cent	TQ
21	68.2	509	.308	19.5	56.9	.94	2.64	6.25	14.39	1.32	.54	.460	.26
	68.1	521	.301	15.7	69.2	.77	2.47	6.35	13.89	1.66	.52	.481	
	68.0	523	.301	13.9	77.8	.69	2.53	6.38	13.18	1.48	.52	.447	
	67.5	526	.304	11.2	97.6	.55	2.30	6.57	15.05	1.44	.51	.486	
	67.5	527	.299	8.1	132.9	.40	1.32	5.63	35.97	9.97	.49	1.786	
22	68.2	689	.398	20.3	70.5	.76	5.11	8.85	17.48	.04	1.14	.410	.17
	67.6	697	.395	20.0	71.0	.75	5.14	9.03	3.48	.02	1.08	.083	
	67.8	700	.373	17.3	77.7	.69	5.38	9.25	3.80	.02	1.02	.091	
	67.8	705	.394	16.7	84.8	.63	5.69	10.35	4.56	.03	1.03	.108	
	67.6	705	.394	11.6	122.3	.44	3.70	8.22	12.1	.47	1.06	.327	
23	68.0	714	.429	24.2	63.8	.84	5.30	8.85	2.57	.05	1.36	.064	.17
	67.8	728	.406	20.6	71.0	.75	-	10.17	2.99	.00	1.40	.069	
	68.0	713	.414	19.2	77.7	.69	5.22	9.25	3.73	.02	-	.088	
	67.8	706	.429	17.7	87.3	.61	4.93	8.96	5.03	.03	1.34	.119	
	67.8	702	.430	14.0	110.2	.49	4.03	8.29	10.53	.29	1.34	.272	
	67.7	699	.416	10.4	144.1	.37	3.30	7.37	13.59	.53	1.31	.366	
24	67.6	697	.479	25.6	67.4	.79	5.10	8.90	3.50	.04	1.75	.085	.16
	67.5	697	.491	23.9	73.9	.72	4.96	8.68	4.13	.00	1.82	.096	
	67.5	697	.491	21.4	82.5	.65	4.93	8.62	4.92	.03	1.84	.117	
	67.6	696	.479	19.0	91.0	.59	4.95	9.05	5.86	.06	1.76	.141	
	67.6	697	.491	13.7	129.0	.41	3.26	7.22	13.31	.47	1.82	.354	

TABLE X (CONTINUED)

RESULTS OF COMBUSTION TESTS FOR COMBUSTOR B WITH NOZZLE B1.1 AND "FULL OPEN" VARIABLE-GEOMETRY SETTING

Design Nozzle Air/Fuel Ratio = 2:1
Swirler Setting, l_{sw} = .35 in
Secondary-Hole Setting, l_{sy} = .75 in
Estimated Effective Primary-Zone Flow Rate = 27.7 per cent

Run No.	P_{03} psia	T_{03} deg F	$\dot{m}_a$ lbm per sec	$\dot{m}_{fu}$ lbm per hr	Z	Φ_p	EI_{NO} mg per gm fuel	EI_{NO_x} mg per gm fuel	EI_{CO} mg per gm fuel	EI_{HC} mg per gm fuel	ΔP per cent	$1-\eta_c$ per cent	TQ
25	68.3	689	.553	28.6	69.6	.77	4.75	8.51	4.91	.17	2.24	.130	.12
	67.4	691	.541	26.7	72.9	.73	4.59	8.21	5.49	.08	2.24	.135	
	67.4	689	.553	24.4	81.5	.66	4.53	8.12	6.61	.08	2.31	.161	
	67.4	689	.534	21.4	89.7	.60	4.60	8.35	7.45	.11	2.20	.183	
	67.9	693	.542	14.3	136.3	.39	2.91	6.75	16.58	1.00	2.17	.480	
26	67.4	877	.841	31.3	96.6	.55	4.04	7.43	10.93	.18	6.48	.271	.13
	67.2	877	.835	27.6	108.8	.49	3.52	6.80	14.54	.37	6.39	.372	
	67.6	877	.847	23.2	131.7	.41	3.02	6.32	21.66	.73	6.35	.572	
	67.4	878	.846	19.0	160.5	.33	2.17	5.13	30.11	1.18	6.22	.811	
	67.8	877	.843	14.3	212.2	.25	1.54	4.74	42.63	1.88	5.94	1.168	
27	87.5	722	.766	42.7	64.5	.83	5.16	9.36	3.93	.30	2.78	.120	.15
	87.5	703	.773	30.7	90.6	.59	4.55	8.43	6.37	.06	2.84	.153	
	87.5	703	.789	26.6	106.9	.50	3.91	7.71	9.80	.20	2.93	.246	
	87.9	706	.770	23.0	120.8	.44	2.39	5.60	13.64	.70	2.67	.384	
	87.7	706	.789	15.3	185.6	.29	1.93	5.03	22.53	1.47	2.63	.663	
28	52.2	691	.325	19.3	60.7	.88	5.04	8.32	4.65	.07	1.33	.115	.23
	52.2	701	.323	18.7	62.1	.86	4.83	8.31	4.08	.06	1.31	.100	
	52.4	703	.316	16.4	69.3	.77	5.10	8.82	4.69	.07	1.22	.116	
	53.0	706	.325	11.2	104.5	.51	3.71	7.70	13.66	.48	1.33	.363	
	52.7	706	.316	8.7	131.2	.41	3.28	7.13	15.96	.80	1.19	.447	

TABLE X (CONTINUED)

RESULTS OF COMBUSTION TESTS FOR COMBUSTOR B WITH NOZZLE B1.1 AND "FULL OPEN" VARIABLE-GEOMETRY SETTING

Design Nozzle Air/Fuel Ratio = 2:1
Swirler Setting, l_{sw} = .35 in
Secondary-Hole Setting, l_{sy} = .75 in
Estimated Effective Primary-Zone Flow Rate = 27.7 per cent

Run No.	P_{03} psia	T_{03} deg F	$\dot{m}_a$ lbm per sec	m_{fu} lbm per hr	z	ϕ_P	EI_{NO} mg per gm fuel	EI_{NO_2} mg per gm fuel	EI_{CO} mg per gm fuel	EI_{HC} mg per gm fuel	ΔP per cent	$1-\eta_c$ per cent	TQ
30	67.5	692	.853	31.9	96.3	.55	2.92	6.02	22.47	1.33	5.85	.648	.13
	67.5	694	.847	27.5	111.0	.48	1.97	5.33	34.07	3.06	5.76	1.083	
	67.5	692	.853	24.0	127.8	.42	1.47	4.60	46.28	6.06	5.66	1.653	
	67.7	694	.854	19.9	154.7	.35	.98	3.95	58.66	8.51	5.48	2.174	
	67.5	693	.853	17.5	175.4	.30	.95	3.64	66.46	9.38	5.44	2.437	
31	77.6	517	.385	19.2	72.3	.74	-	6.63	6.90	.45	.71	.203	.15
	77.4	510	.386	16.0	86.5	.62	2.72	6.81	12.01	.93	.70	.367	
	77.2	508	.398	14.0	102.2	.52	2.14	6.55	18.04	1.72	.72	.583	
	77.4	507	.398	11.5	124.3	.43	1.75	6.36	22.27	2.78	.75	.782	
	77.6	506	.387	11.3	123.1	.43	1.99	6.50	19.18	2.19	.71	.654	

TABLE XI

RESULTS OF COMBUSTION TESTS FOR COMBUSTOR B WITH NOZZLE B2.1 AND "CLOSED" VARIABLE-GEOMETRY SETTING

Design Nozzle Air/Fuel Ratio = 4:1
Swirler Setting, l_{sw} = .1 in
Secondary-Hole Setting, l_{sy} = .3 in
Estimated Effective Primary-Zone Flow Rate = 21.8 per cent

Run No.	P_{03} psia	T_{03} deg F	$\dot{m}_a$ lbm per sec	$\dot{m}_{fu}$ lbm per hr	Z	ϕ_p	EI_{NO} mg per gm fuel	EI_{NO_2} mg per gm fuel	EI_{CO} mg per gm fuel	EI_{HC} mg per gm fuel	ΔP per cent	$1-\eta_c$ per cent	TQ
37	68.0	695	.396	18.8	75.8	.90	6.84	11.70	1.86	.68	2.03	.108	.13
	68.1	699	.396	16.3	87.4	.78	6.40	11.01	1.45	.21	1.45	.054	
	68.2	700	.377	12.8	106.3	.64	5.22	8.51	1.35	.00	1.80	.031	
	68.2	701	.386	10.9	127.2	.53	4.25	7.73	4.71	.56	1.83	.163	
38	67.8	700	.431	20.4	76.1	.89	6.31	10.77	2.01	.14	2.45	.060	.16
	68.0	701	.431	16.1	96.1	.71	6.23	10.56	1.41	.00	2.32	.033	
	68.2	703	.427	12.5	122.9	.55	4.74	8.45	2.99	.15	2.16	.084	
	67.9	705	.430	11.9	129.7	.52	4.87	8.50	3.66	.12	2.11	.096	
39	67.7	694	.541	32.2	60.4	1.12	6.10	10.81	3.02	.41	3.78	.109	.18
	67.9	692	.542	30.6	63.8	.97	6.10	10.79	3.00	.89	3.73	.154	
	67.6	692	.549	27.4	72.0	.94	5.89	10.08	3.17	3.33	3.92	.391	
	67.8	691	.550	25.5	77.7	.87	6.19	10.62	2.89	.55	3.89	.120	.17
	68.1	691	.551	20.1	98.8	.69	5.37	9.50	1.54	.17	3.82	.052	
	67.3	691	.540	16.2	120.2	.57	4.64	7.88	1.76	.06	3.63	.046	
40	78.1	511	.387	22.6	61.6	1.10	4.47	7.95	2.48	.19	1.19	.076	.22
	77.4	512	.385	14.2	97.8	.69	4.29	7.84	4.39	.06	1.24	.108	
	77.9	513	.386	12.9	107.5	.63	3.59	7.40	8.80	.07	1.21	.211	
	77.9	513	.398	11.1	128.6	.53	1.95	6.38	35.18	5.12	1.26	1.305	
	78.0	515	.386	9.5	146.3	.46	1.26	5.43	52.21	23.26	1.15	3.433	

TABLE XI (CONTINUED)

RESULTS OF COMBUSTION TESTS FOR COMBUSTOR B WITH NOZZLE B2.1 AND "CLOSED" VARIABLE-GEOMETRY SETTING

Design Nozzle Air/Fuel Ratio = 4:1
Swirler Setting, ℓ_{sw} = .1 in
Secondary-Hole Setting, ℓ_{sy} = .3 in
Estimated Effective Primary-Zone Flow Rate = 21.8 per cent

Run No.	P_{04} psia	T_{03} deg F	$\dot{m}_a$ lbm per sec	$\dot{m}_f$ lbm per hr	λ	ϕ_p	EI_{NO} mg per gm fuel	EI_{NO_x} mg per gm fuel	EI_{CO} mg per gm fuel	EI_{HC} mg per gm fuel	ΔP per cent	$1-\eta_c$ per cent	TQ
41	67.9	889	.845	31.0	98.2	.69	5.65	9.61	4.22	-	10.46	.098	
	68.2	887	.838	29 0	104.1	.65	5.22	8.50	3.96	-	10.85	.092	
	68.2	889	.840	27.6	109.5	.62	5.03	8.24	3.63	-	10.41	.084	
	68.1	886	.842	24.5	123.6	.55	4.38	7.31	3.85	-	11.01	.089	
	67.9	895	.838	22.9	131.9	.51	3.44	5.69	6.93	-	10.90	.161	.17
42	87.9	707	.773	38.9	71.5	.95	5.86	10.59	1.89	.00	4.57	.044	
	87.9	706	.780	32.0	87.8	.77	5.70	9.86	1.63	.00	4.80	.038	
	88.1	705	.792	29.0	98.2	.69	5.03	8.82	1.34	1.81	4.80	.204	
	87.9	699	.776	23.3	119.9	.57	3.75	6.14	5.49	.86	4.75	.210	.10
	87.9	701	.789	21.1	134.5	.50	2.38	4.84	19.37	6.59	4.59	1.078	

TABLE XII

RESULTS OF COMBUSTION TESTS FOR COMBUSTOR B WITH NOZZLE B2.1 AND "FULL OPEN" VARIABLE-GEOMETRY SETTING

Design Nozzle Air/Fuel Ratio = 4:1
Swirler Setting, ℓ_{sw} = .35 in
Secondary-Hole Setting, ℓ_{sy} = .75 in
Estimated Effective Primary-Zone Flow Rate = 30.0 per cent

Run No.	P_{03} psia	T_{03} deg F	$\dot{m}_a$ lbm per sec	$\dot{m}_{fu}$ lbm per hr	Z	ϕ_p	EI_{NO} mg per gm fuel	EI_{NO_2} mg per gm fuel	EI_{CO} mg per gm fuel	EI_{HC} mg per gm fuel	ΔP per cent	$1-\eta_c$ per cent	TQ
32	67.8	697	.385	18.7	73.9	.67	5.66	9.52	3.91	.06	.98	.096	.18
	67.6	697	.334	15.9	87.2	.57	6.02	10.50	6.73	.07	1.02	.163	
	67.8	697	.385	13.3	104.2	.47	4.25	8.68	10.87	.27	.98	.278	
	67.6	697	.384	10.7	129.3	.38	2.97	7.24	24.30	4.95	.99	1.036	
	67.8	700	.395	10.3	138.1	.36	.89	3.31	33.05	20.28	1.00	2.703	
33	68.3	701	.432	20.4	76.1	.65	5.58	9.79	3.50	.05	1.20	.086	.18
	67.6	703	.444	18.3	87.4	.56	3.39	6.60	8.97	.43	1.31	.249	
	68.0	703	.431	12.8	121.1	.41	2.72	6.78	18.40	1.65	1.22	.584	
	67.9	704	.430	12.7	122.3	.40	1.85	5.48	30.49	9.36	1.26	1.602	
34	68.1	692	.563	29.2	69.5	.71	3.72	6.65	4.56	1.71	2.15	.269	.16
	68.0	692	.613	29.1	75.8	.65	3.42	5.54	6.31	2.57	2.17	.391	
35	77.8	515	.385	18.3	76.0	.65	3.27	7.21	12.56	.72	.67	.361	.23
	77.2	525	.382	12.7	108.3	.46	2.60	7.46	17.84	1.99	.67	.604	
	77.3	520	.383	12.8	107.7	.46	1.69	6.21	29.82	3.63	.64	1.039	
	77.6	523	.395	9.0	157.5	.31	.98	3.52	> 76.6	60.17	.60	> 7.523	
	77.8	524	.384	8.0	171.7	.29	.97	3.29	> 83.5	73.46	.61	> 8.953	
36	87.7	702	.779	31.1	90.2	.55	4.62	8.39	5.64	.72	2.59	.200	.15
	87.5	702	.778	30.3	92.5	.53	4.35	8.16	6.32	.77	2.58	.220	
	87.7	703	.779	26.7	105.0	.47	3.51	7.40	11.16	2.06	2.52	.456	
	87.8	702	.780	25.9	108.5	.46	4.30	8.34	9.41	1.36	2.49	.349	
	87.1	705	.776	23.6	118.4	.42	2.32	6.06	21.68	5.62	2.58	1.040	

TABLE XIII

RESULTS OF COMBUSTION TESTS FOR MODIFIED COMBUSTOR B WITH NOZZLE B2.1 AND "CLOSED" VARIABLE-GEOMETRY SETTING

Design Nozzle Air/Fuel Ratio = 4:1
Swirler Setting, ℓ_{sw} = .1 in
Secondary-Hole Setting, ℓ_{sy} = .3 in
Estimated Effective Primary-Zone Flow Rate = 29.6 per cent

Run No.	P_{03} psia	T_{03} deg F	$\dot{m}_a$ lbm per sec	$\dot{m}_{fu}$ lbm per hr	Z	ϕ_p	EI_{NO} mg per gm fuel	EI_{NO_x} mg per gm fuel	EI_{CO} mg per gm fuel	EI_{HC} mg per gm fuel	ΔP per cent	$1-\eta_c$ per cent	TQ
43	67.4	691	.385	32.6	42.5	1.18	5.74	10.01	.46	.98	4.05	.105	.19
	67.4	680	.387	30.4	45.8	1.09	4.84	8.35	.54	1.08	3.97	.116	
	67.4	697	.384	27.0	51.3	.98	4.54	7.46	.56	.13	3.99	.025	.19
	67.0	700	.382	23.6	58.4	.86	3.94	6.51	.80	1.46	4.05	.158	
	67.2	700	.383	18.9	73.0	.68	3.45	5.75	1.79	.13	3.89	.054	
44	67.6	694	.430	26.5	58.3	.86	3.93	6.50	.97	-	4.91	.023	
	67.8	694	.430	21.8	71.0	.70	3.05	5.25	5.14	-	4.90	.119	.22
	67.6	694	.430	21.5	71.9	.70	2.94	5.32	6.41	-	4.91	.149	
45	67.9	725	.535	41.9	45.9	1.09	4.18	7.67	1.13	-	7.82	.026	.21
	67.4	695	.547	33.8	58.3	.86	3.44	5.84	1.49	-	8.19	.035	.22
	67.1	696	.546	30.8	63.8	.78	2.95	5.35	2.88	-	8.56	.067	
	67.8	741	.538	29.6	65.3	.77	3.43	5.90	3.97	-	7.85	.092	
46	77.4	510	.380	26.8	51.1	.98	2.64	6.12	.96	.13	2.50	.034	.15
	77.4	520	.395	24.5	58.1	.86	3.30	5.63	1.48	4.04	2.63	.420	
	77.4	519	.396	18.4	77.4	.65	1.05	4.11	28.17	11.43	2.56	1.745	
	77.4	513	.397	18.1	78.9	.63	1.65	4.31	18.20	.90	2.67	.508	
	77.4	515	.384	14.4	96.2	.52	.48	3.01	>46.5	33.94	2.51	>4.343	
47	67.9	895	.657	42.7	55.4	.90	4.32	7.70	1.58	-	13.41	.037	.25
	67.7	897	.656	36.3	65.0	.77	3.69	6.28	2.17	-	13.59	.050	
	67.5	898	.666	31.6	75.8	.66	2.74	4.87	4.30	-	14.21	.100	
	67.4	897	.665	29.9	80.0	.63	2.68	4.76	5.79	-	14.10	.134	

TABLE XIII (CONTINUED)

RESULTS OF COMBUSTION TESTS FOR MODIFIED COMBUSTOR B WITH NOZZLE B2.1 AND "CLOSED" VARIABLE-GEOMETRY SETTING

Design Nozzle Air Fuel Ratio = 4:1
Swirler Setting, ℓ_{sw} = .1 in
Secondary-Hole Setting, ℓ_{sy} = .3 in
Estimated Effective Primary-Zone Flow Rate = 29.6 per cent

Run No.	P_{03} psia	T_{03} deg F	m_a lbm per sec	$\dot{m}_{fu}$ lbm per hr	Z	ϕ_p	EI_{NO} mg per gm fuel	EI_{NO_x} mg per gm fuel	EI_{CO} mg per gm fuel	EI_{HC} mg per gm fuel	ΔP per cent	$1-\eta_c$ per cent	TQ
48	87.4	682	.618	36.4	61.1	.82	3.86	6.56	1.50	-	5.92	.035	.21
	87.1	682	.626	33.8	66.6	.75	3.50	5.95	2.55	-	6.05	.059	
	87.0	682	.625	30.2	74.5	.67	2.81	5.27	11.37	-	6.22	.264	
	86.9	680	.629	27.7	81.6	.61	1.11	3.93	>39.5	-	6.27	>.916	

TABLE XIV

SUMMARY OF TEST CONDITIONS EXAMINED WITH COMBUSTOR A*

Run No.	ℓ_{sw} in	ℓ_{sy} in	P_{os} psia	T_{os} deg F	$\dot{m}_a$ lbm per sec	ΔP per cent of inlet pressure	$\bar{\tau}_p$ msec
49	.2	.4	24	700	.920	6.5	19
50	↓	↓	↓	900	.315	.9	51
51	↓	↓	↓	900	.840	6.6	18
52	↓	↓	↓	1100	.790	6.7	17
53	↓	↓	↓	1185	.775	6.9	17
54	↓	↓	59	895	.500	.4	80
55	↓	↓	↓	870	.910	1.2	45
56	↓	↓	↓	900	1.310	2.5	30
60	.3	.7	40	900	.435	.6	55
61	↓	↓	↓	900	1.145	3.7	20
62	↓	↓	↓	1100	1.070	3.7	19
63	↓	↓	↓	1150	1.055	3.6	20
64	↓	↓	59	905	.53	.3	67
65	↓	↓	↓	900	.955	1.1	37
66	↓	↓	↓	895	1.390	2.4	25
68	↓	↓	88	890	.655	.2	81

---

*All tests were performed with Nozzle A2.1.

TABLE XV

RESULTS OF COMBUSTION TESTS FOR COMBUSTOR A WITH NOZZLE A2.1 AND "CLOSED" VARIABLE-GEOMETRY SETTING

Design Nozzle Air/Fuel Ratio = 4:1
Swirler Setting, ℓ_{sw} = .2 in
Secondary-Hole Setting, ℓ_{sy} = .4 in
Estimated Effective Primary-Zone Flow Rate = 11.8 per cent

Run No.	P_{03} psia	T_{03} deg F	$\dot{m}_a$ lbm per sec	$\dot{m}_{fu}$ lbm per hr	Z	ϕ_p	EI_{NO} mg per gm fuel	EI_{NO_x} mg per gm fuel	EI_{CO} mg per gm fuel	EI_{HC} mg per gm fuel	ΔP per cent	$1-\eta_c$ per cent	TQ
49	24.1	701	.924	45.9	72.5	1.89	3.95	6.65	10.36	-	6.45	.240	.08
	24.1	698	.920	41.5	79.8	1.71	4.01	6.93	10.46	-	6.45	.243	
50	23.9	899	.318	19.3	59.4	2.30	7.00	11.50	2.57	-	6.93	.060	.13
	23.8	901	.317	17.4	65.6	2.09	7.30	12.47	2.77	-	6.96	.064	
	23.8	900	.317	14.6	78.1	1.75	6.87	11.04	2.90	-	6.90	.067	
	23.8	900	.317	11.4	100.2	1.37	7.33	11.72	3.13	-	6.89	.072	
	23.8	899	.317	8.6	132.1	1.04	7.72	12.25	3.60	-	6.86	.083	
51	23.6	899	.837	39.1	77.0	1.78	5.98	10.15	7.76	-	6.69	.180	.10
	23.5	902	.841	34.9	86.8	1.58	5.81	10.03	8.31	-	6.67	.193	
	23.6	899	.841	32.6	92.8	1.47	5.83	9.83	8.70	-	6.58	.202	
	23.5	898	.842	31.2	97.1	1.41	5.69	9.65	9.38	-	6.71	.218	
	23.5	901	.841	27.5	110.3	1.24	5.76	9.19	9.35	-	6.72	.217	
	23.6	901	.841	24.3	124.7	1.10	5.46	8.98	8.99	-	6.55	.208	
	23.5	900	.842	22.7	133.4	1.02	4.73	8.11	8.83	-	6.60	.205	
	23.6	900	.841	19.2	157.4	.87	4.26	7.04	10.25	-	6.51	.238	
52	23.7	1098	.787	39.2	72.4	1.73	8.73	14.67	4.82	.60	6.45	.169	.14
	23.7	1099	.786	35.4	80.0	1.57	8.55	14.27	4.85	.32	6.75	.143	
	23.6	1098	.788	31.8	89.1	1.41	8.76	14.58	5.48	.14	6.86	.141	
	23.6	1101	.787	29.1	97.3	1.29	8.65	14.35	5.41	.10	6.80	.135	
	23.7	1097	.790	25.9	109.9	1.14	8.61	13.91	5.25	.05	6.72	.125	
	23.6	1101	.787	20.2	139.9	.90	7.59	11.86	4.77	.00	6.75	.111	
	23.6	1097	.788	18.1	156.7	.80	6.69	10.76	4.87	.00	6.70	.113	

TABLE XV (CONTINUED)

RESULTS OF COMBUSTION TESTS FOR COMBUSTOR A WITH NOZZLE A2.1 AND "CLOSED" VARIABLE-GEOMETRY SETTING

Design Nozzle Air Fuel Ratio = 4:1
Swirler Setting, ℓ_{sw} = .2 in
Secondary-Hole Setting, ℓ_{sy} = .4 in
Estimated Effective Primary-Zone Flow Rate = 11.8 per cent

Run No.	P_{03} psia	T_{c3} deg F	$\dot{m}_a$ lbm per sec	$\dot{m}_{fu}$ lbm per hr	Z	ϕ_p	EI_{NO} mg per gm fuel	EI_{NO_x} mg per gm fuel	EI_{CO} mg per gm fuel	EI_{HC} mg per gm fuel	ΔP per cent	$1-\eta_c$ per cent	TQ
53	23.7	1184	.769	40.9	67.6	1.86	9.94	17.42	3.71	.28	6.72	.113	.16
	23.8	1182	.771	36.1	76.8	1.63	10.31	17.67	3.99	.50	6.64	.140	
	23.5	1182	.787	32.5	87.3	1.44	9.96	16.81	4.52	.02	7.28	.107	
	23.6	1181	.768	27.9	99.1	1.27	10.36	17.48	4.64	.00	6.78	.108	
	23.6	1182	.775	25.6	108.9	1.15	8.98	14.82	4.35	.00	6.99	.101	
	23.6	1185	.768	24.3	113.6	1.11	9.13	14.91	3.98	.00	6.87	.092	
	23.6	1184	.773	20.3	137.3	.92	8.30	13.60	3.87	.00	6.94	.090	
	23.8	1183	.770	17.5	157.9	.80	8.06	13.12	3.68	.00	6.61	.085	
	23.6	1182	.768	12.9	214.5	.59	6.24	9.92	4.16	.00	6.68	.097	
	23.7	1185	.769	10.8	256.6	.49	5.12	8.38	4.73	.00	6.61	.110	
54	59.5	896	.503	23.6	76.7	1.78	10.78	17.88	1.65	-	.37	.038	.14
	58.3	898	.498	21.3	84.0	1.63	11.08	18.07	1.81	-	.34	.042	
	58.2	892	.498	18.1	99.3	1.38	11.41	18.30	2.13	-	.39	.049	
	58.7	896	.500	15.3	117.4	1.17	12.01	18.98	2.75	-	.37	.064	
	58.7	893	.500	14.5	124.3	1.10	10.77	17.70	3.03	-	.37	.070	
	59.0	896	.501	11.9	152.1	.90	12.36	21.39	4.59	-	.33	.106	
	59.0	893	.501	8.7	208.0	.66	13.63	22.56	4.85	-	.32	.112	
55	59.0	873	.906	28.9	113.0	1.21	10.62	17.19	2.86	-	1.19	.066	.16
	59.1	872	.910	27.0	121.5	1.13	10.77	17.88	3.19	-	1.22	.074	
	59.3	870	.910	24.5	133.8	1.02	10.74	17.54	3.39	-	1.20	.079	
	59.1	871	.908	22.6	144.9	.94	10.87	17.59	3.38	-	1.25	.078	
	59.3	872	.909	19.9	164.1	.83	10.59	17.29	3.83	-	1.22	.089	
	59.3	873	.906	17.2	189.2	.72	9.84	15.69	4.96	-	1.19	.115	
	59.2	873	.908	15.2	214.3	.64	8.69	14.69	5.62	-	1.18	.130	
	59.4	869	.911	13.7	238.8	.57	8.94	14.84	5.79	-	1.16	.134	
	59.2	871	.909	10.7	305.0	.45	6.97	11.66	7.33	-	1.14	.171	
	59.4	869	.911	7.5	434.9	.31	2.89	6.78	34.53	-	1.12	.801	

TABLE XV (CONTINUED)

RESULTS OF COMBUSTION TESTS FOR COMBUSTOR A WITH NOZZLE A2.1 AND "CLOSED" VARIABLE-GEOMETRY SETTING

Design Nozzle Air Fuel Ratio = 4:1
Swirler Setting, ℓ_{sw} = .2 in
Secondary-Hole Setting, ℓ_{sy} = .4 in
Estimated Effective Primary-Zone Flow Rate = 11.8 per cent

Run No.	P_{o3} psia	T_{o3} deg F	$\dot{m}_a$ lbm per sec	$\dot{m}_{fu}$ lbm per hr	z	ϕ_p	EI_{NO} mg per gm fuel	EI_{NO_x} mg per gm fuel	EI_{CO} mg per gm fuel	EI_{HC} mg per gm fuel	ΔP per cent	$1-\eta_c$ per cent	TQ
56	58.8	903	1.316	43.0	110.2	1.14	9.66	15.70	.97	.17	2.61	.038	.13
	58.9	902	1.315	39.8	118.9	1.06	9.80	15.60	.93	.12	2.58	.033	
	58.9	902	1.315	36.9	128.3	.98	9.90	15.80	.75	.10	2.58	.027	
	58.6	903	1.311	33.9	139.3	.90	9.44	15.36	.75	.10	2.57	.027	
	58.9	903	1.302	32.1	146.0	.86	8.83	14.24	.78	.12	2.52	.030	
	58.7	898	1.304	22.1	212.3	.59	7.06	11.51	2.47	.97	2.47	.150	
	58.6	896	1.311	20.9	226.2	.55	6.59	10.82	2.41	.17	2.48	.072	
	58.3	899	1.309	18.6	253.7	.50	6.33	10.51	2.71	.07	2.54	.069	
	58.5	898	1.311	17.7	266.6	.47	6.09	10.19	3.10	.00	2.47	.072	
	58.3	899	1.308	13.5	350.1	.36	4.00	7.52	13.90	.59	2.49	.379	
	58.7	897	1.307	10.8	437.1	.29	1.81	5.01	47.40	9.98	2.41	2.053	

TABLE XVI

RESULTS OF COMBUSTION TESTS FOR COMBUSTOR A WITH NOZZLE A2.1 AND "PART OPEN" VARIABLE-GEOMETRY SETTING

Design Nozzle Air Fuel Ratio = 4:1
Swirler Setting, ℓ_{sw} = .3 in
Secondary-Hole Setting, ℓ_{sy} = .7 in
Estimated Effective Primary-Zone Flow Rate = 14.8 per cent

Run No.	P_{o3} psia	T_{o3} deg F	$\dot{m}_a$ lbm per sec	$\dot{m}_{fu}$ lbm per hr	Z	ϕ_p	EI_{NO} mg per gm fuel	EI_{NO_x} mg per gm fuel	EI_{CO} mg per gm fuel	EI_{HC} mg per gm fuel	ΔP per cent	$1-\eta_c$ per cent	TQ
60	39.5	900	.424	18.8	81.4	1.23	11.09	17.66	.72	.10	.54	.026	.11
	39.4	899	.436	16.7	93.6	1.07	12.53	19.67	.73	.21	.57	.037	
	39.5	897	.438	14.0	113.1	.88	9.45	14.85	.77	.21	.54	.038	
	39.5	897	.438	12.2	129.8	.77	8.26	13.08	.88	.21	.58	.040	
	39.8	898	.437	8.1	193.0	.52	6.83	11.08	1.31	.24	.51	.053	
61	39.5	899	1.139	48.3	84.9	1.18	12.54	20.19	1.74	.18	3.75	.058	.10
	39.5	899	1.141	41.0	100.2	1.00	10.06	16.06	1.76	.12	3.72	.052	
	39.2	899	1.141	36.1	113.7	.88	8.31	13.65	1.66	.09	3.81	.047	
	39.7	897	1.147	34.7	118.8	.84	7.32	11.79	1.50	.07	3.72	.042	
	39.8	894	1.152	30.2	137.4	.73	6.59	10.54	1.74	.08	3.68	.048	
	39.6	897	1.147	26.5	155.7	.64	6.00	9.70	2.12	.09	3.70	.057	
62	40.0	1105	1.074	47.3	81.7	1.22	15.41	24.94	1.04	.15	3.74	.038	.06
	40.0	1099	1.072	37.6	102.7	.97	14.48	23.30	1.25	.13	3.64	.041	
	39.6	1099	1.071	32.4	118.8	.84	13.39	21.30	1.39	.11	3.76	.043	
	39.8	1097	1.070	28.8	133.9	.75	10.33	16.17	1.56	.12	3.63	.048	
	39.7	1099	1.072	23.1	166.8	.60	7.73	11.99	1.78	.14	3.58	.055	
	39.4	1096	1.069	17.7	216.9	.46	6.09	9.68	2.63	.07	3.63	.067	
63	39.9	1150	1.057	35.0	108.7	.92	12.60	20.01	1.80	.61	3.72	.10	.26
	40.2	1150	1.061	31.2	122.6	.82	10.62	16.48	1.61	.22	3.63	.058	
	40.0	1147	1.063	28.4	134.8	.74	9.42	14.65	.98	.23	3.42	.044	
	39.8	1153	1.055	22.2	171.0	.58	7.48	11.46	.66	.29	3.50	.043	
	39.5	1154	1.051	18.0	210.4	.48	6.35	9.90	1.02	.32	3.53	.054	
	39.4	1149	1.051	16.4	231.3	.43	5.89	9.58	1.68	.42	3.54	.079	

TABLE XVI (CONTINUED)

RESULTS OF COMBUSTION TESTS FOR COMBUSTOR A WITH NOZZLE A2.1 AND "PART OPEN" VARIABLE-GEOMETRY SETTING

Design Nozzle Air/Fuel Ratio = 4:1
Swirler Setting, ℓ_{sw} = .3 in
Secondary-Hole Setting, ℓ_{sy} = .7 in
Estimated Effective Primary-Zone Flow Rate = 14.8 per cent

Run No.	P_{03} psia	T_{03} deg F	$\dot{m}_a$ lbm per sec	$\dot{m}_{fa}$ lbm per hr	Z	ϕ_p	EI_{NO} mg per gm fuel	EI_{NO_x} mg per gm fuel	EI_{CO} mg per gm fuel	EI_{HC} mg per gm fuel	ΔP per cent	$1-\eta_c$ per cent	TQ
64	58.7	907	.533	19.7	97.5	1.03	10.71	16.88	.48	.02	.33	.013	.20
	58.4	905	.532	17.4	110.2	.91	11.51	18.53	.54	.02	.34	.014	
	58.6	906	.533	15.3	125.2	.80	12.02	19.83	.98	.01	.40	.023	
	58.6	905	.529	12.3	154.6	.65	12.08	20.25	1.65	.02	.31	.041	
65	59.1	899	.949	41.5	82.4	1.21	15.10	25.27	.48	.28	1.13	.038	.07
	59.2	899	.959	36.0	95.7	1.04	15.42	25.18	.56	.13	1.24	.026	
	58.9	898	.957	30.1	114.4	.87	13.25	21.60	.45	.13	1.11	.023	
	58.7	901	.954	27.3	126.0	.79	11.70	19.14	.43	.14	1.11	.023	
	58.7	901	.954	24.0	143.1	.70	10.74	17.38	.42	.12	1.24	.021	
	58.7	896	.952	21.2	161.8	.62	9.60	15.76	.71	.27	.98	.042	
	58.5	899	.953	18.6	184.6	.54	9.22	14.73	.36	.17	1.13	.025	
	58.2	897	.951	13.3	256.8	.39	6.40	10.64	2.74	.26	1.10	.088	
	58.6	901	.953	7.2	479.2	.21	1.29	5.94	80.71	27.72	1.04	4.520	
66	59.2	897	1.396	63.6	79.0	1.27	13.74	22.84	1.24	.24	2.38	.052	.07
	58.3	897	1.390	55.1	90.8	1.10	12.73	20.68	1.20	.35	2.62	.061	
	58.6	898	1.393	49.8	100.7	.99	11.68	19.37	1.28	.30	2.57	.058	
	58.9	898	1.397	45.2	111.3	.90	11.39	18.71	1.08	.26	2.46	.050	
	58.5	898	1.392	40.5	123.7	.81	8.91	14.65	1.08	.25	2.53	.049	
	59.0	897	1.393	36.3	138.4	.72	8.37	13.93	.81	.19	2.38	.037	
	58.3	893	1.387	28.0	178.2	.56	6.77	11.09	1.21	.30	2.45	.067	
	58.6	891	1.392	21.0	239.1	.42	5.34	8.76	2.44	.42	2.27	.097	
	58.7	891	1.393	16.9	296.4	.34	4.56	7.79	5.46	.66	2.32	.189	

TABLE XVI (CONTINUED)

RESULTS OF COMBUSTION TESTS FOR COMBUSTOR A WITH NOZZLE A2.1 AND "PART OPEN" VARIABLE-GEOMETRY SETTING

Design Nozzle Air/Fuel Ratio = 4:1
Swirler Setting, ℓ_{sw} = .3 in
Secondary-Hole Setting, ℓ_{sy} = .7 in
Estimated Effective Primary-Zone Flow Rate = 14.8 per cent

Run No.	P_{03} psia	T_{03} deg F	$\dot{m}_a$ lbm per sec	$\dot{m}_{fu}$ lbm per hr	Z —	ϕ_p —	EI_{NO} mg per gm fuel	EI_{NO_x} mg per gm fuel	EI_{CO} mg per gm fuel	EI_{HC} mg per gm fuel	ΔP per cent	$1-\eta_c$ per cent	TQ
68	87.2	890	.654	36.6	64.3	1.56	12.83	22.27	.50	.13	.22	.024	.13
	88.0	890	.657	26.6	88.9	1.13	10.98	18.98	.61	.04	.21	.017	
	87.5	891	.655	22.5	104.7	.95	11.49	20.14	.66	.02	.24	.018	
	86.7	889	.652	18.9	124.5	.80	12.73	22.30	.85	.02	.24	.021	
	87.7	887	.656	14.3	165.6	.60	13.79	23.80	1.13	.03	.24	.029	
	87.9	887	.657	11.4	208.3	.48	13.22	23.36	1.52	.05	.23	.040	
	87.5	886	.656	7.5	314.8	.32	11.11	19.04	3.51	.14	.25	.095	
	87.9	888	.657	7.3	324.4	.31	11.79	20.66	4.40	.19	.23	.120	

TABLE XVII

SUMMARY OF TEST CONDITIONS EXAMINED WITH MODIFIED COMBUSTOR A*

Run No.	Modification No.**	Nozzle Combination***	ℓ_{sy} in	P_{t3} psia	T_{t3} deg F	$\dot{m}_a$ lbm/sec	Nozzle Air Pressure Drop, ΔP_{Noz} per cent of inlet pressure	$\bar{\tau}_p$ msec
71	1	M	.3	29	880	.595	23.8	18
72	↓	P	↓	↓	880	.605	25.3	17
73	↓	P	↓	52	890	.85	14.1	25
74	↓	M	↓	↓	885	.85	14.3	25
75	↓	M+P	↓	↓	905	.855	13.9	24
76	↓	M	↓	56	900	1.11	21.0	19
77	↓	P	↓	↓	900	1.11	21.2	18
78	↓	M	.6	32	905	.63	20.9	18
79	↓	P	↓	↓	905	.63	21.1	18
80	↓	M	↓	35	915	.755	29.5	14
81	↓	P	↓	↓	915	.755	29.5	14
82	2	M	.4	28	910	.575	12.4	17
83	↓	P	↓	↓	910	.58	12.3	17
84	↓	M+P	↓	↓	910	.58	12.3	17
85	↓	M+P	↓	30	905	.785	19.2	13

*All tests conducted with Nozzle A2.2 and secondary-hole setting (ℓ_{sy}) of 0.6 in.

**See Figure 31.

***M - Fuel through main airblast portion of nozzle only.
P - Fuel through pilot only.
M+P - Fuel through both pilot and main.

TABLE XVIII

CALCULATED NOZZLE AND SWIRLER AIR FLOWS FOR MODIFIED COMBUSTOR A

Modification No.*	Swirler Setting,** l_{sw} in	$\dot{m}_{FN}$ per cent	$\dot{m}_{sw}$ per cent	$\dot{m}_{p,eff}$ per cent
1	0.3	9.4	2.8	21.3
1	0.6	9.4	5.8	23.5
2	0.4	8.6	9.8	26.4

---

*See Figure 31.

**In all cases, the secondary-hole setting (l_{sy}) was 0.6 in.

TABLE XIX

RESULTS OF COMBUSTION TESTS FOR MODIFICATION NO. 1 OF COMBUSTOR A WITH NOZZLE A2.2 AND "CLOSED" SWIRLER SETTING

Design Nozzle Air/Fuel Ratio = 4:1
Swirler Setting, ℓ_{sw} = .3 in
Secondary-Hole Setting, ℓ_{sy} = .6 in
Estimated Effective Primary-Zone Flow Rate = 21.3 per cent

Run No.	P_{03} psia	T_{03} deg F	$\dot{m}_a$ lbm per sec	$\dot{m}_{fu}$ lbm per hr	Z	ϕ_p	EI_{NO} mg per gm fuel	EI_{NO_x} mg per gm fuel	EI_{CO} mg per gm fuel	EI_{HC} mg per gm fuel	ΔP_{Noz} per cent	$1-\eta_c$ per cent
71	28.7	880	.599	27.3	79.0	.88	4.97	8.38	1.78	-	24.41	.041
	28.7	880	.605	24.4	89.2	.78	3.92	6.44	1.96	-	25.43	.045
	29.1	880	.587	21.3	99.3	.70	2.91	4.93	2.03	-	22.67	.047
	29.1	880	.587	19.0	111.2	.63	1.74	2.97	4.23	-	22.67	.098
72	28.9	880	.608	24.5	89.2	.78	4.48	7.45	2.27	-	25.57	.053
	28.7	880	.605	20.5	106.1	.65	2.44	4.25	4.50	-	25.75	.104
	28.9	880	.603	17.9	121.4	.57	.96	1.94	16.31	-	24.52	.378
73	51.7	889	.851	27.1	113.1	.61	4.49	7.24	1.10	-	14.51	.026
	51.7	888	.848	26.6	114.9	.60	3.12	5.24	1.90	-	13.91	.044
	51.6	890	.851	24.6	124.4	.56	2.34	4.08	2.79	-	14.14	.065
	52.0	889	.850	23.5	130.5	.53	2.18	3.88	3.81	-	14.03	.088
74	51.5	885	.851	34.6	88.6	.78	8.44	13.50	.43	-	14.57	.010
	51.6	882	.854	29.6	103.7	.67	4.77	8.14	.56	-	14.32	.013
	51.6	884	.848	28.6	106.7	.65	2.68	4.53	3.12	-	14.14	.072
75	52.0	904	.844	39.8	76.4	.91	12.91	20.53	.97	-	13.63	.023
	52.0	905	.860	36.0	86.0	.81	9.28	14.64	1.09	-	14.42	.025
	52.0	905	.850	28.1	109.0	.64	5.01	8.21	1.38	-	13.82	.032
	51.9	904	.856	25.6	120.2	.58	2.13	3.62	1.64	-	14.04	.038
	51.7	903	.860	23.3	133.0	.52	1.73	3.08	2.20	-	13.90	.051
	51.7	903	.860	22.5	137.4	.51	1.43	2.74	2.54	-	13.90	.059
	51.7	903	.860	18.8	164.9	.42	1.10	2.26	9.94	-	13.90	.230
	51.7	903	.860	17.9	172.6	.40	.83	2.12	15.76	-	13.90	.366

TABLE XIX (CONTINUED)

RESULTS OF COMBUSTION TESTS FOR MODIFICATION NO. 1 OF COMBUSTOR A WITH NOZZLE A2.2 AND "CLOSED" SWIRLER SETTING

Design Nozzle Air/Fuel Ratio = 4:1
Swirler Setting, ℓ_{sw} = .3 in
Secondary-Hole Setting, ℓ_{sy} = .6 in
Estimated Effective Primary-Zone Flow Rate = 21.3 per cent

Run No.	P_{03} psia	T_{03} deg F	$\dot{m}_a$ lbm per sec	$\dot{m}_{fu}$ lbm per hr	Z	ϕ_p	EI_{NO} mg per gm fuel	EI_{NO_x} mg per gm fuel	EI_{CO} mg per gm fuel	EI_{HC} mg per gm fuel	ΔP_{NOZ} per cent	$1-\eta_c$ per cent
76	56.0	906	1.111	50.6	79.0	.88	10.8	17.3	1.159	-	21.1	.027
	56.4	903	1.108	44.7	89.3	.78	8.69	13.9	1.177	-	20.7	.027
	56.1	902	1.112	39.9	100.2	.69	6.08	9.56	1.271	-	21.0	.030
	56.4	900	1.116	36.5	110.1	.63	3.91	6.53	1.525	-	21.2	.035
	56.4	900	1.116	35.7	112.4	.62	2.70	4.41	2.85	-	21.2	.066
77	56.0	900	1.107	36.9	107.9	.64	6.09	9.68	1.473	-	20.9	.034
	56.0	900	1.113	36.8	109.0	.64	4.44	7.16	1.743	-	21.6	.040
	56.1	901	1.113	32.6	122.9	.57	2.95	4.82	2.75	-	21.4	.044
	56.4	902	1.109	27.7	144.2	.48	1.58	3.22	13.18	-	21.1	.306

TABLE XX

RESULTS OF COMBUSTION TESTS FOR MODIFICATION NO. 1 OF COMBUSTOR A WITH NOZZLE A2.2 AND "OPEN" SWIRLER SETTING

Design Nozzle Air/Fuel Ratio = 4:1
Swirler Setting, ℓ_{sw} = .6 in
Secondary-Hole Setting, ℓ_{sy} = .6 in
Estimated Effective Primary-Zone Flow Rate = 23.5 per cent

Run No.	P_{03} psia	T_{03} deg F	$\dot{m}_a$ lbm per sec	$\dot{m}_{fu}$ lbm per hr	Z	ϕ_p	EI_{NO} mg per gm fuel	EI_{NO_x} mg per gm fuel	EI_{CO} mg per gm fuel	EI_{HC} mg per gm fuel	ΔP_{NOZ} per cent	$1-\eta_c$ per cent
78	31.7	905	.630	27.9	81.4	.77	4.26	6.80	1.15	.00	20.7	.027
	31.7	904	.630	25.6	88.5	.71	2.96	4.97	1.43	.00	21.7	.033
	31.7	906	.626	22.7	99.2	.64	1.91	3.05	3.05	.00	20.7	.071
	31.8	907	.625	20.4	110.1	.57	1.15	2.38	34.87	.00	20.6	.809
79	31.8	906	.627	33.2	67.9	.93	6.21	10.17	1.26	.12	20.7	.041
	32.1	907	.633	28.3	80.5	.78	5.73	9.31	1.46	.01	20.8	.035
	32.2	908	.630	25.1	90.4	.70	4.92	7.83	1.72	.00	21.0	.040
	32.0	910	.628	20.5	110	.57	2.22	3.79	3.97	.00	20.9	.092
	31.9	906	.631	19.6	115.9	.54	1.75	3.06	6.66	.00	21.2	.155
	31.9	906	.633	18.0	126.5	.50	.369	1.62	59.8	3.10	21.5	1.684
	31.9	906	.633	16.7	136.3	.46	.291	1.42	>66.4	22.90	21.5	>3.727
	31.9	906	.633	16.2	140.4	.45	.293	1.12	>68.3	51.60	21.5	>6.512
80	34.7	913	.750	41.9	64.4	.98	5.82	9.76	1.65	.20	29.1	.057
	34.6	914	.755	38.2	71.1	.89	5.07	8.46	1.71	.11	29.5	.050
	34.6	915	.753	33.7	80.5	.78	4.05	6.72	1.69	.00	29.2	.039
	34.7	915	.759	32.5	84.0	.75	3.43	5.73	1.80	.00	29.7	.042
	34.7	917	.760	29.6	92.3	.68	2.30	4.15	2.48	.00	29.7	.058
	34.7	919	.753	25.7	105.3	.60	0.92	1.94	18.69	.90	29.5	.520

TABLE XX (CONTINUED)

RESULTS OF COMBUSTION TESTS FOR MODIFICATION NO. 1 OF COMBUSTOR A WITH NOZZLE A2.2 AND "OPEN" SWIRLER SETTING

Design Nozzle Air/Fuel Ratio = 4:1
Swirler Setting, l_{sw} = .6 in
Secondary-Hole Setting, l_{sy} = .6 in
Estimated Effective Primary-Zone Flow Rate = 23.5 per cent

Run No.	P_{03} psia	T_{03} deg F	$\dot{m}_a$ lbm per sec	$\dot{m}_{fu}$ lbm per hr	Z	ϕ_p	EI_{NO} mg per gm fuel	EI_{NO_x} mg per gm fuel	EI_{CO} mg per gm fuel	EI_{HC} mg per gm fuel	ΔP_{Noz} per cent	$1-\eta_c$ per cent
81	34.6	917	.757	35.7	76.4	.82	5.29	8.84	1.55	.24	29.8	.058
	34.7	915	.750	32.7	82.6	.76	4.68	7.70	1.58	.06	29.1	.043
	34.5	916	.751	29.7	91.1	.69	3.62	6.14	1.95	.00	29.6	.045
	34.6	915	.758	27.5	99.2	.63	2.70	4.61	2.41	.00	29.5	.056
	34.7	918	.753	24.9	108.9	.58	1.82	3.23	3.62	.00	29.1	.084
	34.5	915	.752	24.0	112.6	.56	1.01	1.98	10.75	.00	29.6	.249
	34.5	915	.752	23.4	115.8	.54	.75	1.61	19.74	.53	29.6	.509
	34.5	915	.752	23.0	117.4	.54	.64	1.56	24.14	.65	29.6	.622
	34.5	915	.752	22.6	119.6	.53	.41	1.42	36.10	1.83	29.6	1.013
	34.5	915	.752	22.4	120.7	.52	.27	1.35	50.18	3.70	29.6	1.517

TABLE XXI

RESULTS OF COMBUSTION TESTS FOR MODIFICATION NO. 2 OF COMBUSTOR A WITH NOZZLE A2.2

Design Nozzle Air/Fuel Ratio = 4:1
Swirler Setting, ℓ_{sw} = .4 in
Secondary-Hole Setting, ℓ_{sy} = .6 in
Estimated Effective Primary-Zone Flow Rate = 26.4 per cent

Run No.	P_{03} psia	T_{03} deg F	$\dot{m}_a$ lbm per sec	$\dot{m}_{fn}$ lbm per hr	Z	ϕ_p	EI_{NO} mg per gm fuel	EI_{NO_x} mg per gm fuel	EI_{CO} mg per gm fuel	EI_{HC} mg per gm fuel	ΔP_{Noz} per cent	$1-\eta_c$ per cent
82	27.8	914	.568	31.1	65.8	.85	4.98	8.38	1.13	-	12.27	.026
	27.9	912	.582	27.2	77.0	.73	3.71	6.31	1.73	-	12.70	.040
	27.9	911	.580	25.1	83.2	.67	3.31	5.55	3.90	-	12.54	.091
	27.9	911	.580	24.0	86.8	.65	2.73	5.09	7.55	-	12.54	.175
83	28.0	909	.577	25.8	80.5	.70	5.23	8.53	1.38	-	12.44	.032
	23.0	910	.581	23.6	88.5	.63	4.58	7.67	1.99	-	12.46	.046
	28.0	909	.573	21.0	98.3	.57	3.65	6.06	3.93	-	12.15	.091
	27.8	909	.586	17.9	118.2	.47	1.11	2.69	35.91	-	12.78	.833
	27.8	909	.586	17.4	121.5	.46	.79	2.59	49.12	-	12.78	1.140
	27.8	909	.586	16.4	128.3	.44	.40	1.85	>62.0	-	12.78	>1.438
84	27.9	908	.578	34.5	60.3	.93	6.53	11.28	.98	-	12.15	.023
	28.0	908	.581	30.3	69.0	.81	5.00	8.33	1.01	-	12.29	.023
	27.8	908	.579	26.5	78.7	.71	3.96	6.70	1.04	-	12.58	.024
	27.8	906	.578	25.6	81.4	.69	3.80	6.08	1.07	-	12.38	.025
	27.9	907	.583	23.8	88.2	.64	3.14	5.23	1.33	-	12.54	.031
	27.8	905	.585	19.4	108.7	.52	1.87	3.13	6.94	-	12.60	.161
	27.8	905	.585	18.7	112.6	.50	1.53	2.88	10.32	-	12.60	.239
	27.8	905	.585	18.4	114.5	.49	1.48	2.82	11.92	-	12.60	.277
	27.8	905	.585	18.3	115.0	.49	1.20	2.61	23.30	-	12.60	.541
85	30.1	906	.781	43.6	64.5	.87	4.47	7.79	.70	-	18.75	.016
	30.0	907	.784	38.7	72.8	.77	4.01	6.79	.89	-	19.49	.021
	30.0	904	.790	33.9	84.0	.67	3.21	5.60	1.19	-	19.45	.028
	30.0	905	.780	29.1	96.6	.58	2.22	3.95	1.70	-	19.19	.039
	30.1	905	.785	26.4	107.1	.52	1.39	2.57	7.05	-	19.05	.163

TABLE XXII

HOT-TEST MEASUREMENTS

Parameter	Instrument
Air-flow rate	Orifice plate
Fuel-flow rate	Flow meter
Inlet pressure	Static pressure tap and pressure gauge
Pressure difference across combustor	Static pressure taps and manometer
Inlet temperature	Thermocouple
Temperature distribution at exit of combustor	High-temperature probes with two-dimensional traversing mechanism
Temperature of combustor liner	Temperature sensitive paints
Chemical composition of exhaust products	Two fixed rakes with continuous analysis of sample

TABLE XXIII

RADIAL COORDINATES OF EXIT TEMPERATURE TRAVERSE FOR EACH THERMOCOUPLE PROBE

Radial Coordinate, in	
Combustor A	Combustor B
0.76	0.44
1.84	1.06
2.39	1.38
2.84	1.63
3.22	

TABLE XXIV

SPECIFICATIONS OF THE EMISSION INSTRUMENTS

Pollutant Species	Method	Instrument Model	Ranges	Accuracy
Nitric Oxide and Total NOx	Chemiluminescent	TECO Model 10A	2.5, 10, 25, 100, 250, 1000, 2500, 10,000, ppm	± 1% Full-scale or better.
Carbon Monoxide	Nondispersive Infrared (NDIR)	Beckman Model 315A	0 - 100 ppm 0 - 500 ppm	± 2% full-scale ± 1% full-scale
Carbon Dioxide	NDIR	Beckman Model 315A	0 - 2% 0 - 5%	± 1% full-scale
Total Hydrocarbons	Flame Ionization Detector (FID)	Beckman Model 402	x1, 5, 10, 50, 100, 500, 1000, 5000	5 ppm to 10% full-scale as CH_4
Smoke	ARP 1179 (Ref 22)	Photovolt Model 670	0 - 100	± 1/2%

TABLE XXV

HOT RIG FLOW CONDITIONS MODELED IN CONDUCTING SPRAY ANALYSIS TESTS OF NOZZLE A2.2

Swirler Setting, ℓ_{sw} (in)	P_{03} (psia)	T_{03} (deg F)	$\dot{m}_a$ (lbm per sec)	$\dot{m}_{fu}$ (lbm per hr)	ΔP (per cent)
0.2*	24	1180	0.77	11	6.8
0.3**	40	1150	1.05	28	3.5

---

* "Closed" corresponding to idle setting.

** "Part open" corresponding to 50 per cent power setting.

TABLE XXVI

EXPERIMENTALLY DETERMINED DROPLET SIZE DISTRIBUTION FOR NOZZLE A2.2

Size Group (microns)	Per Cent of Total Drops	Per Cent of Total Fuel Mass
	(a) $\ell_{sw} = 0.2$ in	
	SMD = 54 microns	
8-16	31.35	0.8
16-32	25.84	5.2
32-64	41.98	67.4
64-128	0.64	8.2
128-192	0.13	7.7
192-256	0.07	10.7
	(b) $\ell_{sw} = 0.3$ in	
	SMD = 57 microns	
8-16	41.27	1.1
16-32	24.94	5.5
32-64	32.65	57.4
64-128	0.95	13.3
128-192	0.13	8.7
192-256	0.04	7.1
320-384	0.01	6.9

FIGURES

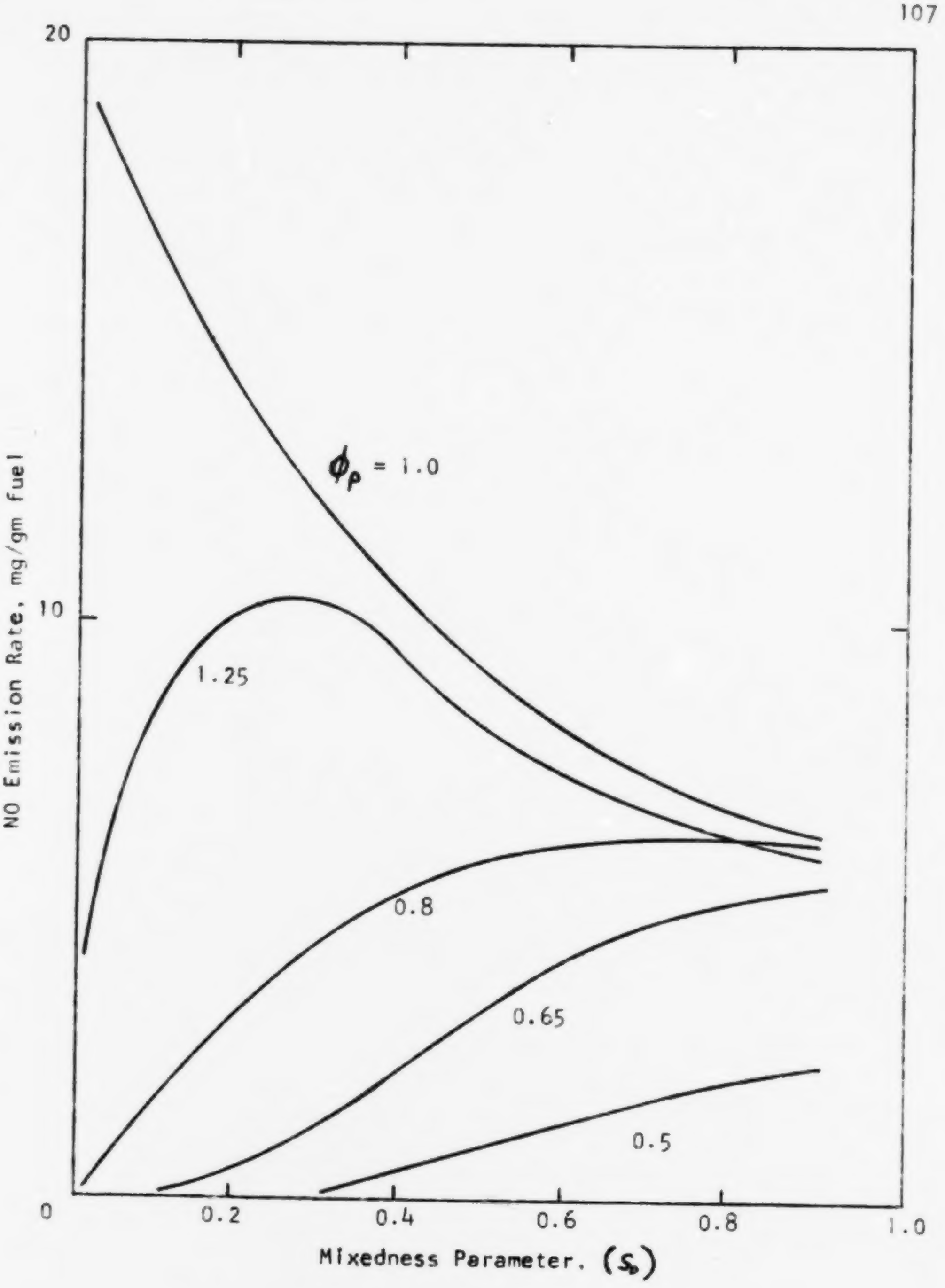

FIGURE 1 - EFFECTS OF FUEL DISTRIBUTION ON PREDICTED NO EMISSION RATE FOR REPRESENTATIVE AIRCRAFT GAS TURBINE COMBUSTOR (REF 2)

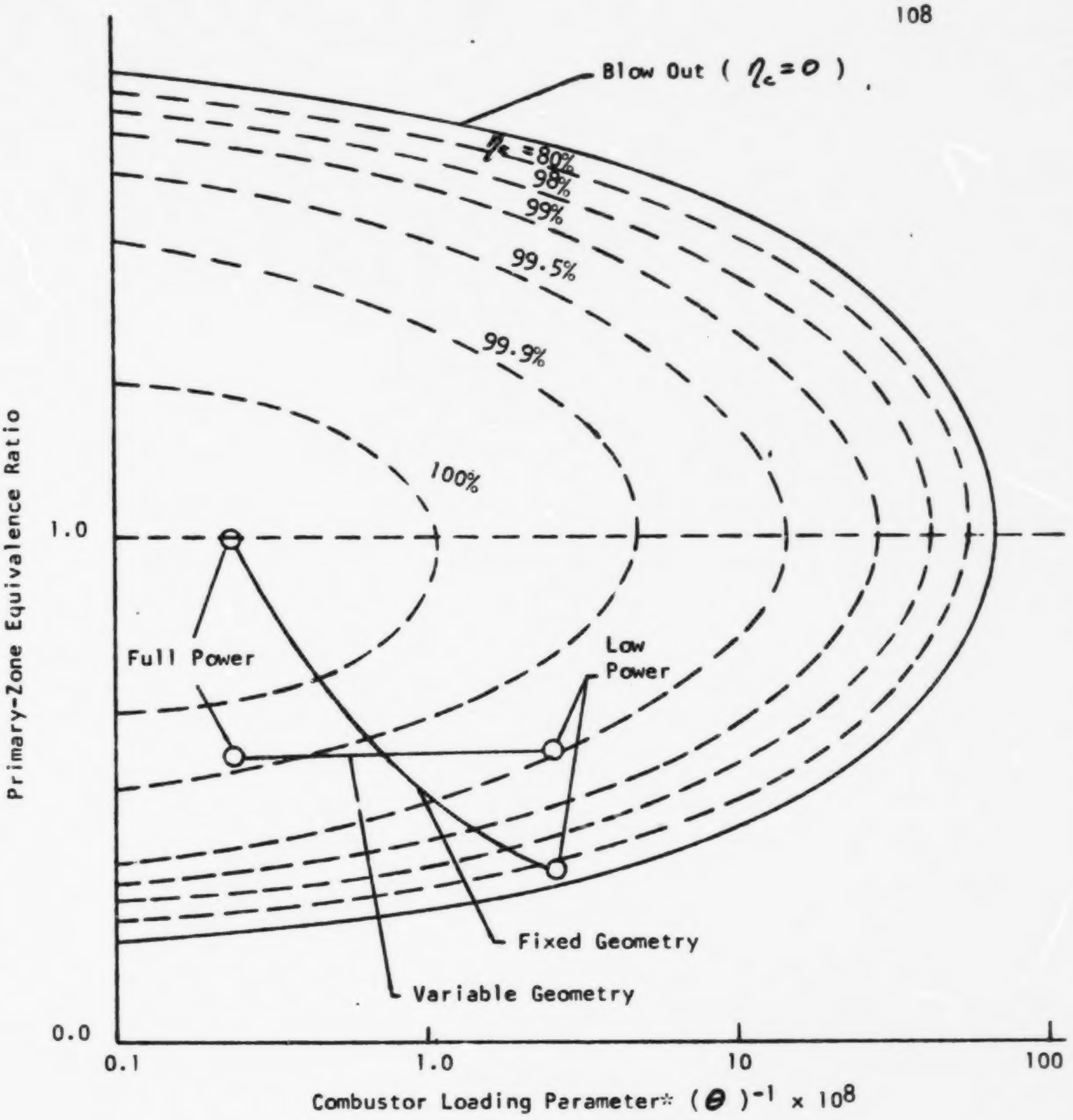

$$\frac{1}{\theta} = \frac{\dot{m}_a}{P_{03}^{1.75} A_{ref} D_{ref}^{0.75} \exp(T_{03}/b)}$$

* Typical values plotted in lbm, lbf, ft, sec, deg R units

FIGURE 2 - COMBUSTION PERFORMANCE MAP FOR FIXED AND VARIABLE-GEOMETRY COMBUSTORS

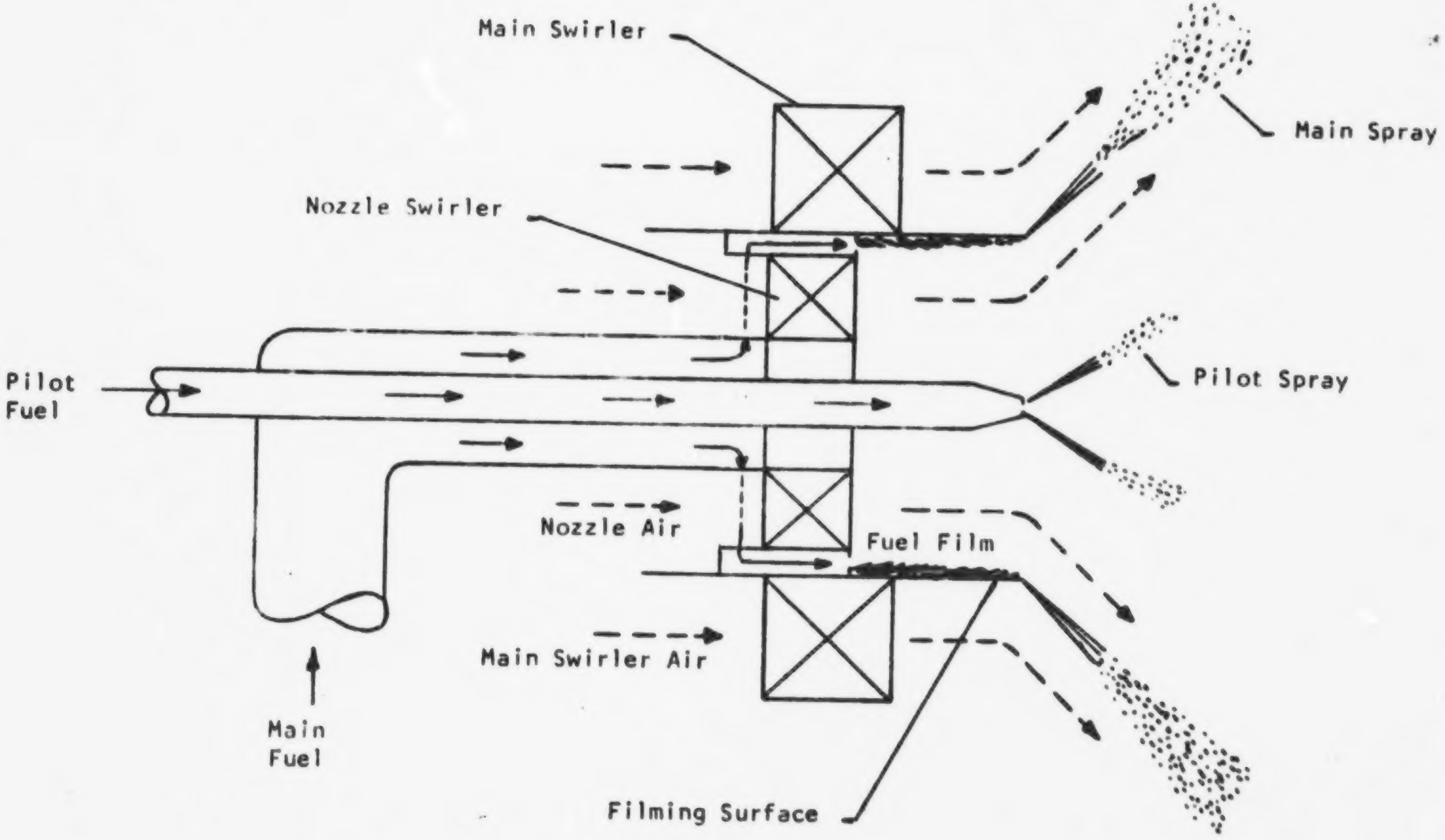
Main Swirler
Main Spray
Nozzle Swirler
Pilot Fuel
Pilot Spray
Nozzle Air
Fuel Film
Main Swirler Air
Main Fuel
Filming Surface

FIGURE 3 - GENERAL CONFIGURATION OF A PILOTED AIRBLAST NOZZLE

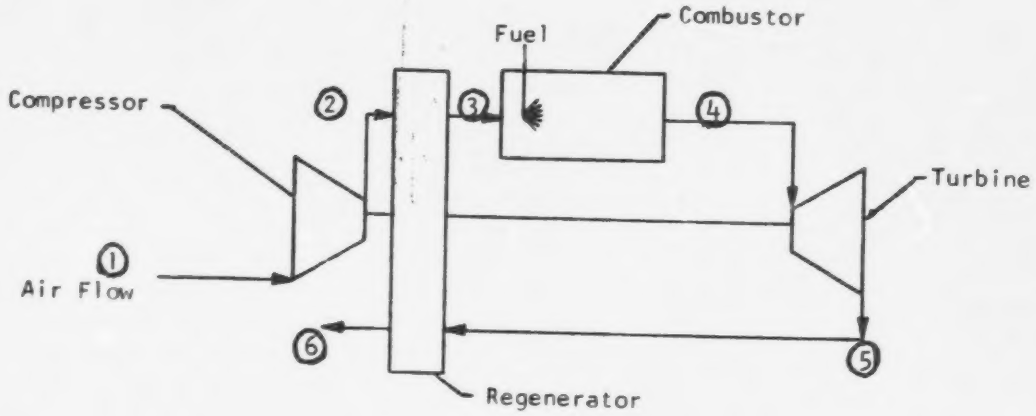
Combustor
Fuel
Compressor
②
③
④
Turbine
①
Air Flow
⑥
⑤
Regenerator

a. Class A Cycle (Regenerative)

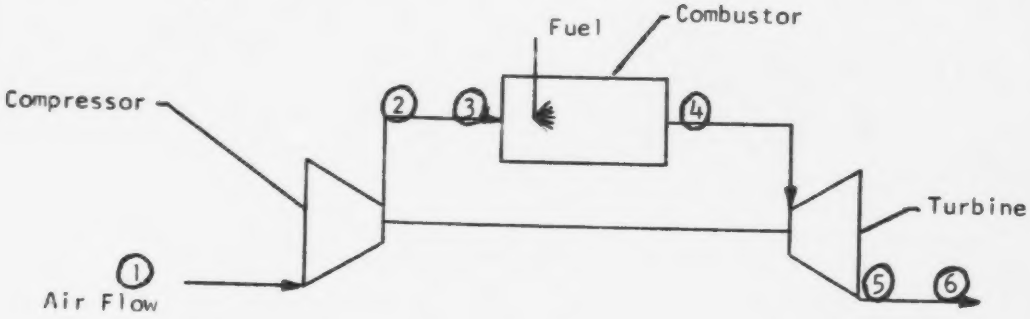
Combustor
Fuel
Compressor
②
③
④
Turbine
①
Air Flow
⑤
⑥

b. Class B Cycle (Nonregenerative)

FIGURE 4 - DIAGRAMMATIC REPRESENTATION OF CLASS A AND CLASS B CYCLES

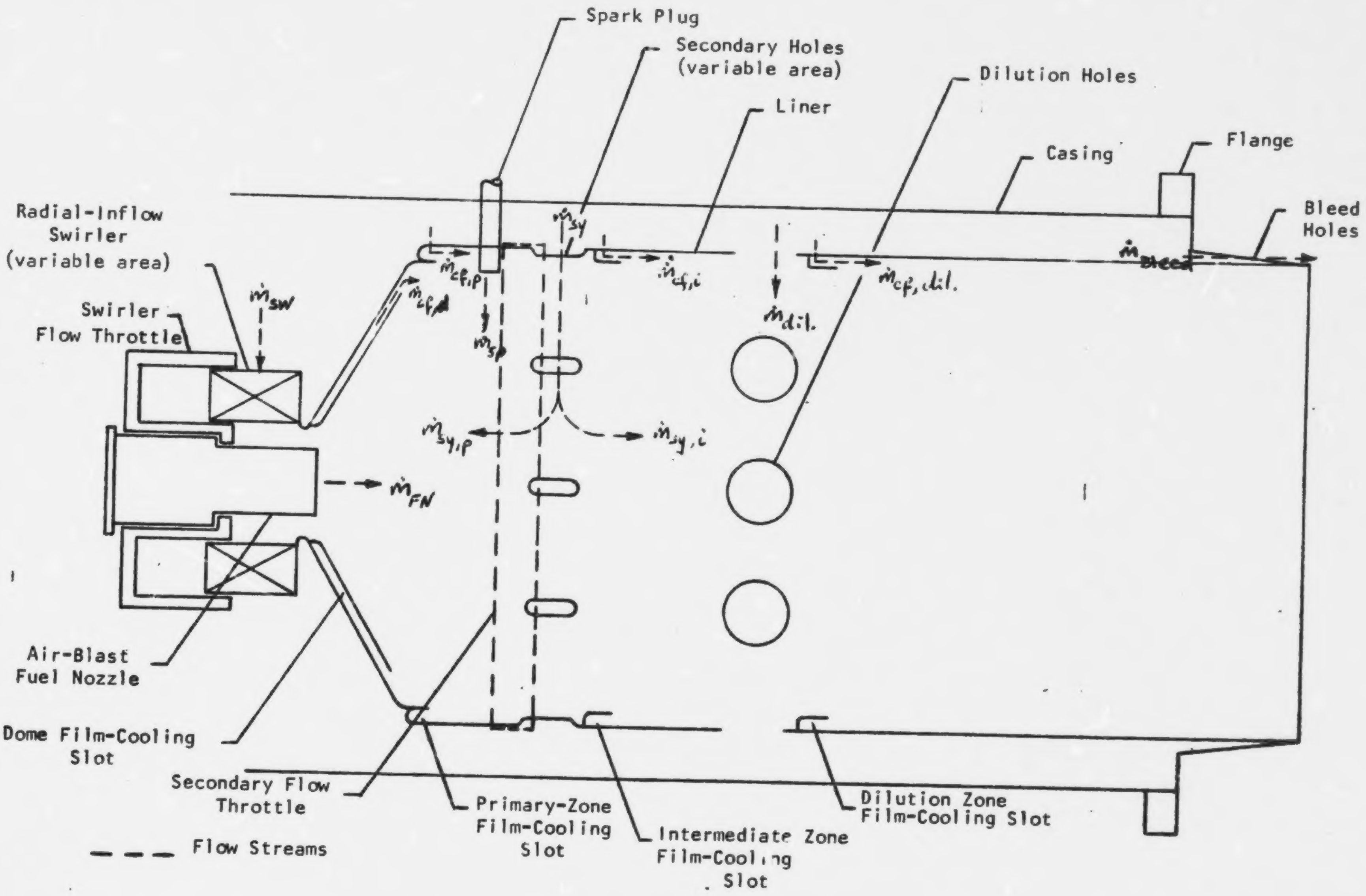
Spark Plug
Secondary Holes (variable area)
Dilution Holes
Liner
Casing
Flange
Bleed Holes
Radial-Inflow Swirler (variable area)
Swirler Flow Throttle
Air-Blast Fuel Nozzle
Dome Film-Cooling Slot
Secondary Flow Throttle
Primary-Zone Film-Cooling Slot
Intermediate Zone Film-Cooling Slot
Dilution Zone Film-Cooling Slot
Flow Streams
$\dot{m}_{SW}$
$\dot{m}_{cf,d}$
$\dot{m}_{cf,p}$
$\dot{m}_{sp}$
$\dot{m}_{sy}$
$\dot{m}_{sy,p}$
$\dot{m}_{sy,i}$
$\dot{m}_{cf,i}$
$\dot{m}_{dil.}$
$\dot{m}_{cf,dil.}$
$\dot{m}_{Bleed}$
$\dot{m}_{FN}$

FIGURE 5 - GENERAL CONFIGURATION OF COMBUSTORS

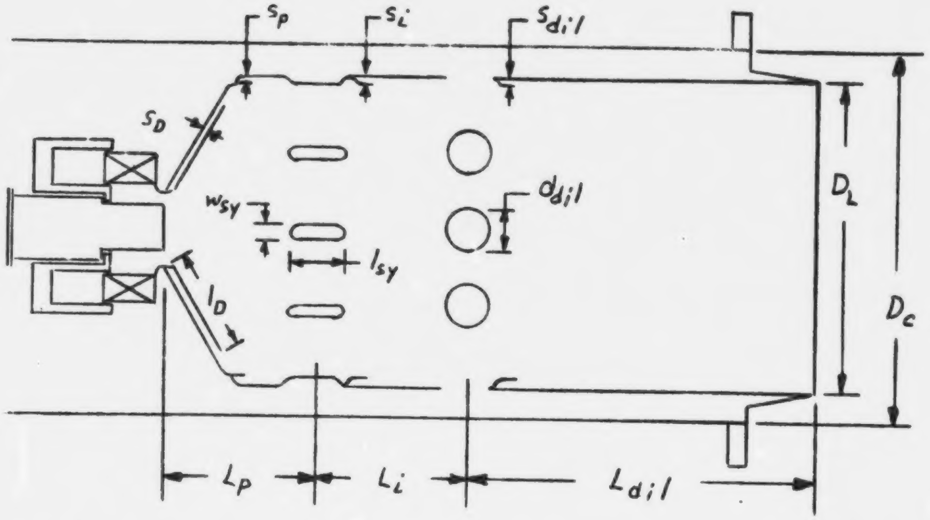
s_p
s_i
s_{dil}
s_D
w_{sy}
d_{dil}
l_{sy}
l_D
D_L
D_c
L_p
L_i
L_{dil}

Dimensions, in	Combustor A	Combustor B
D_c	8.3	4.4
D_L	6.8	3.5
L_p	3.4	1.8
L_i	3.4	1.8
L_{Dil}	7.8	4.4
l_{sy}	1.2	0.75
w_{sy}	0.24	0.15
d_{dil}	0.77	0.47
s_p	0.20	0.10
s_i	0.20	0.10
s_{dil}	0.20	0.10
s_D	0.10	0.10
l_D	2.4	0.60
No. of Secondary Holes	8	8
No. of Dilution Holes	8	4

FIGURE 6 - FINAL DESIGN CONFIGURATIONS

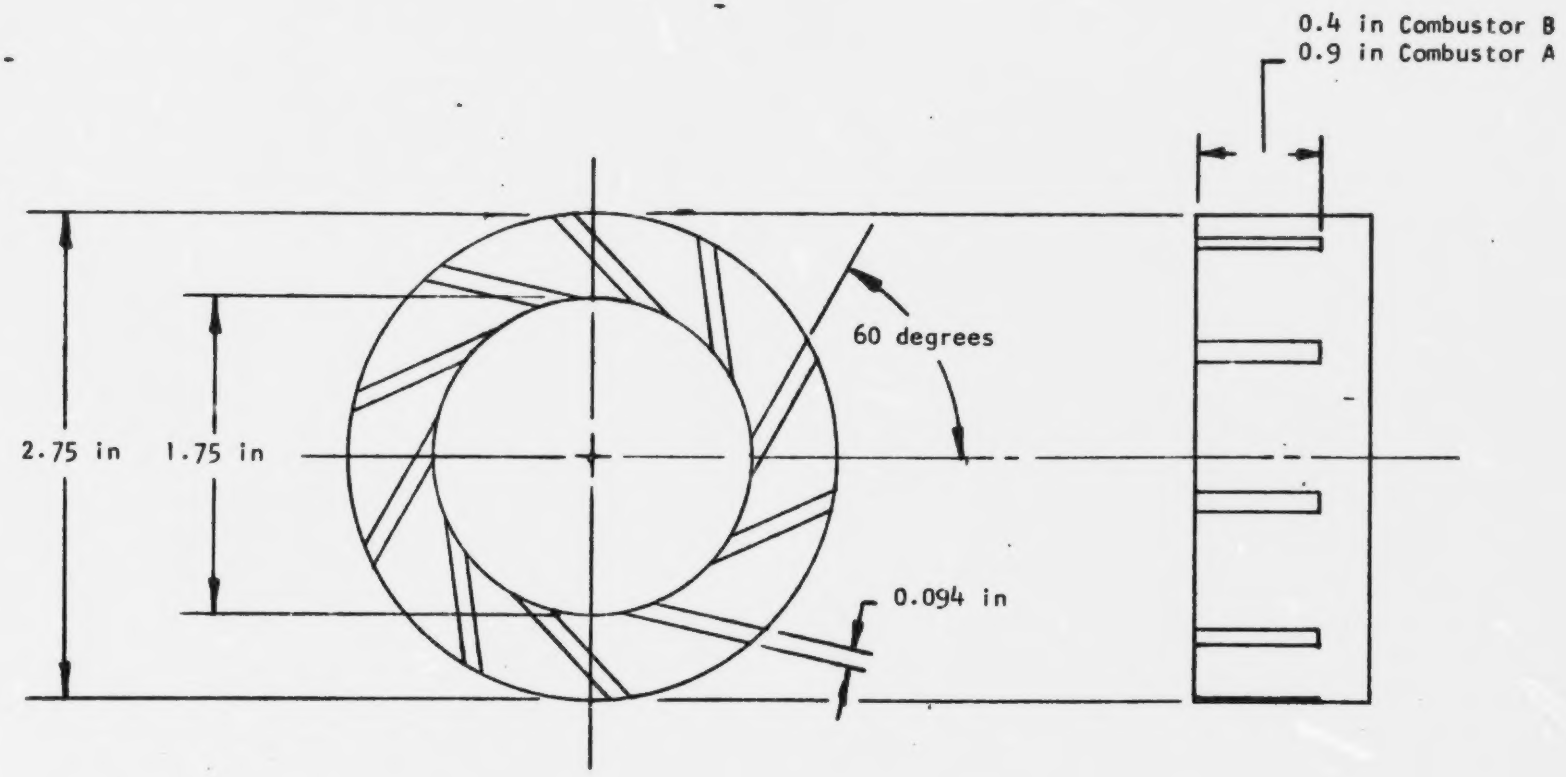
0.4 in Combustor B
0.9 in Combustor A
60 degrees
2.75 in
1.75 in
0.094 in

FIGURE 7 - RADIAL SWIRLER DESIGN

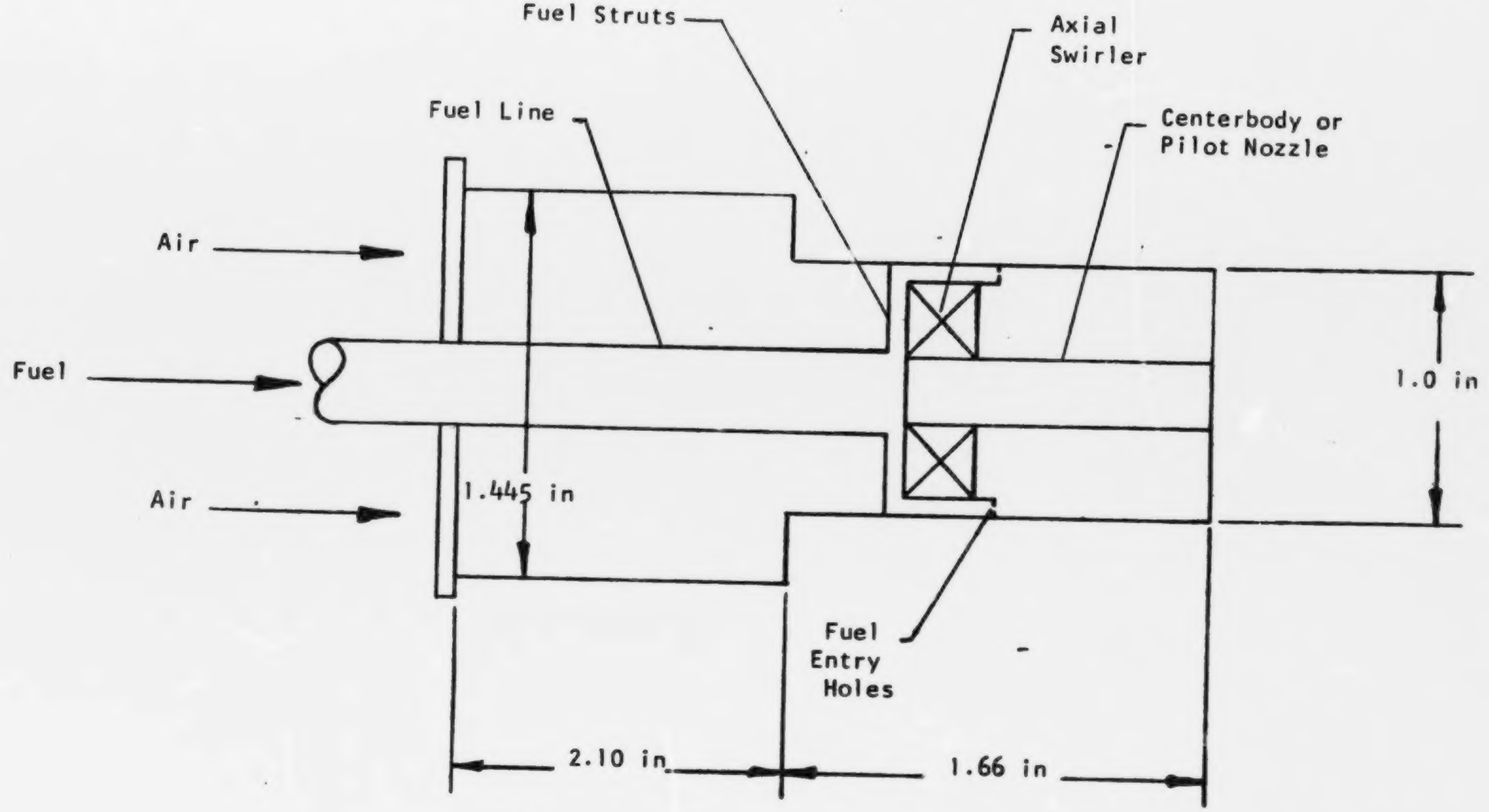
Fuel Struts
Axial Swirler
Fuel Line
Centerbody or Pilot Nozzle
Air
Fuel
Air
1.445 in
1.0 in
Fuel Entry Holes
2.10 in
1.66 in

FIGURE 8 - AIRBLAST NOZZLE CONFIGURATION

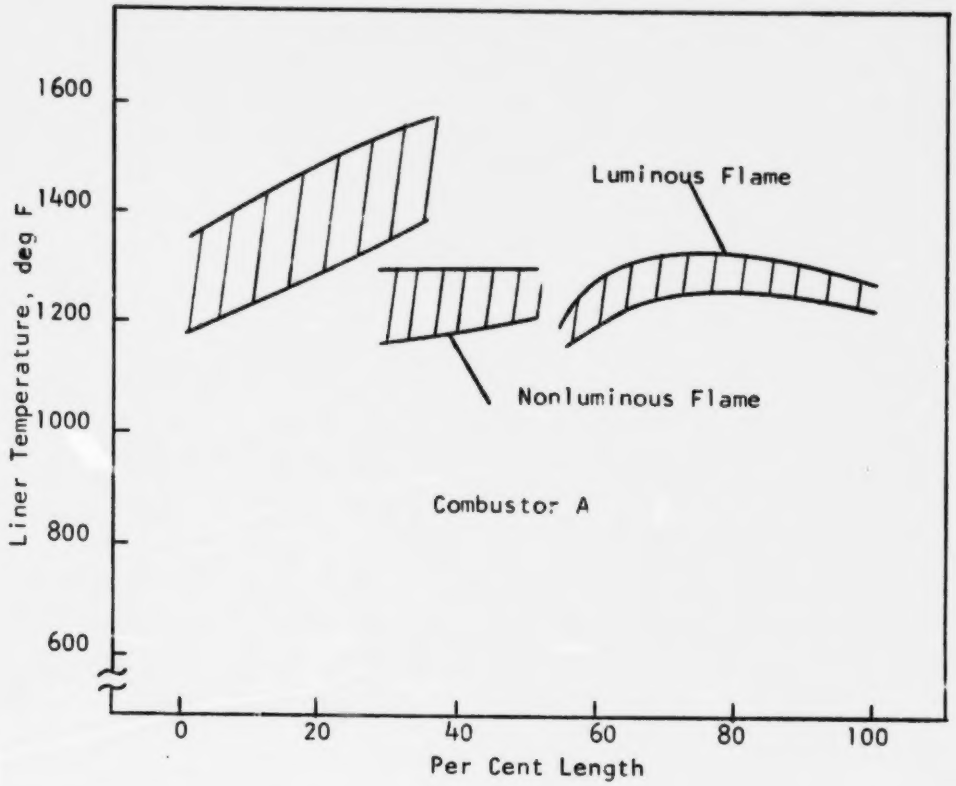

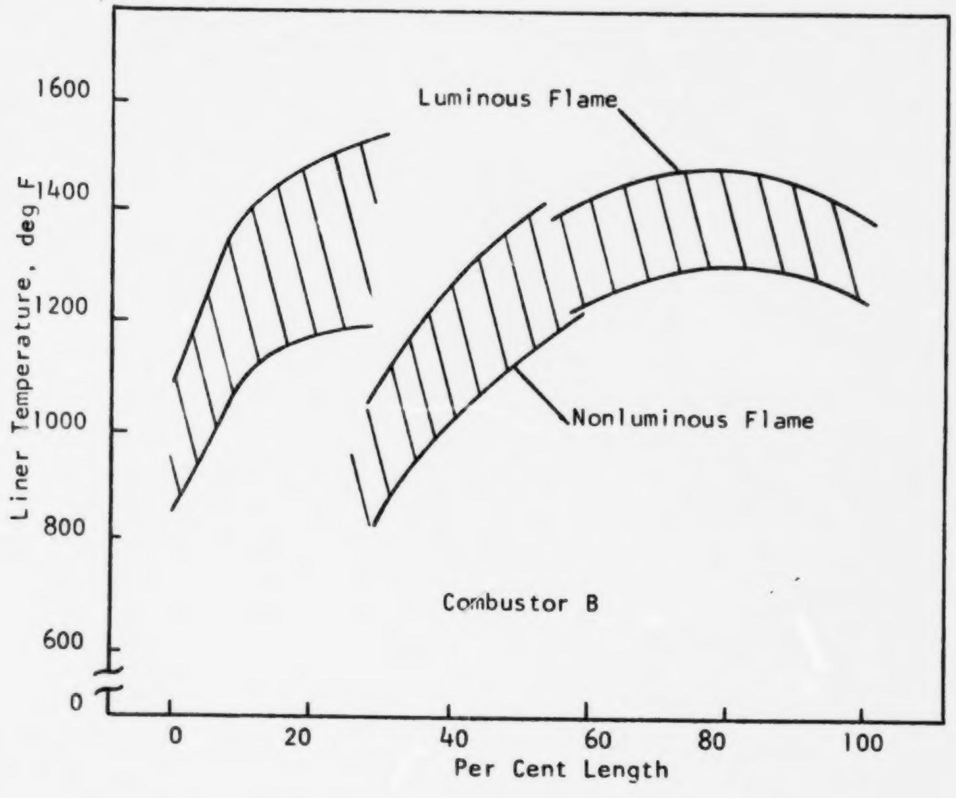

FIGURE 9 - ESTIMATED AXIAL DISTRIBUTIONS OF LINER TEMPERATURE

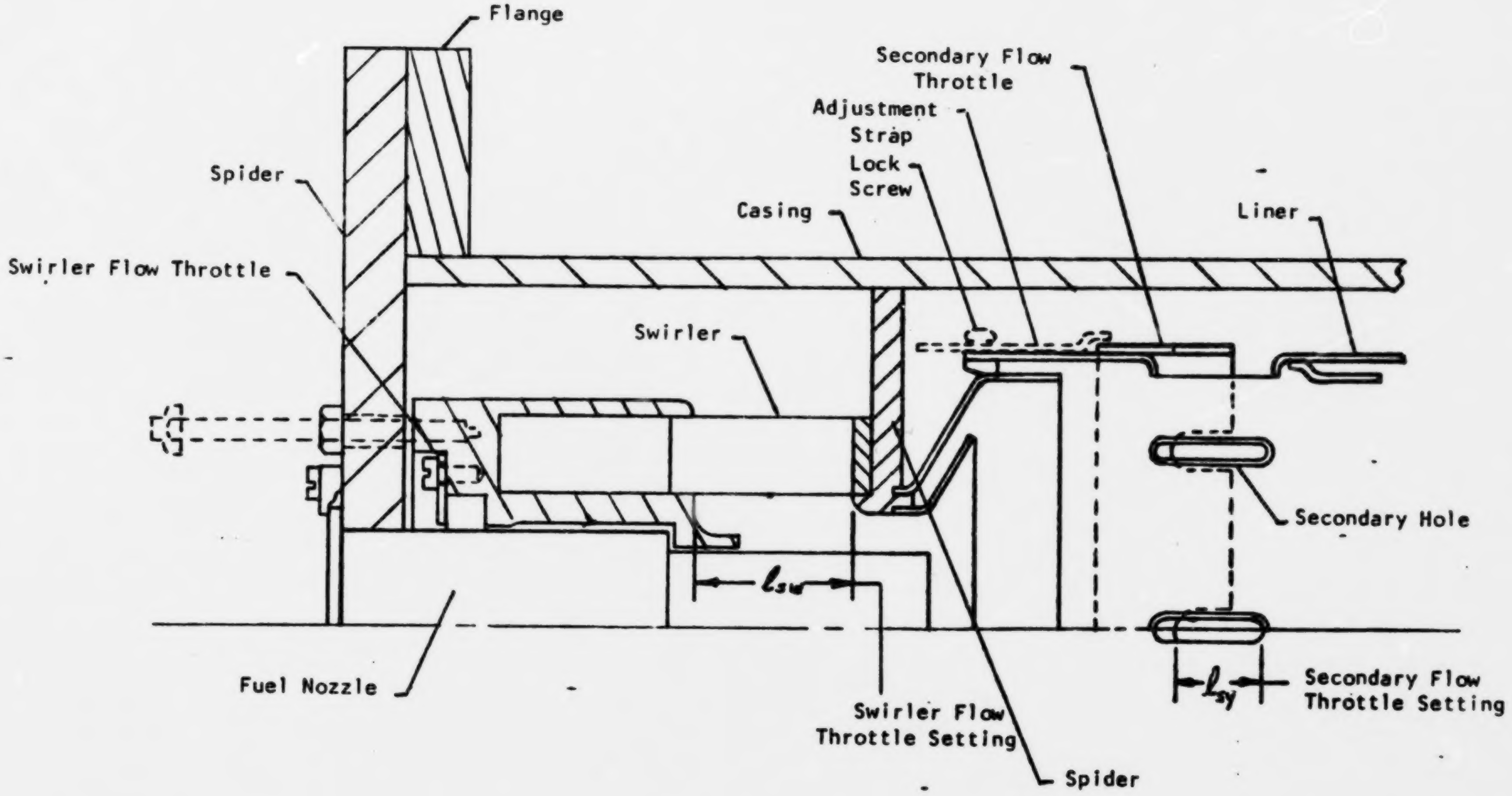
Flange
Spider
Swirler Flow Throttle
Secondary Flow Throttle
Adjustment Strap
Lock Screw
Casing
Liner
Swirler
Secondary Hole
l_{sw}
Fuel Nozzle
Swirler Flow Throttle Setting
Spider
l_{sy}
Secondary Flow Throttle Setting

FIGURE 10 - VARIABLE-GEOMETRY CONFIGURATION

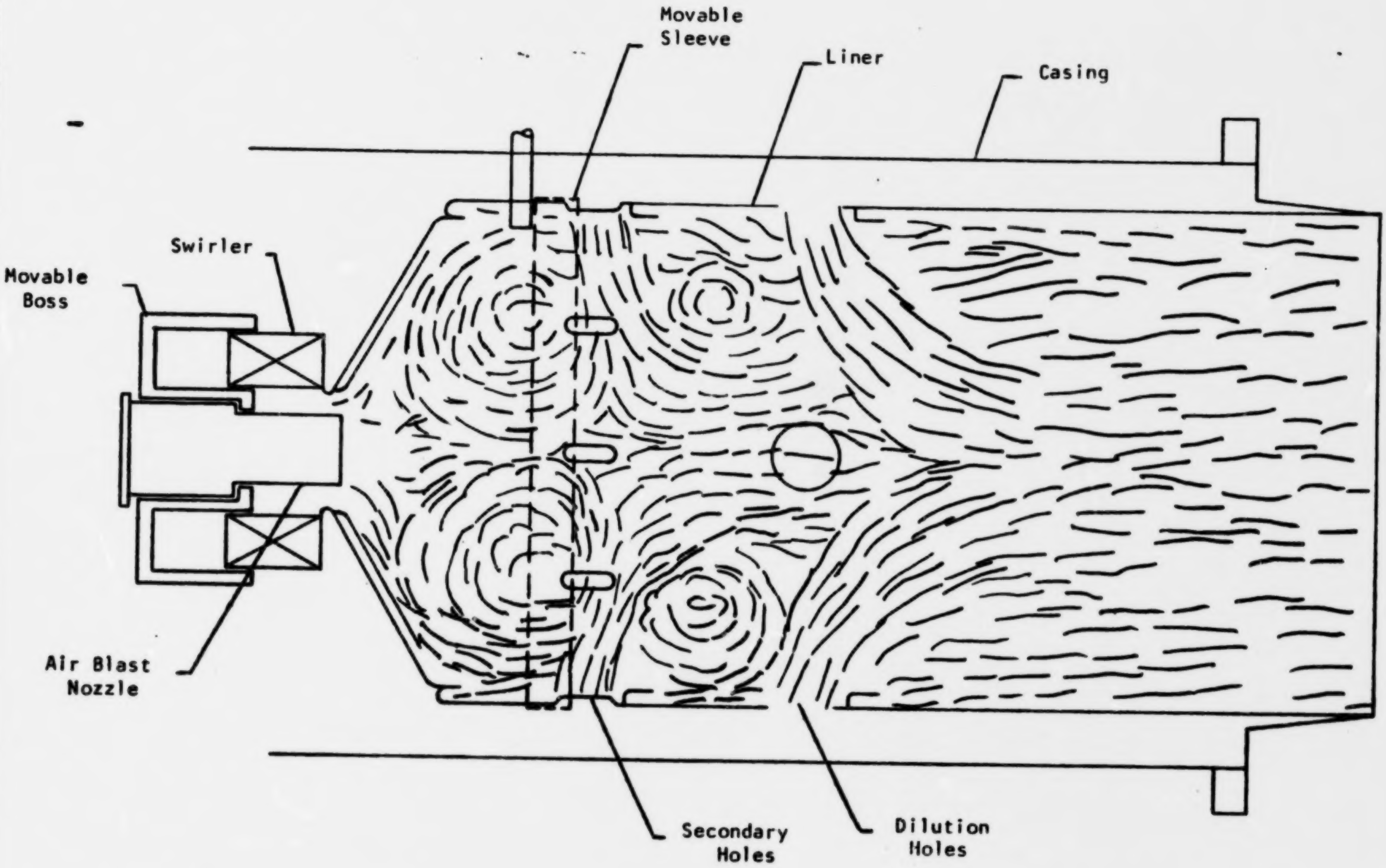
Movable Sleeve
Liner
Casing
Swirler
Movable Boss
Air Blast Nozzle
Secondary Holes
Dilution Holes

FIGURE 11 - GENERAL FLOW PATTERN OBSERVED IN FLOW VISUALIZATION TESTS

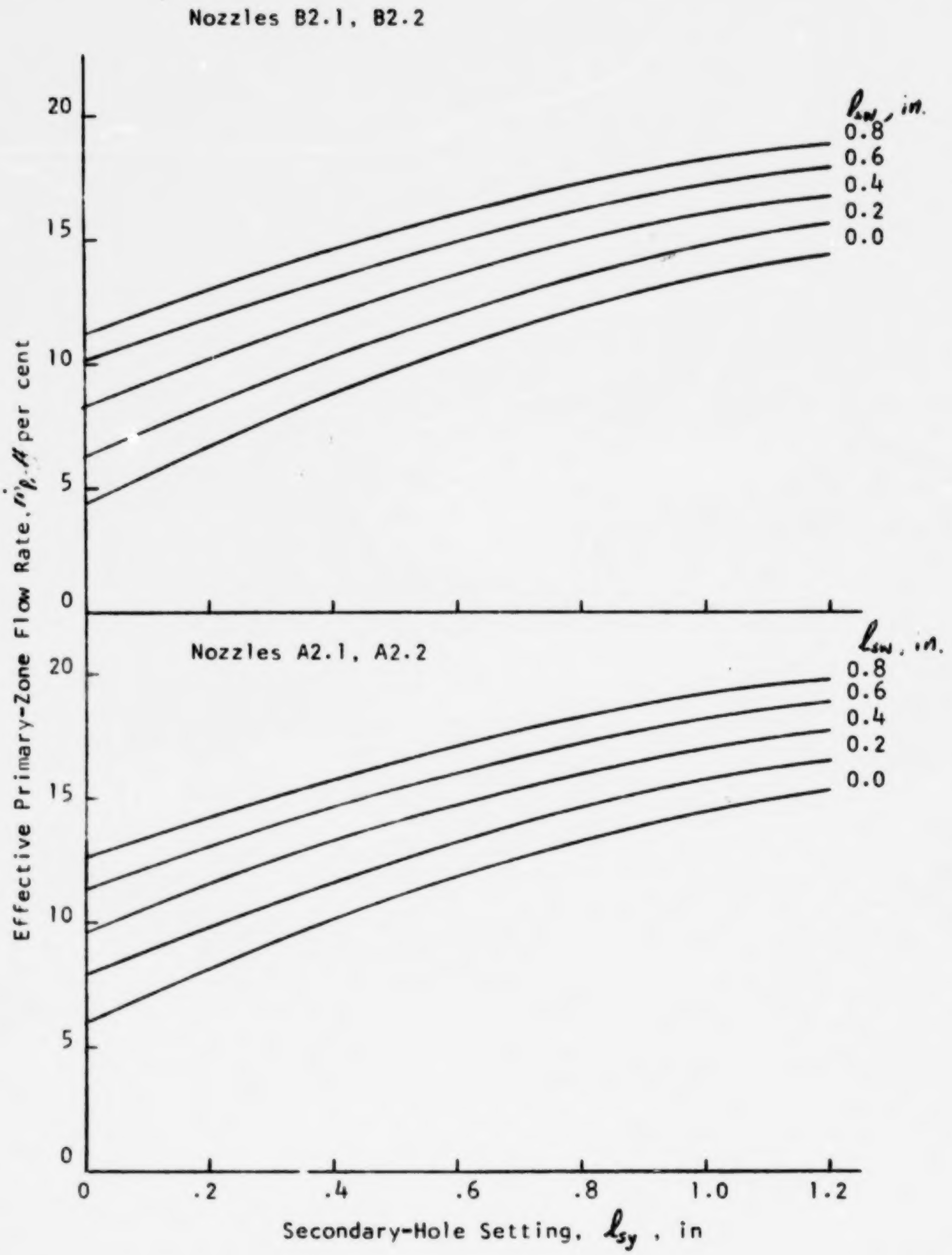

FIGURE 12 - VARIATION OF EFFECTIVE PRIMARY-ZONE FLOW RATE FOR COMBUSTOR A

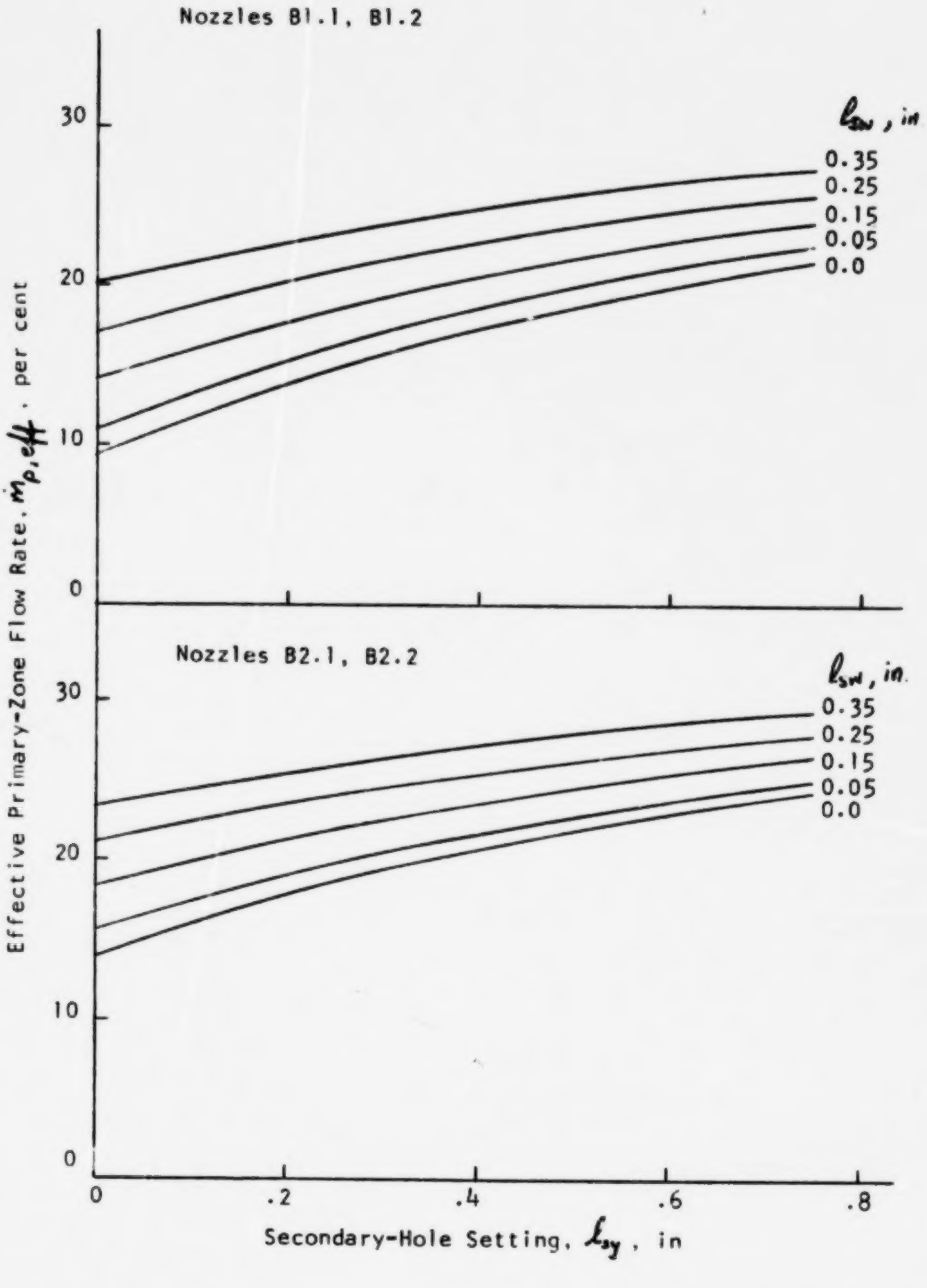

FIGURE 13 - VARIATION OF EFFECTIVE PRIMARY-ZONE FLOW RATE FOR COMBUSTOR B

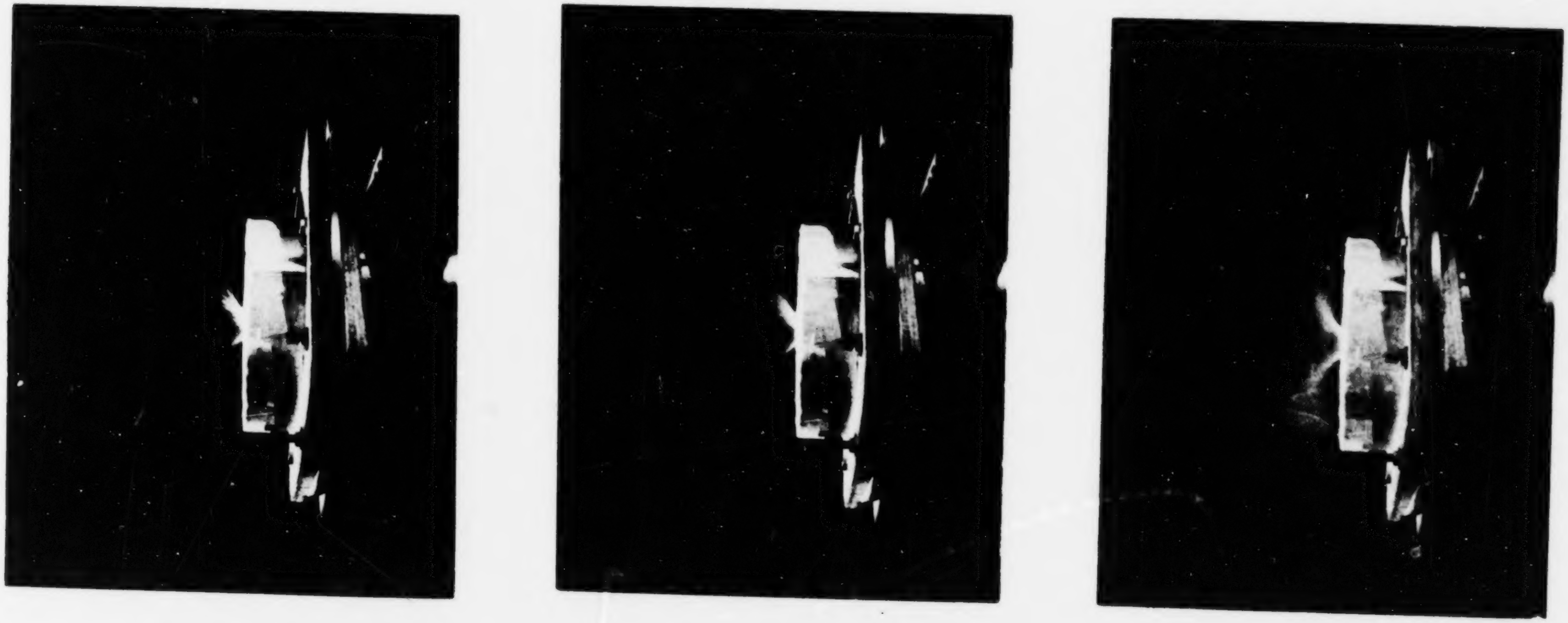

a. $\Delta P = 0.21$ psi

b. $\Delta P = 0.65$ psi

c. $\Delta P = 1.44$ psi

FIGURE 14 - EFFECTS OF NOZZLE AIR PRESSURE DROP ON SPRAY PERFORMANCE

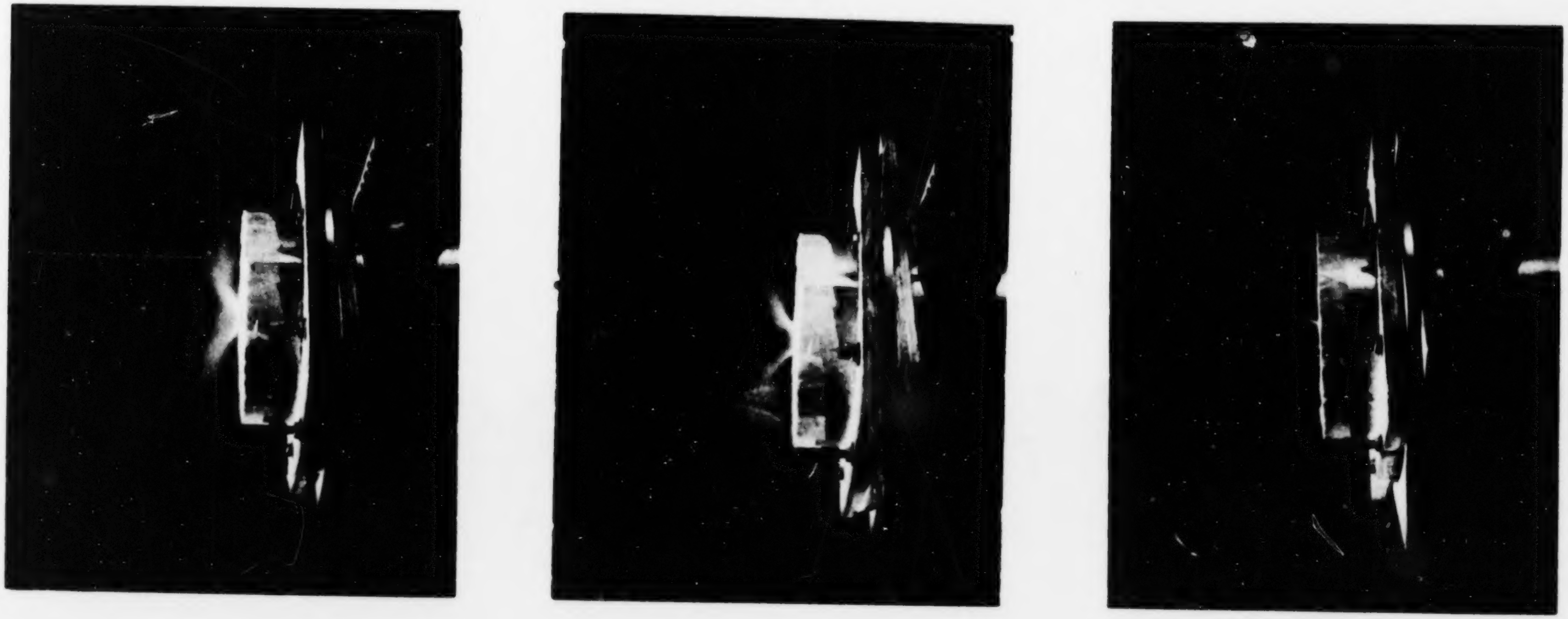

a. Nozzle Moved Axially Downstream (into Combustor)

b. Nozzle at Design Position

c. Nozzle Moved Axially Upstream (out of Combustor)

FIGURE 15 - EFFECTS OF AXIAL POSITION OF NOZZLE ON SPRAY PERFORMANCE

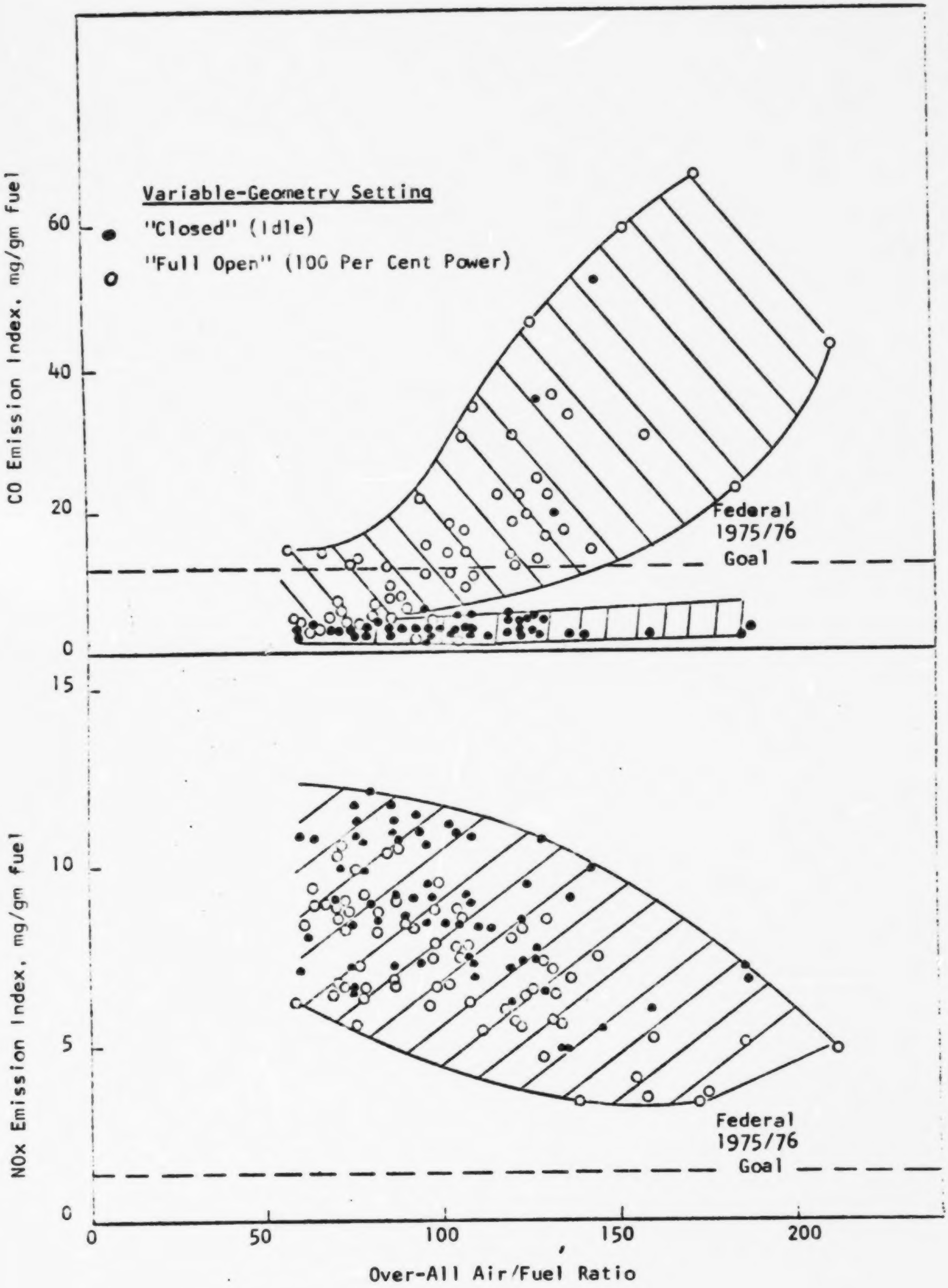

FIGURE 16 - SUMMARY OF NO_x AND CO EMISSIONS FOR COMBUSTOR B

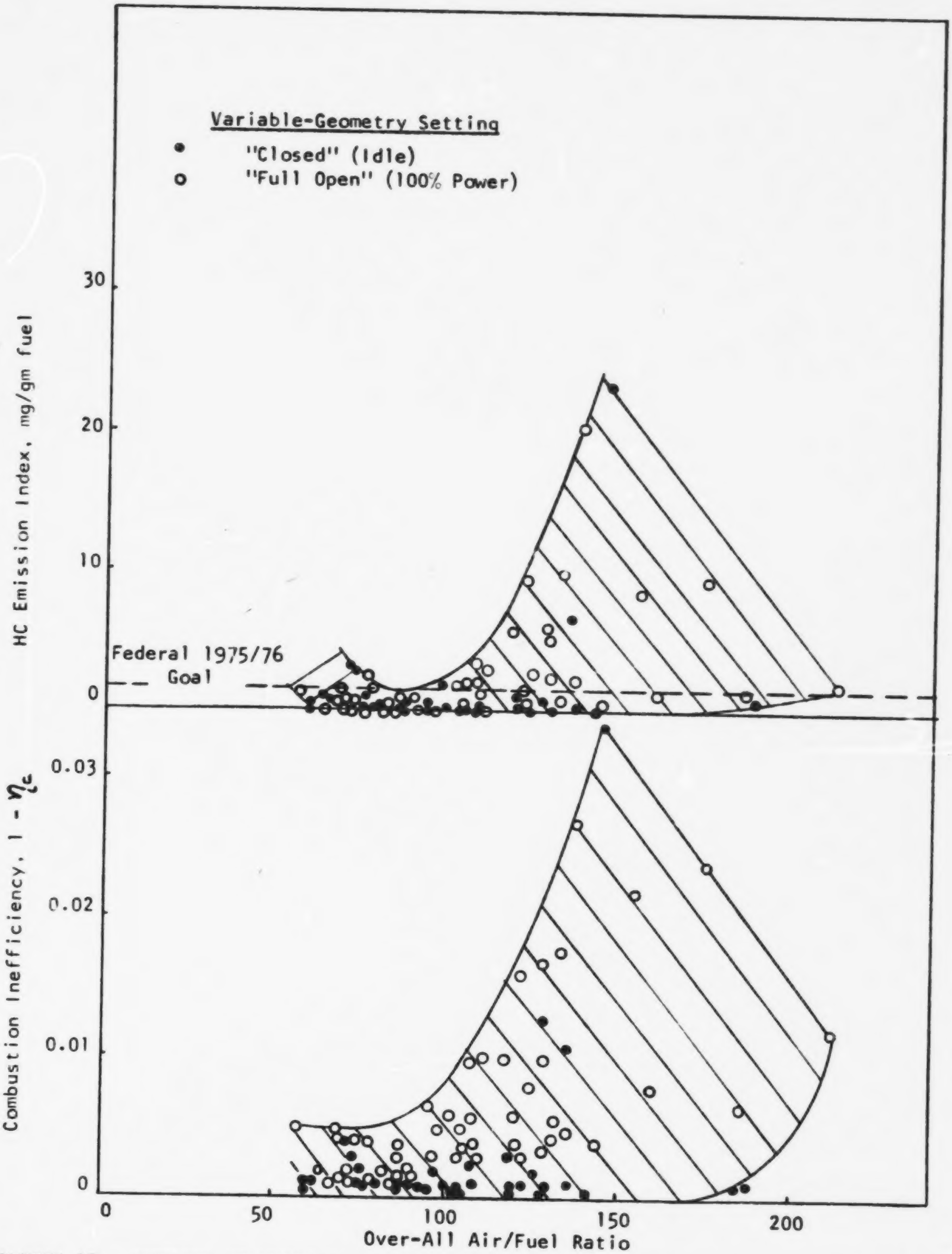

FIGURE 17 - SUMMARY OF HYDROCARBON EMISSIONS (HC) AND COMBUSTION EFFICIENCY (η_c) FOR COMBUSTOR B

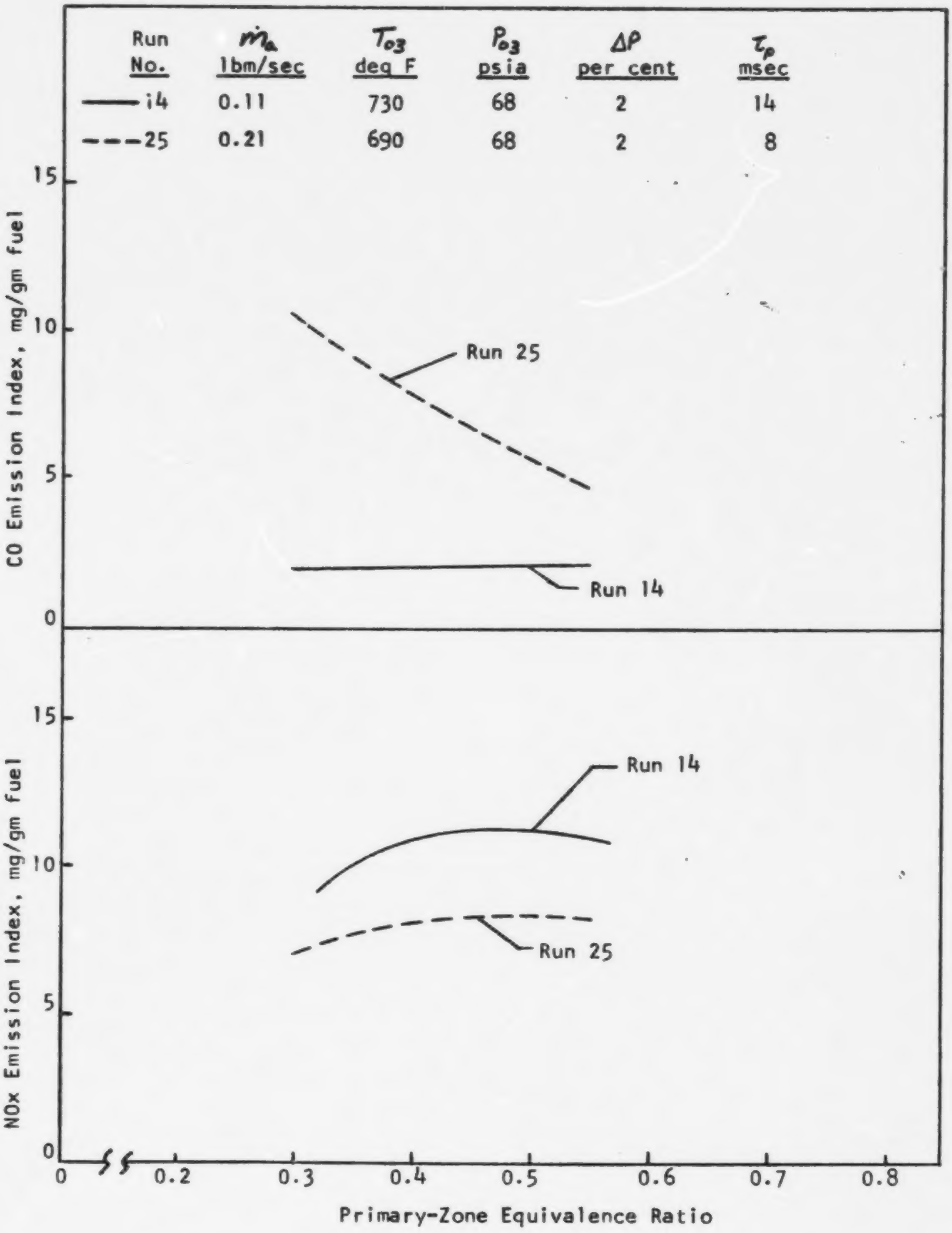

FIGURE 18 - TYPICAL EFFECT OF RESIDENCE TIME ON NOx AND CO EMISSIONS FOR COMBUSTOR B

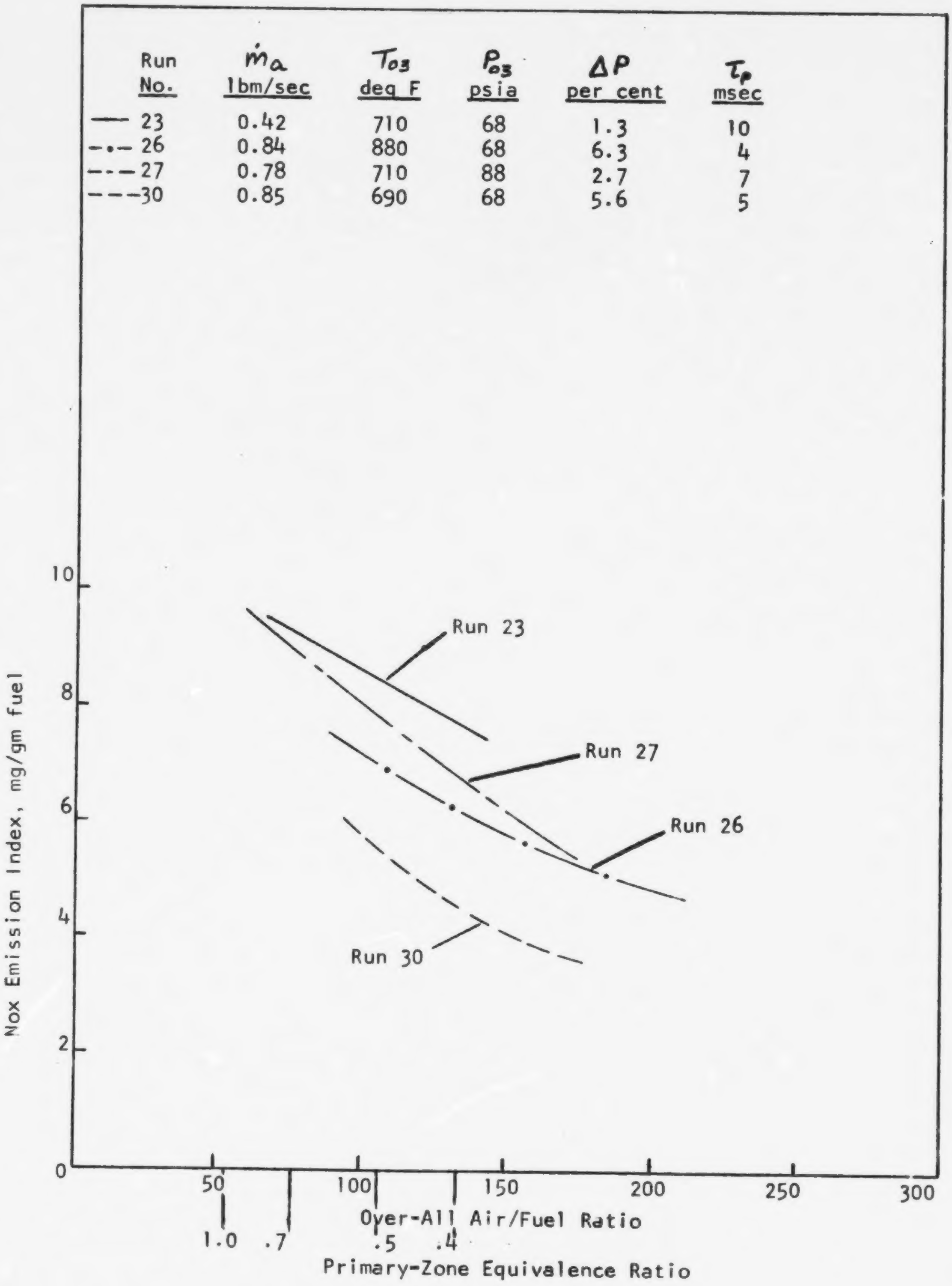

Run No.	$\dot{m}_a$ lbm/sec	T_{o3} deg F	P_{o3} psia	ΔP per cent	τ_p msec
— 23	0.42	710	68	1.3	10
-·- 26	0.84	880	68	6.3	4
-- - 27	0.78	710	88	2.7	7
--- 30	0.85	690	68	5.6	5

FIGURE 19 - TYPICAL VARIATION OF NOx EMISSIONS WITH FLOW CONDITIONS FOR COMBUSTOR B

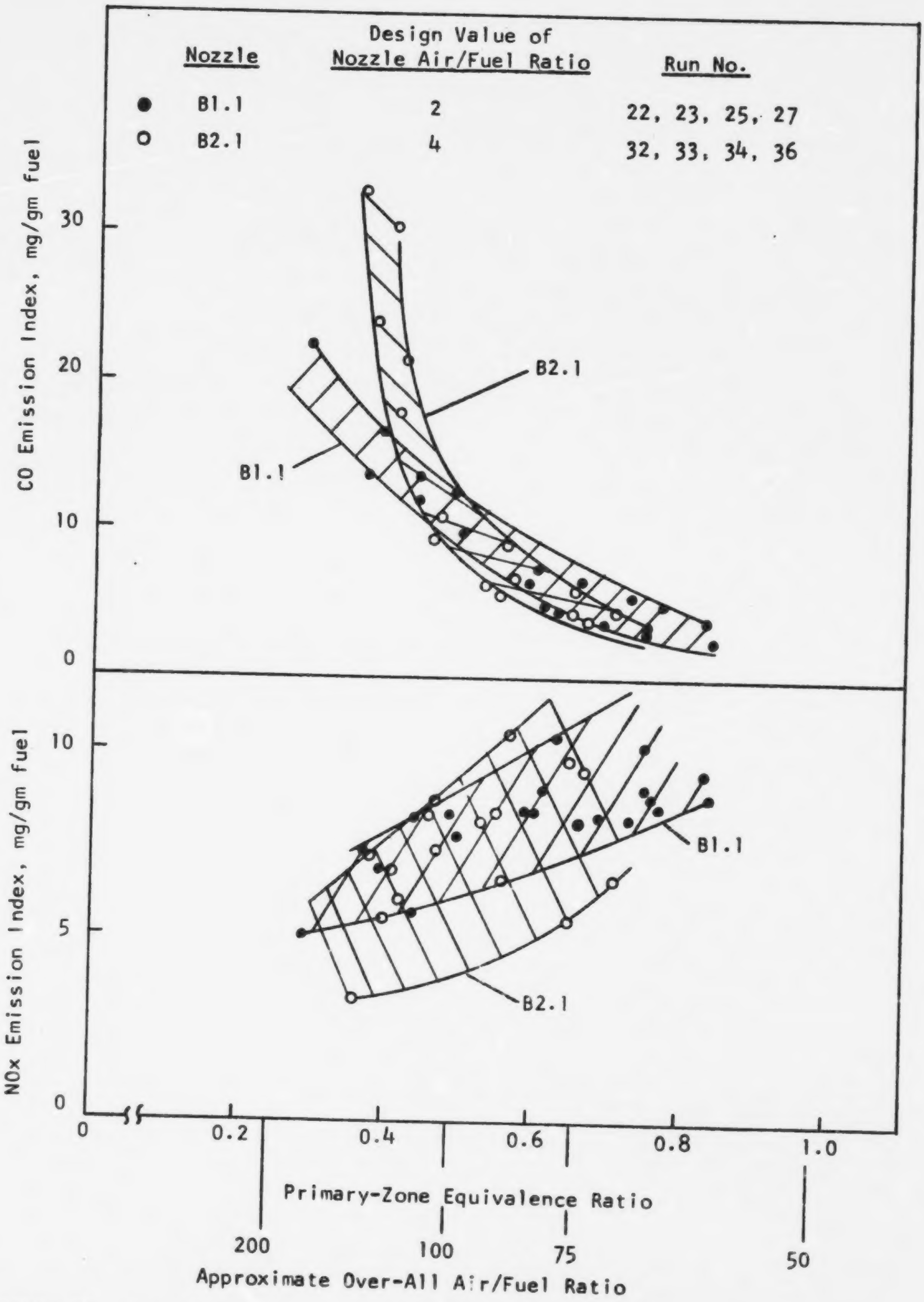

FIGURE 20 - EFFECT OF NOZZLE AIR/FUEL RATIO ON NOx AND CO EMISSIONS

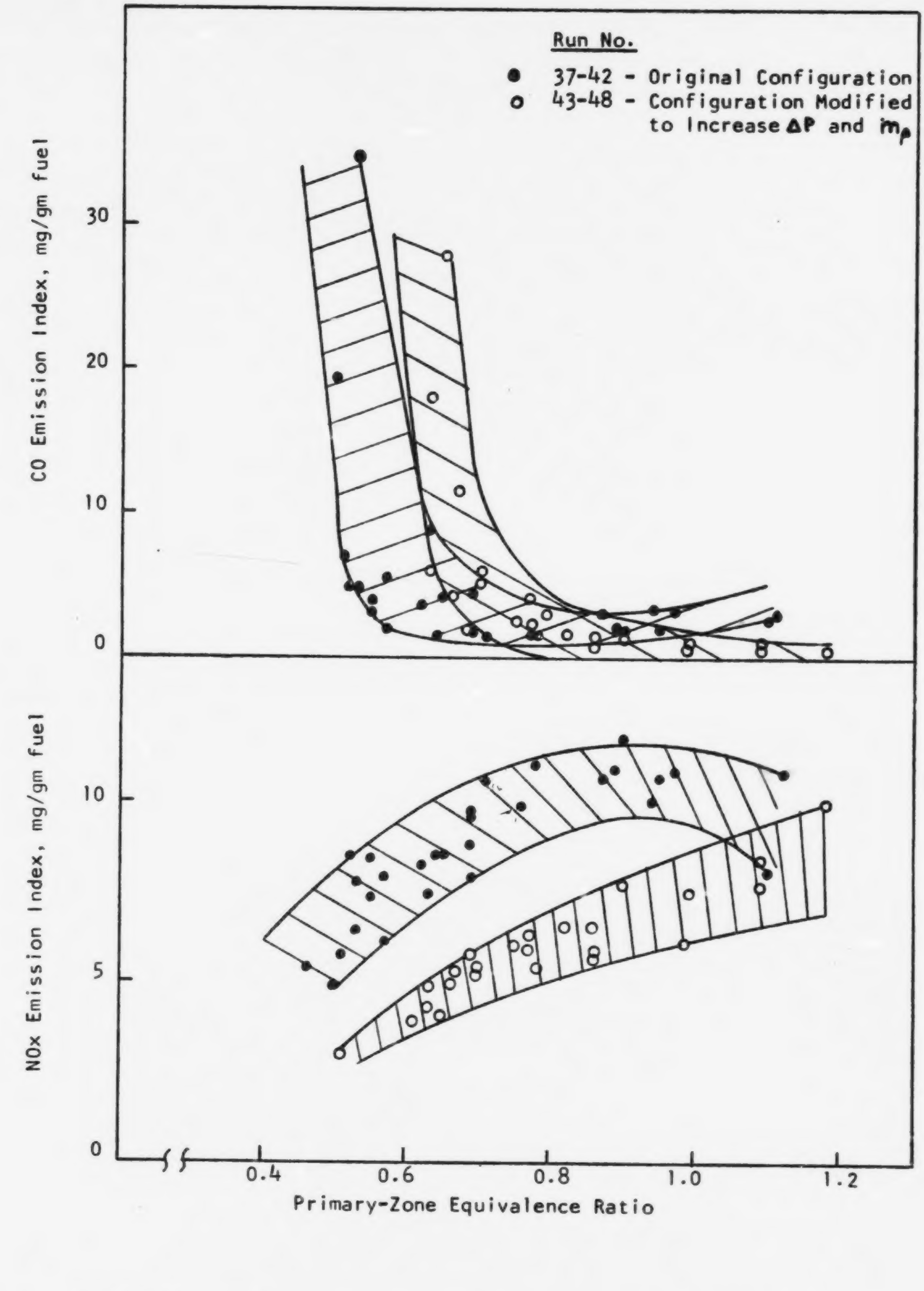

FIGURE 21 - COMPARISON OF NOx AND CO EMISSIONS FOR ORIGINAL AND MODIFIED COMBUSTOR B CONFIGURATIONS

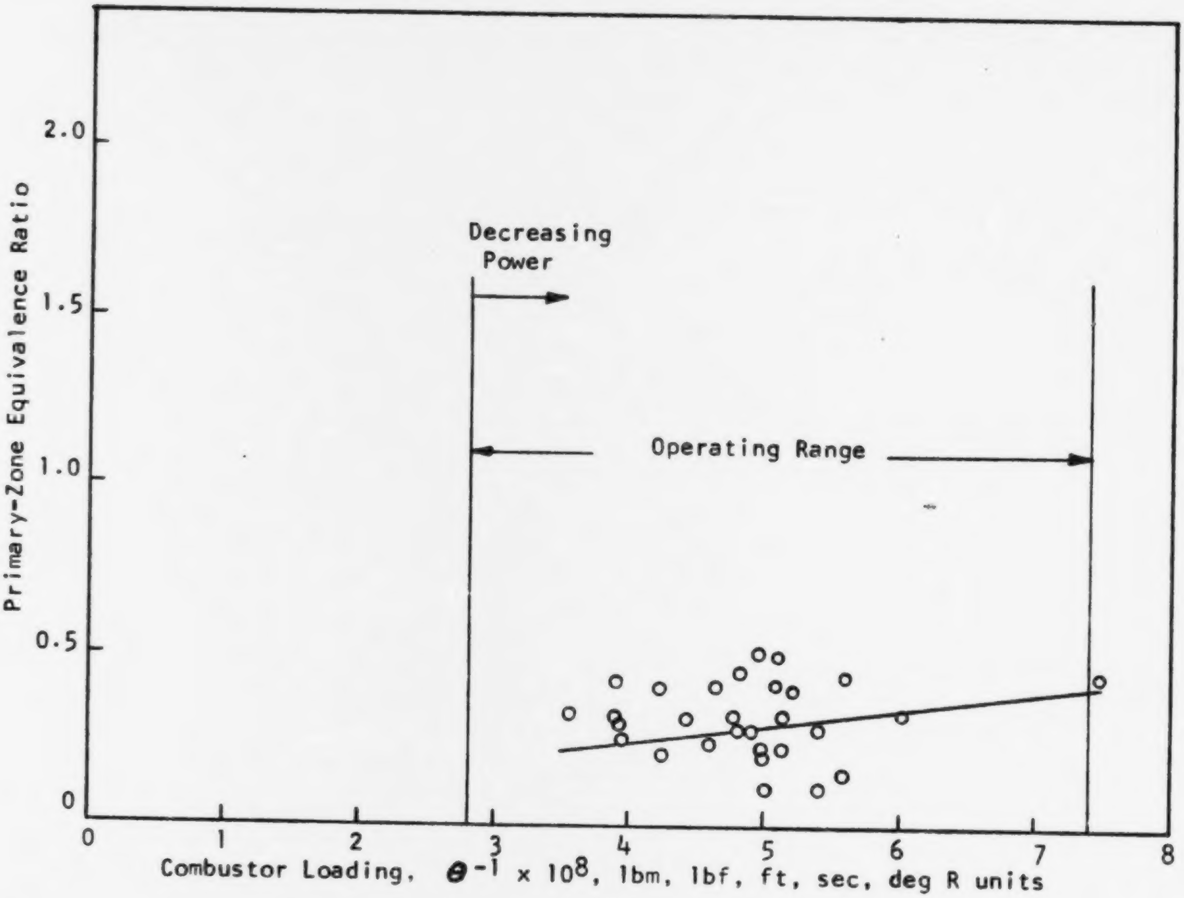

$$\frac{1}{\theta} \equiv \frac{\dot{m}_a}{P_{03}^{1.75} A_{ref} D_{ref}^{0.75} \exp(T_{03}/b)}$$

FIGURE 22 - WEAK EXTINCTION LIMIT FOR COMBUSTOR B

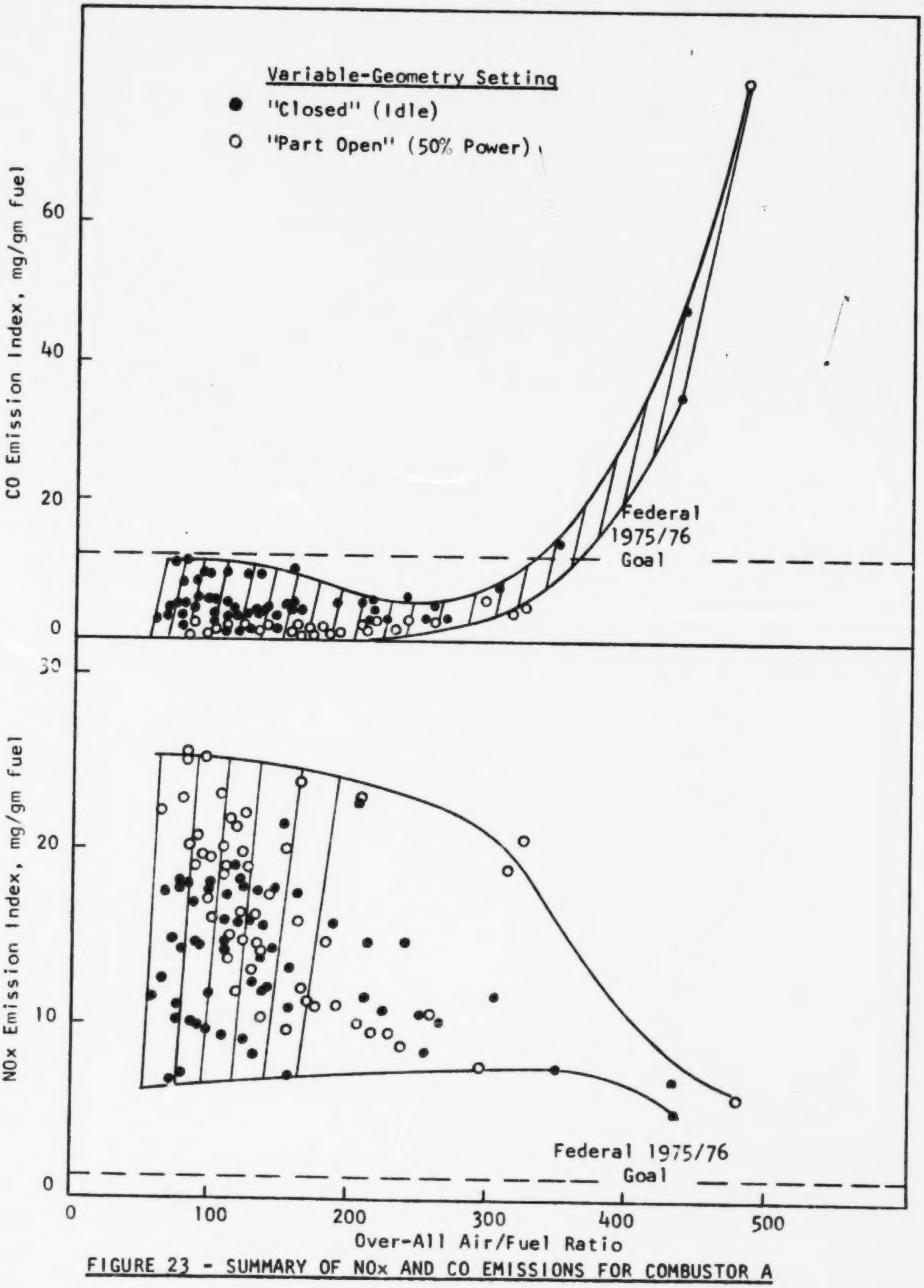

FIGURE 23 - SUMMARY OF NOx AND CO EMISSIONS FOR COMBUSTOR A

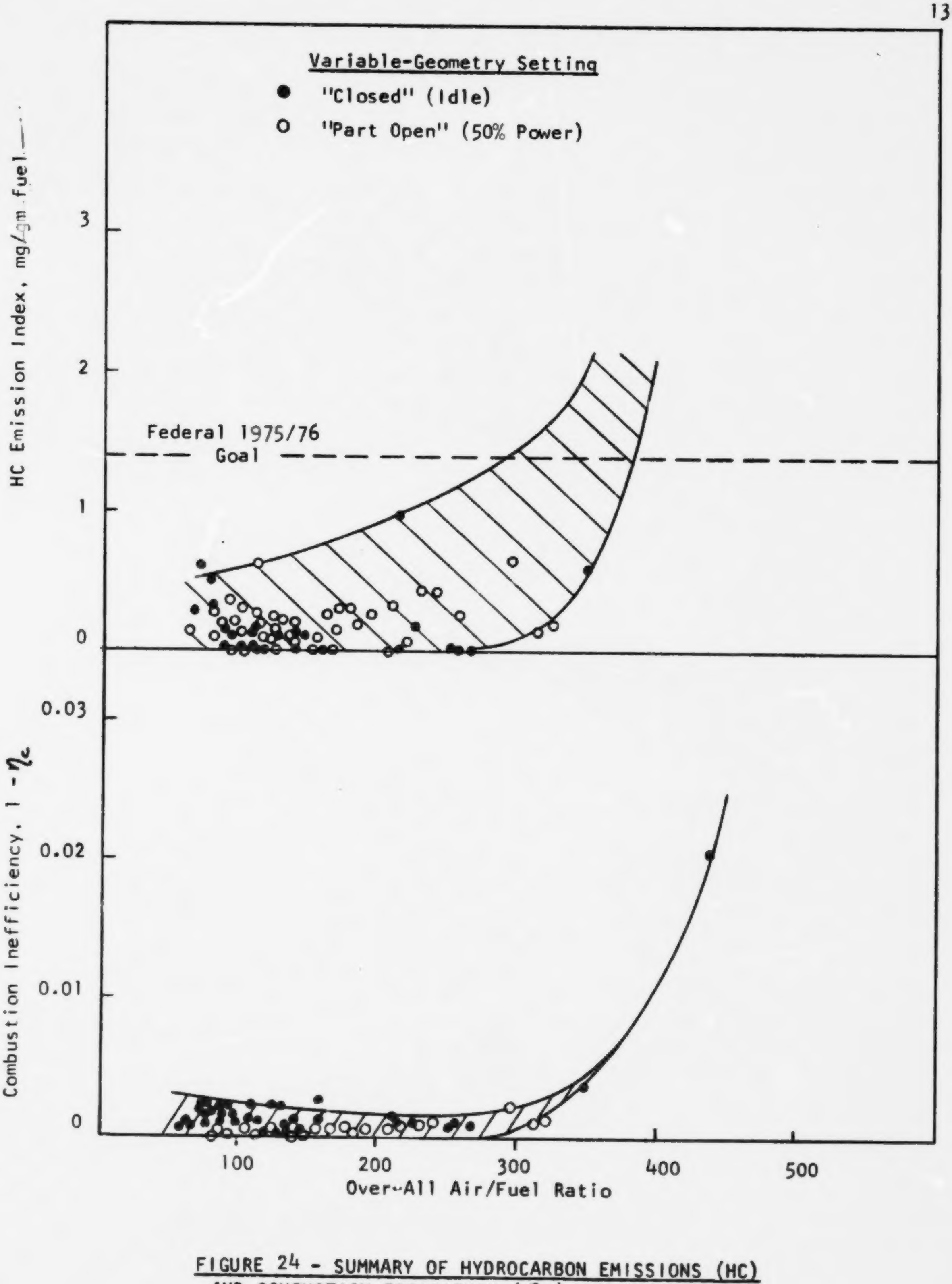

FIGURE 24 - SUMMARY OF HYDROCARBON EMISSIONS (HC) AND COMBUSTION EFFICIENCY (η) FOR COMBUSTOR A

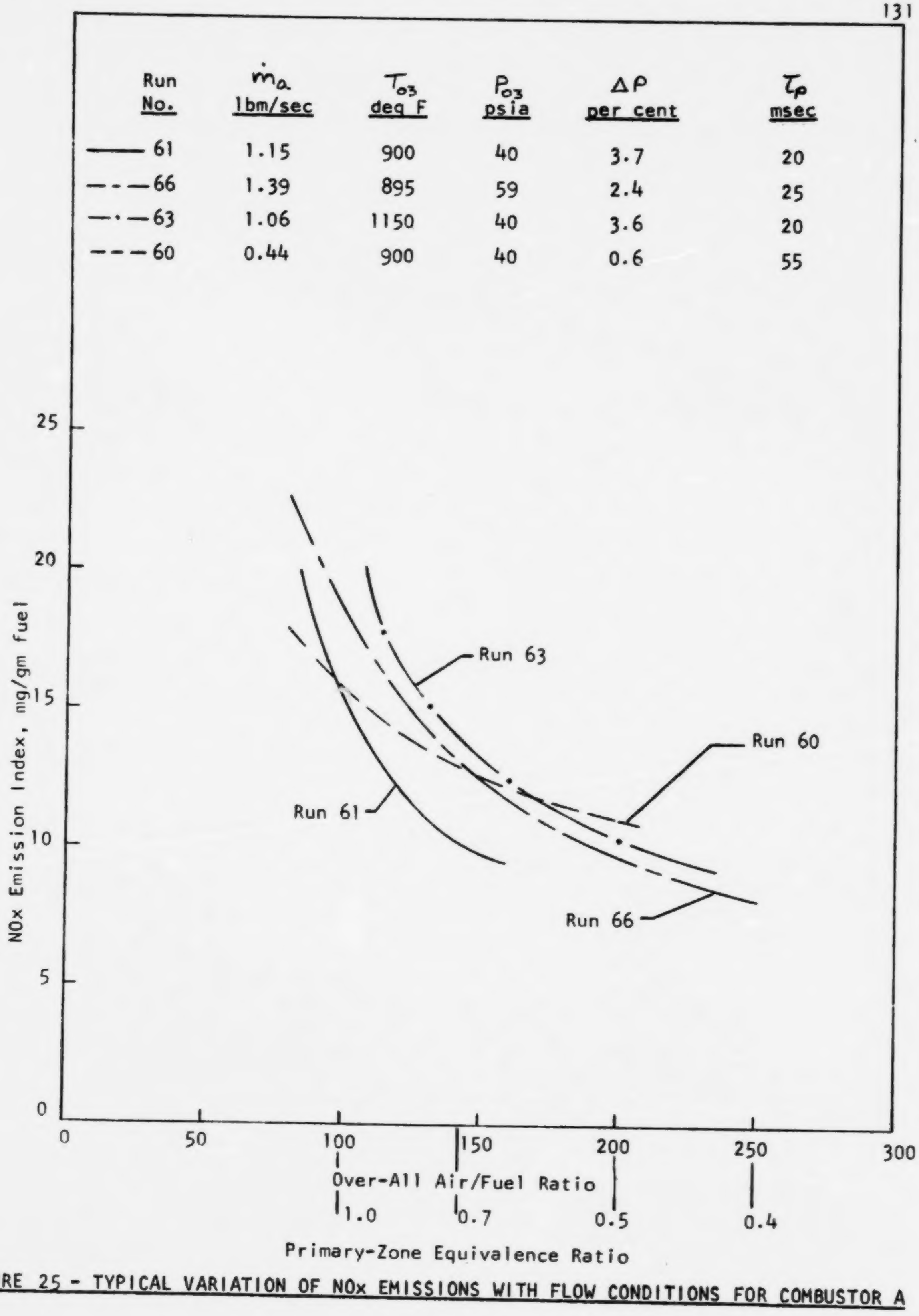

Run No.	$\dot{m}_a$ lbm/sec	T_{03} deg F	P_{03} psia	ΔP per cent	τ_p msec
——— 61	1.15	900	40	3.7	20
— — — 66	1.39	895	59	2.4	25
—·— 63	1.06	1150	40	3.6	20
- - - 60	0.44	900	40	0.6	55

FIGURE 25 - TYPICAL VARIATION OF NOx EMISSIONS WITH FLOW CONDITIONS FOR COMBUSTOR A

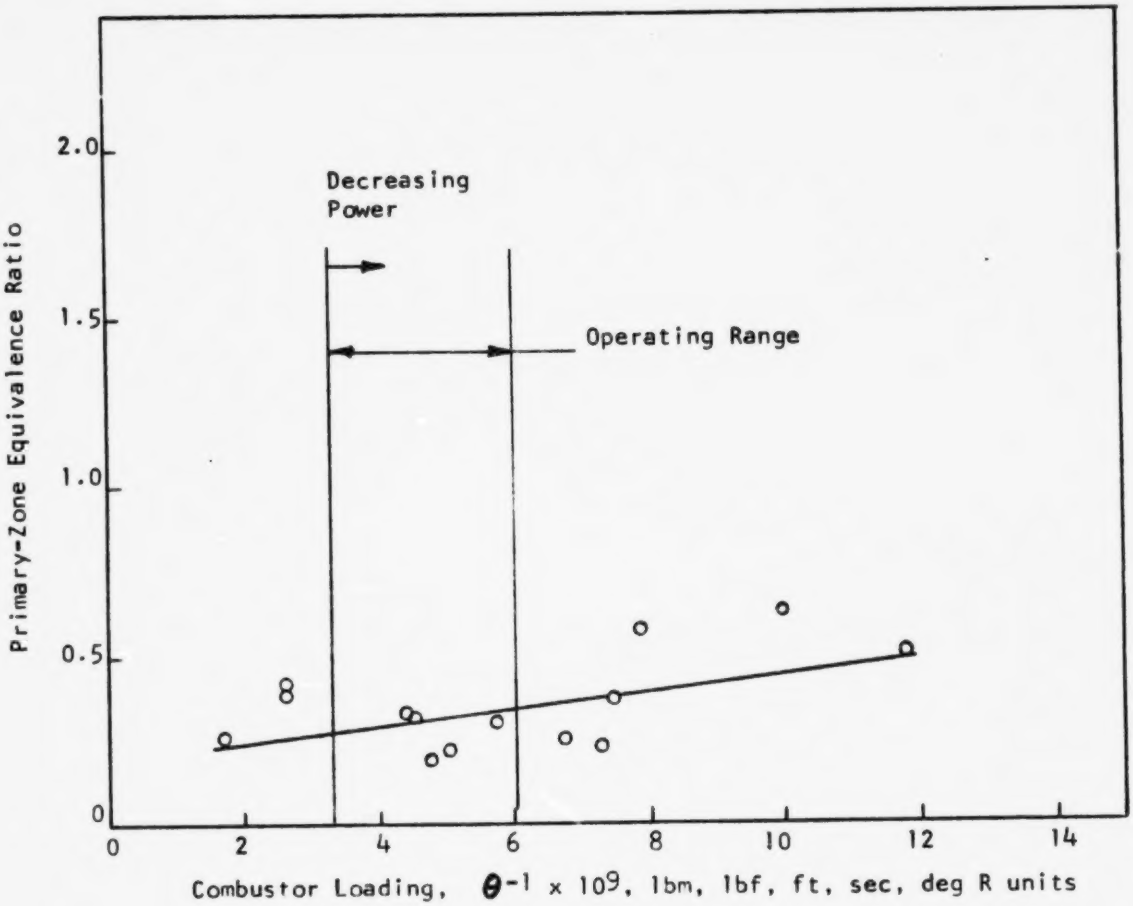

$$\frac{1}{\theta} \equiv \frac{\dot{m}_a}{P_{03}^{1.75} A_{ref} D_{ref}^{0.75} \exp(T_{03}/b)}$$

FIGURE 26 - WEAK EXTINCTION LIMIT FOR COMBUSTOR A

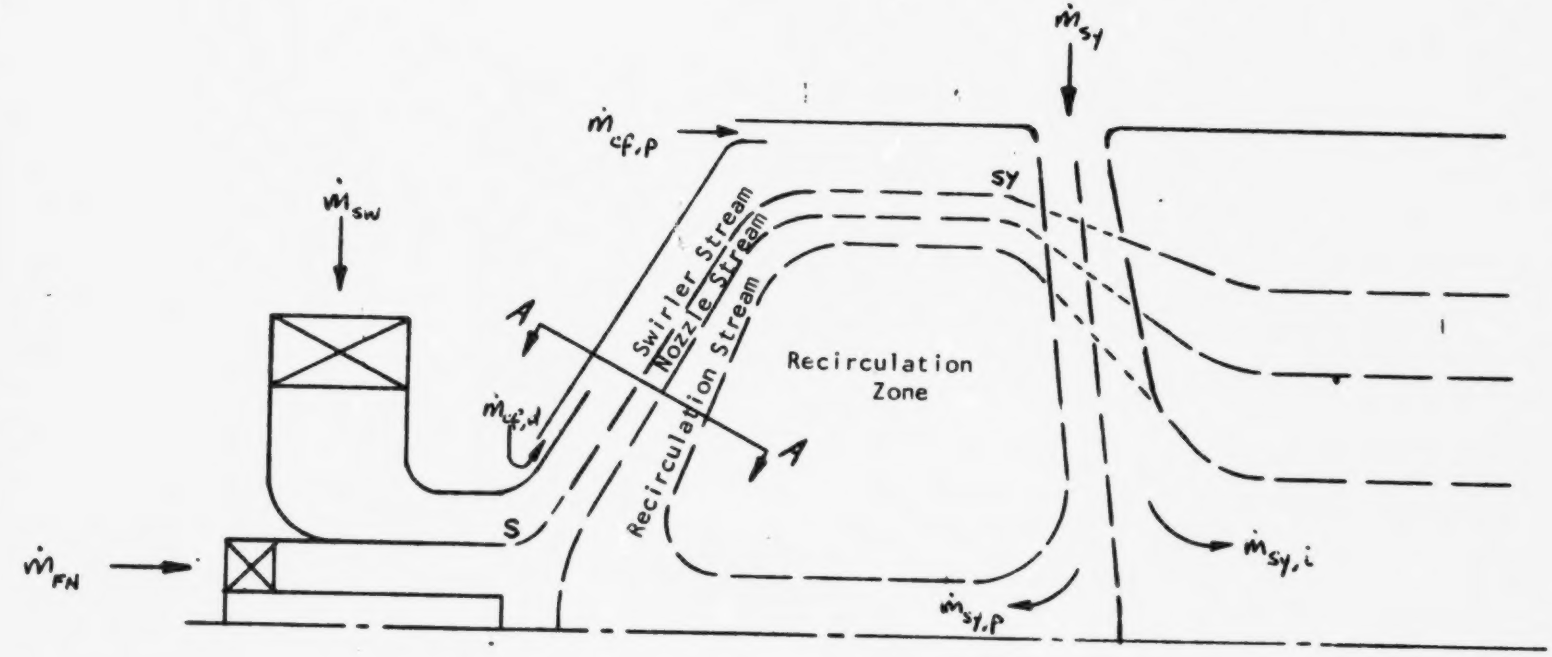
$\dot{m}_{sy}$
$\dot{m}_{cf,p}$
$\dot{m}_{sw}$
SY
Swirler Stream
Nozzle Stream
Recirculation Stream
Recirculation Zone
A
A
$\dot{m}_{cf,d}$
S
$\dot{m}_{FN}$
$\dot{m}_{sy,i}$
$\dot{m}_{sy,p}$

FIGURE 27 - COMBUSTOR FLOW PATTERN SCHEMATIC

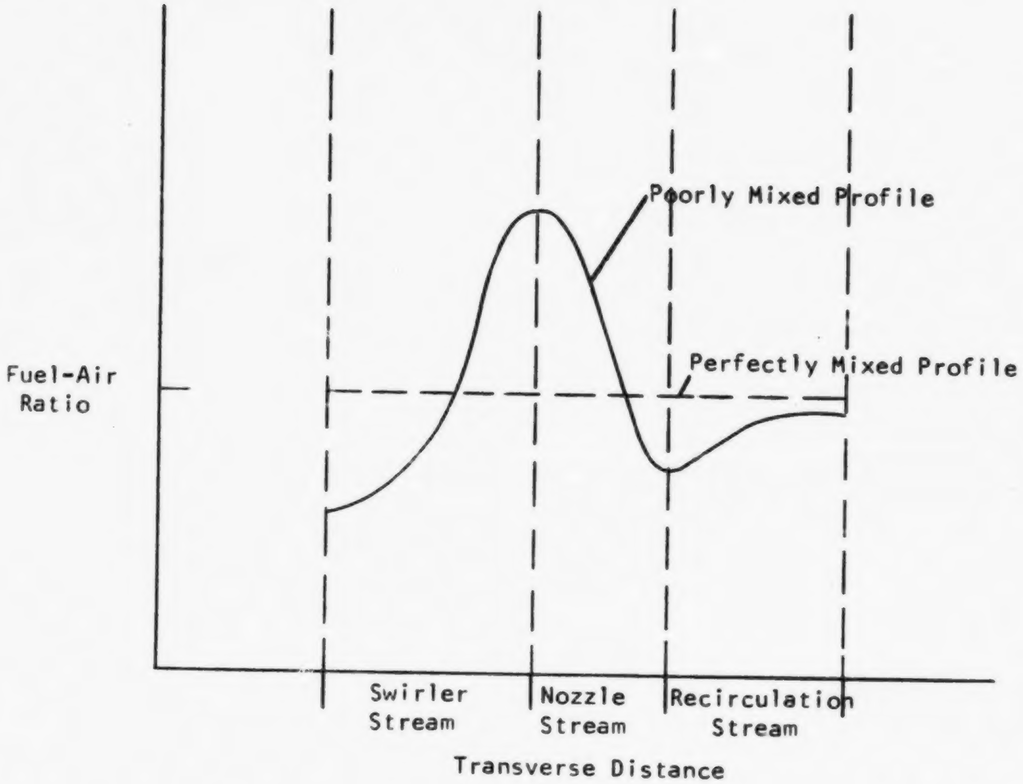

FIGURE 28 - FUEL-AIR DISTRIBUTION IN PRIMARY-ZONE INLET REGION

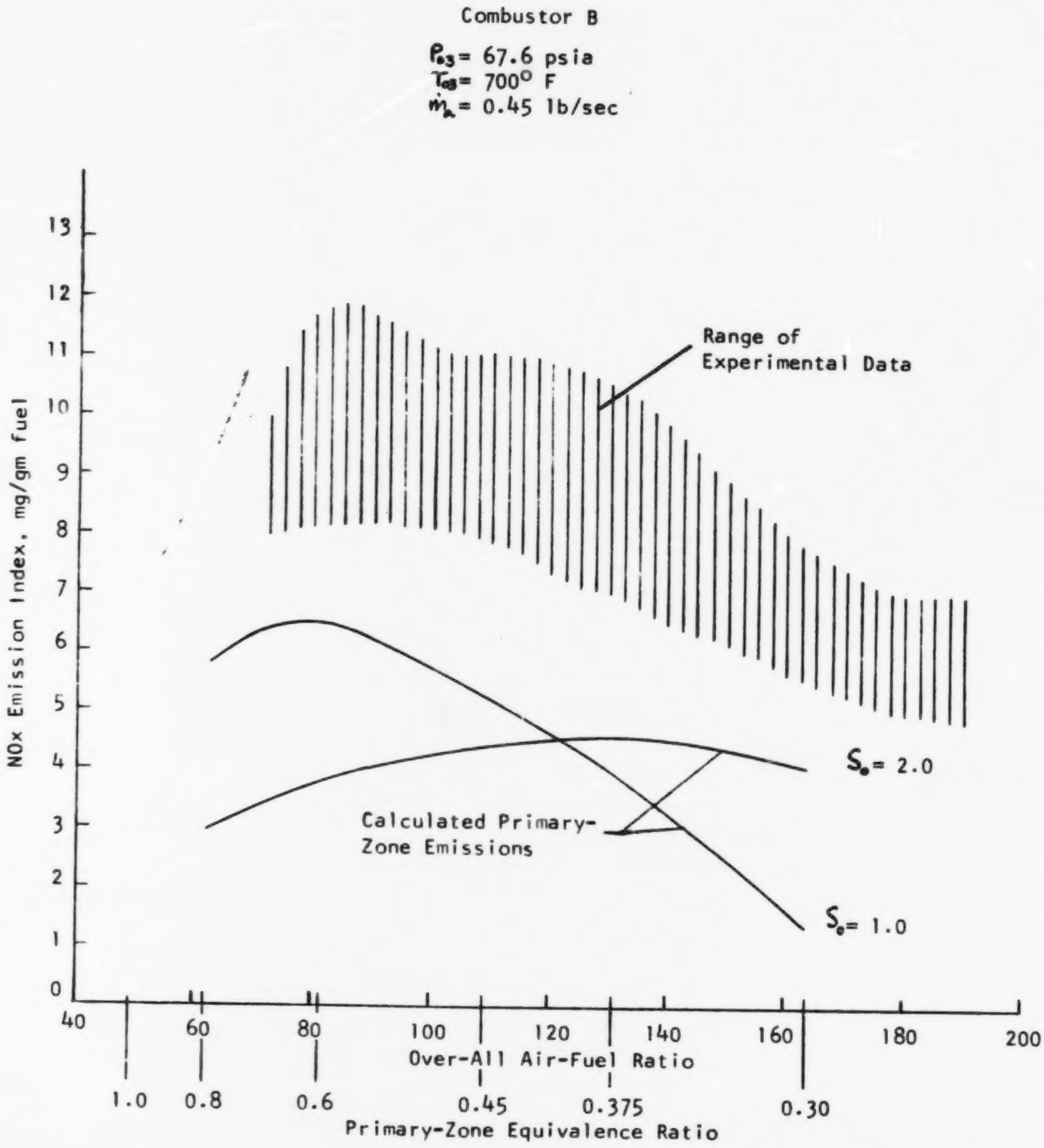

FIGURE 29 - CALCULATED RESULTS FOR COMBUSTOR B

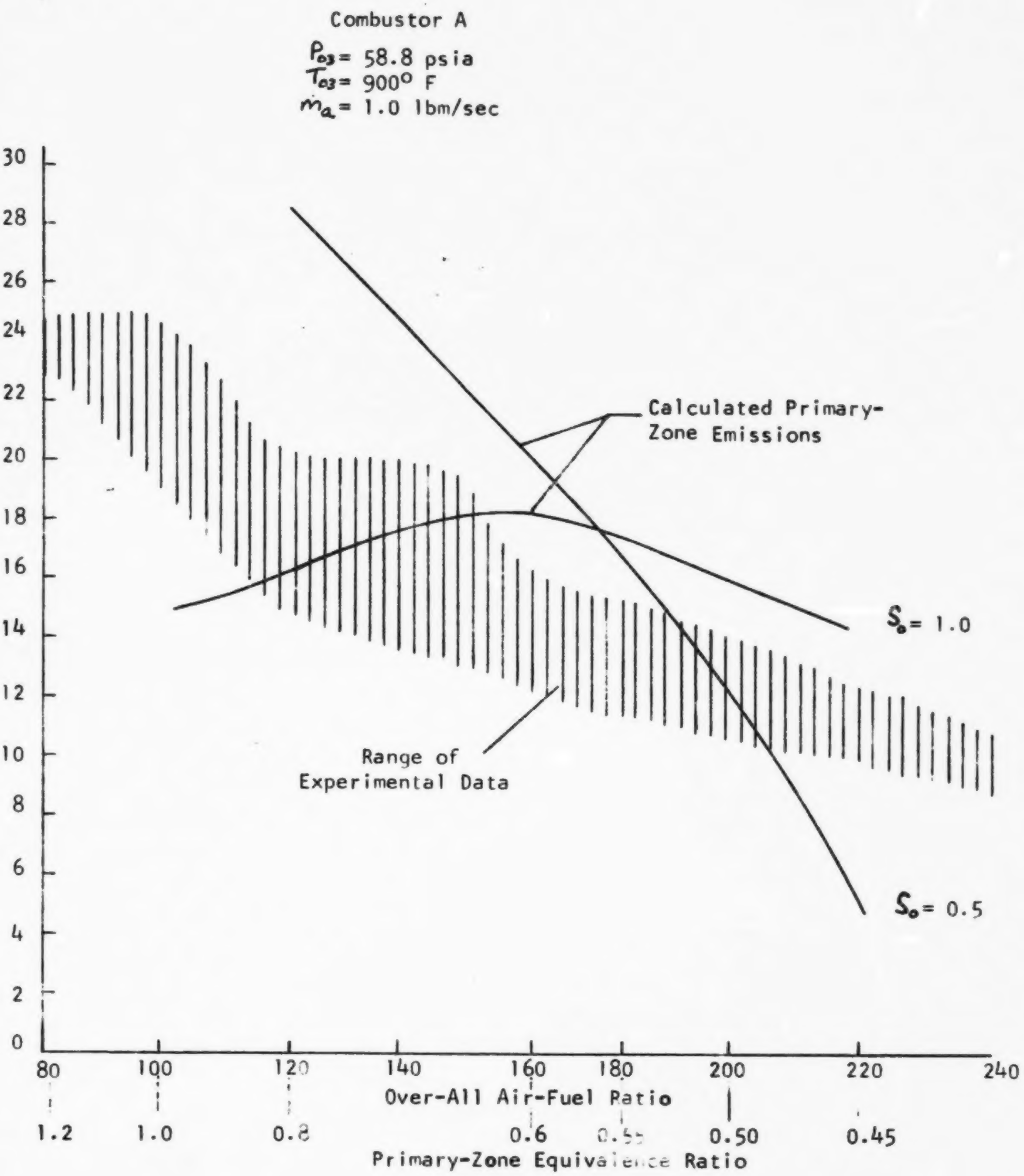

FIGURE 30 - CALCULATED RESULTS FOR COMBUSTOR A

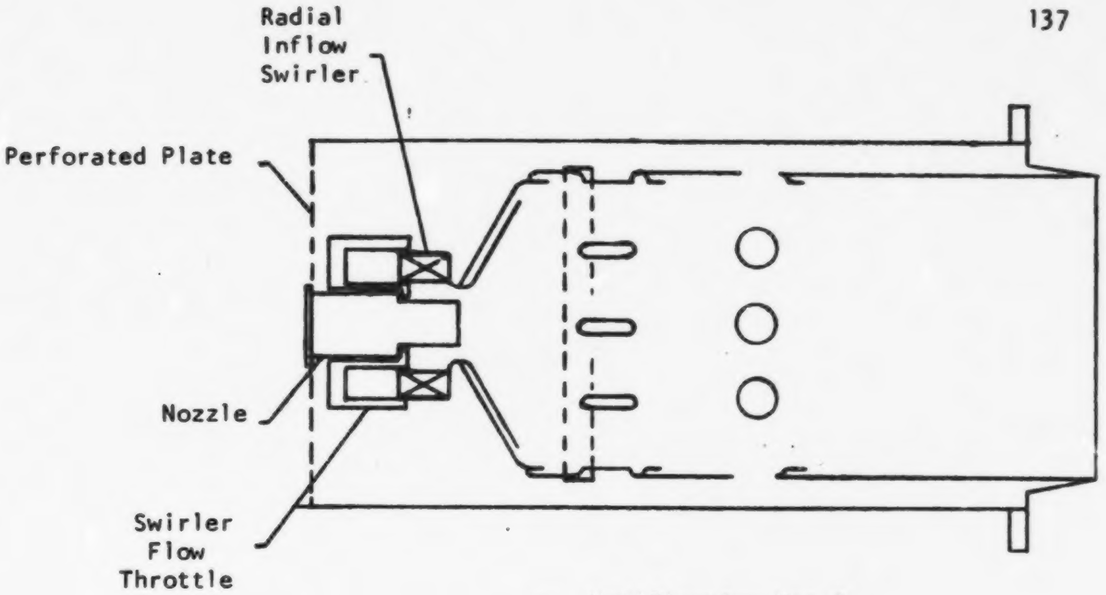
Radial Inflow Swirler
Perforated Plate
Nozzle
Swirler Flow Throttle

a. Modification No. 1

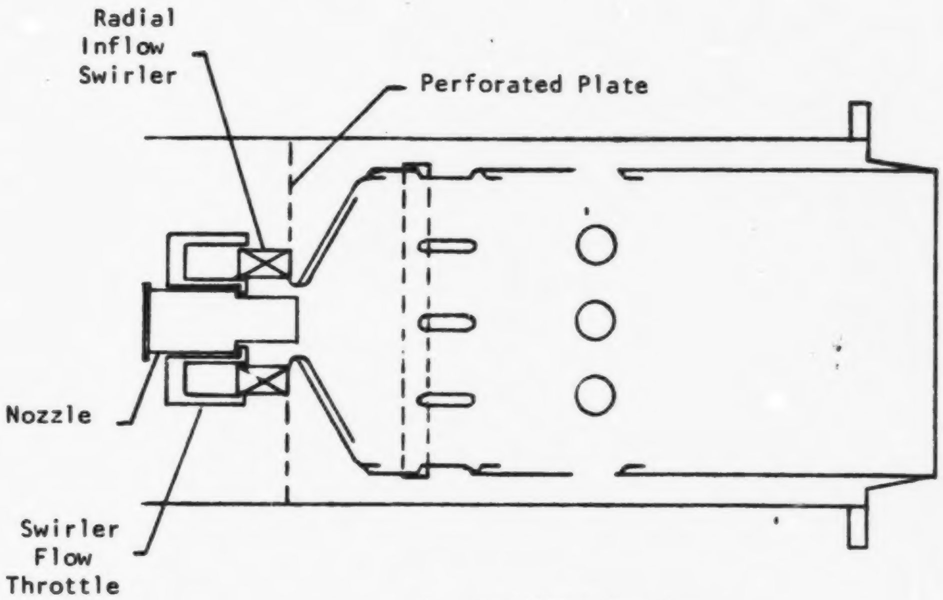
Radial Inflow Swirler
Perforated Plate
Nozzle
Swirler Flow Throttle

b. Modification No. 2

FIGURE 31 - MODIFICATIONS OF COMBUSTOR A TESTED

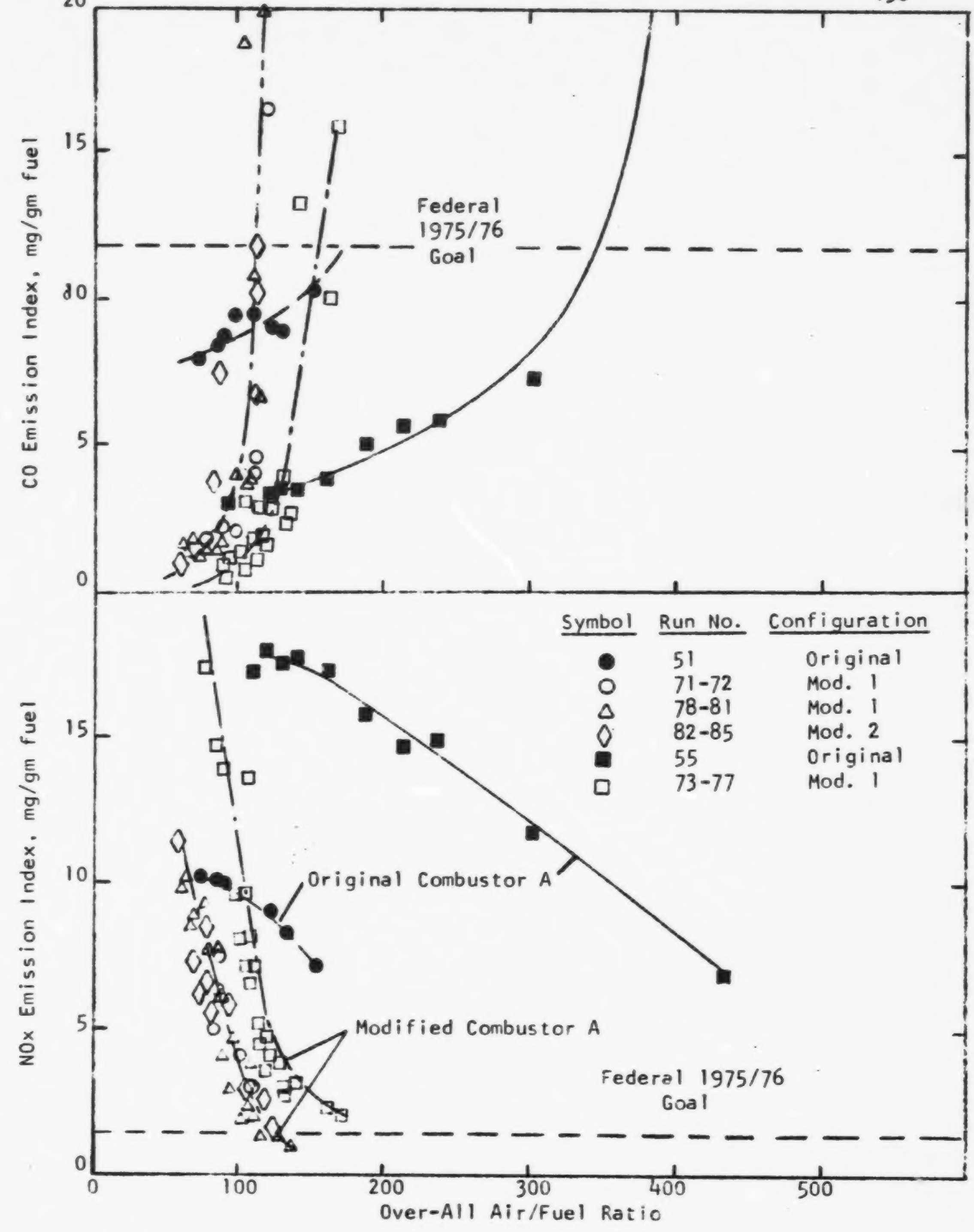

FIGURE 32 - COMPARISON OF NOx AND CO EMISSIONS FOR ORIGINAL AND MODIFIED COMBUSTOR A

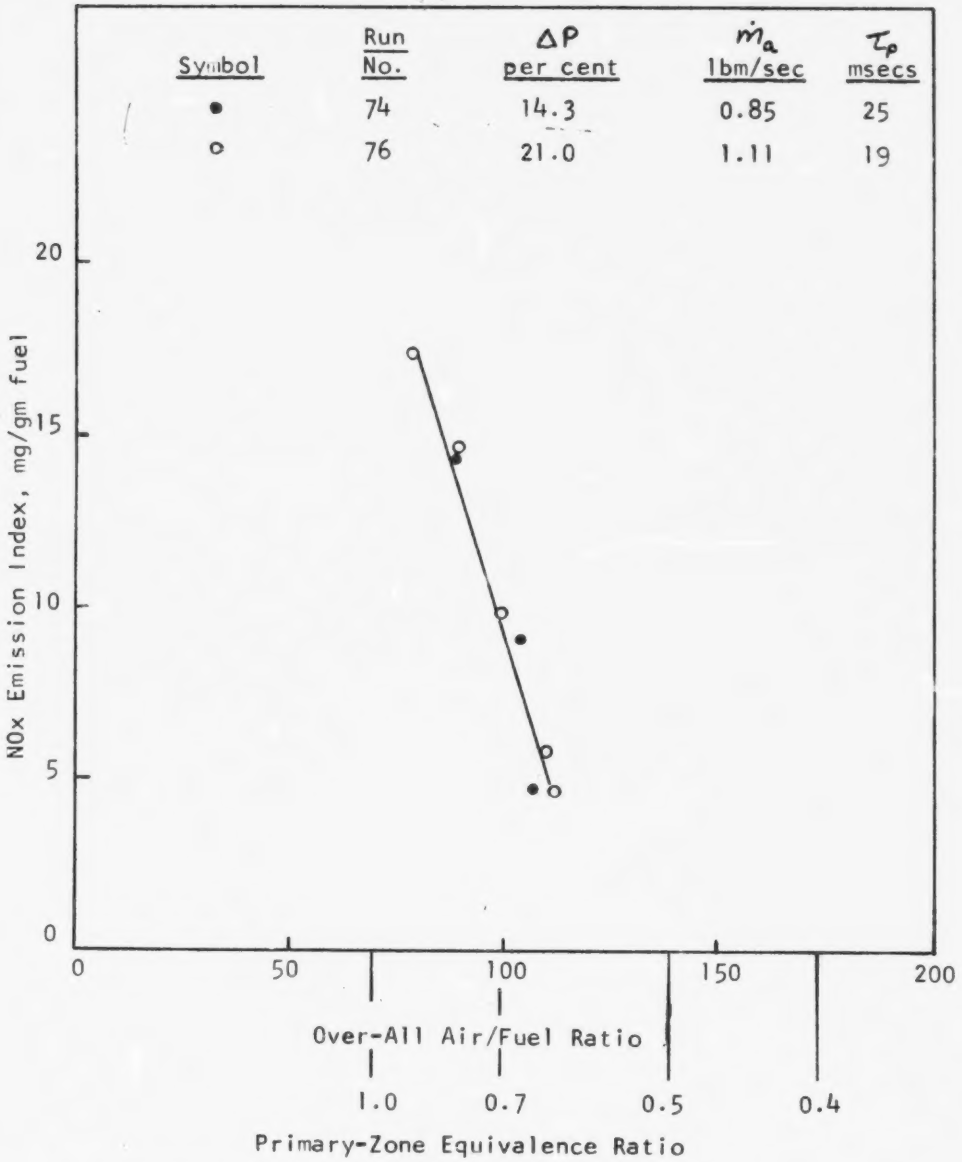

Symbol	Run No.	ΔP per cent	$\dot{m}_a$ lbm/sec	τ_p msecs
●	74	14.3	0.85	25
○	76	21.0	1.11	19

FIGURE 33 - EFFECT OF PRESSURE DROP AND RESIDENCE TIME ON NOx EMISSIONS FOR MODIFIED COMBUSTOR A

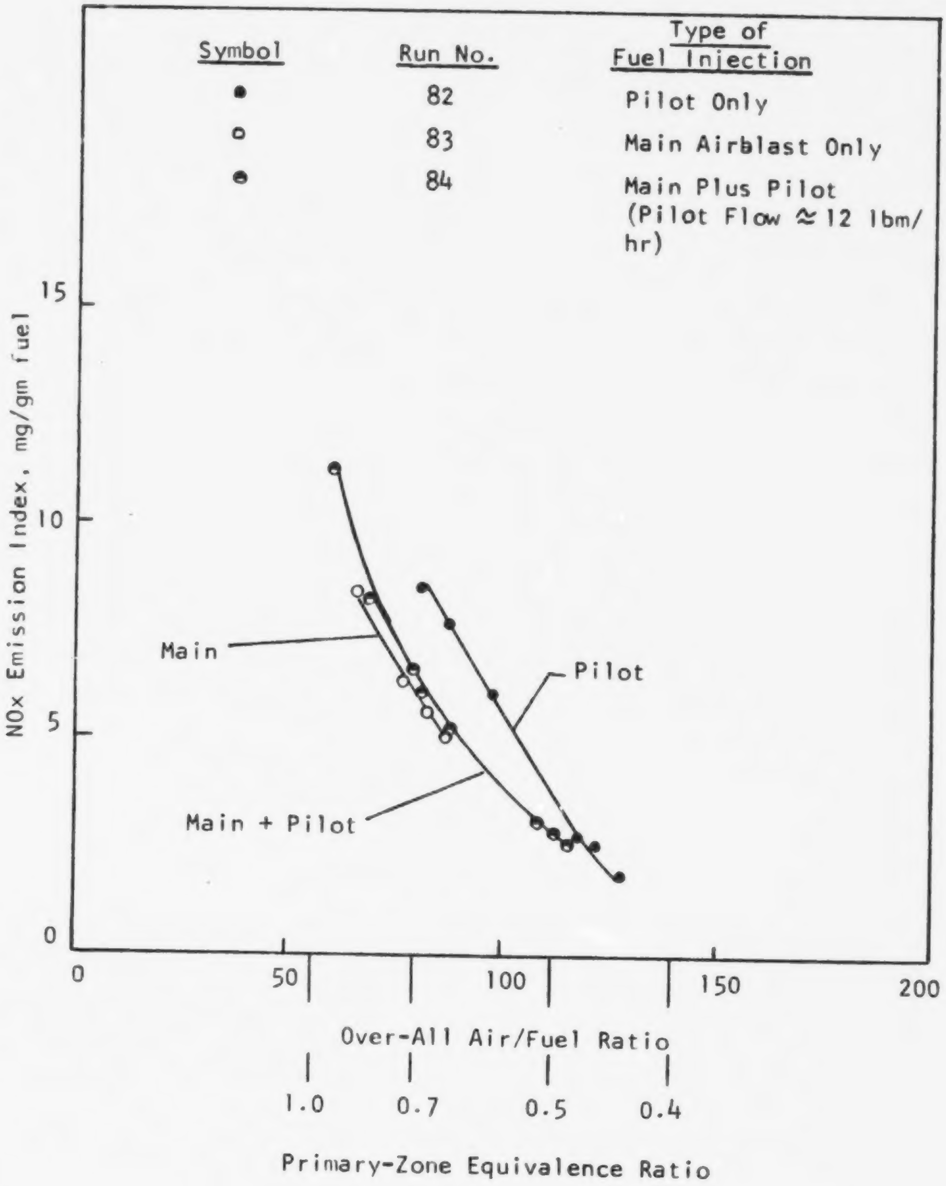

FIGURE 34 - EFFECT OF FUEL INJECTION ON NOx EMISSIONS FOR MODIFIED COMBUSTOR A

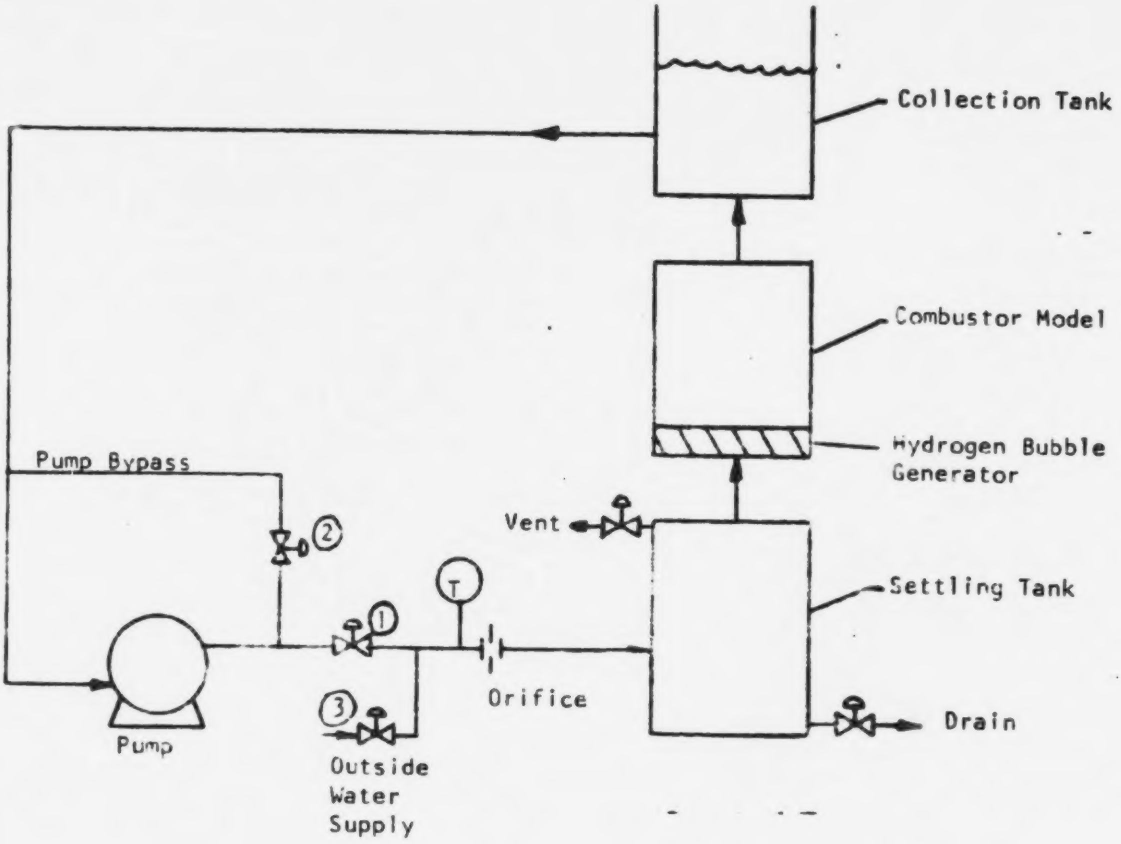
Collection Tank
Combustor Model
Hydrogen Bubble Generator
Settling Tank
Vent
Drain
Pump Bypass
②
①
③
T
Orifice
Pump
Outside Water Supply

FIGURE 35 - FLOW SCHEMATIC OF WATER RIG

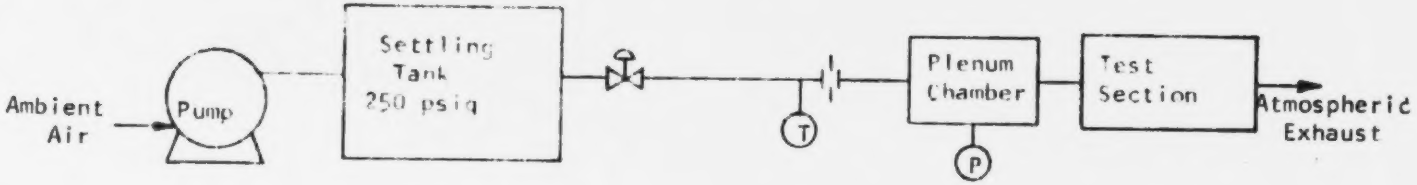
Ambient
Air
Pump
Settling
Tank
250 psig
T
Plenum
Chamber
P
Test
Section
Atmospheric
Exhaust

FIGURE 36 - FLOW SCHEMATIC OF COLD-AIR TEST RIG

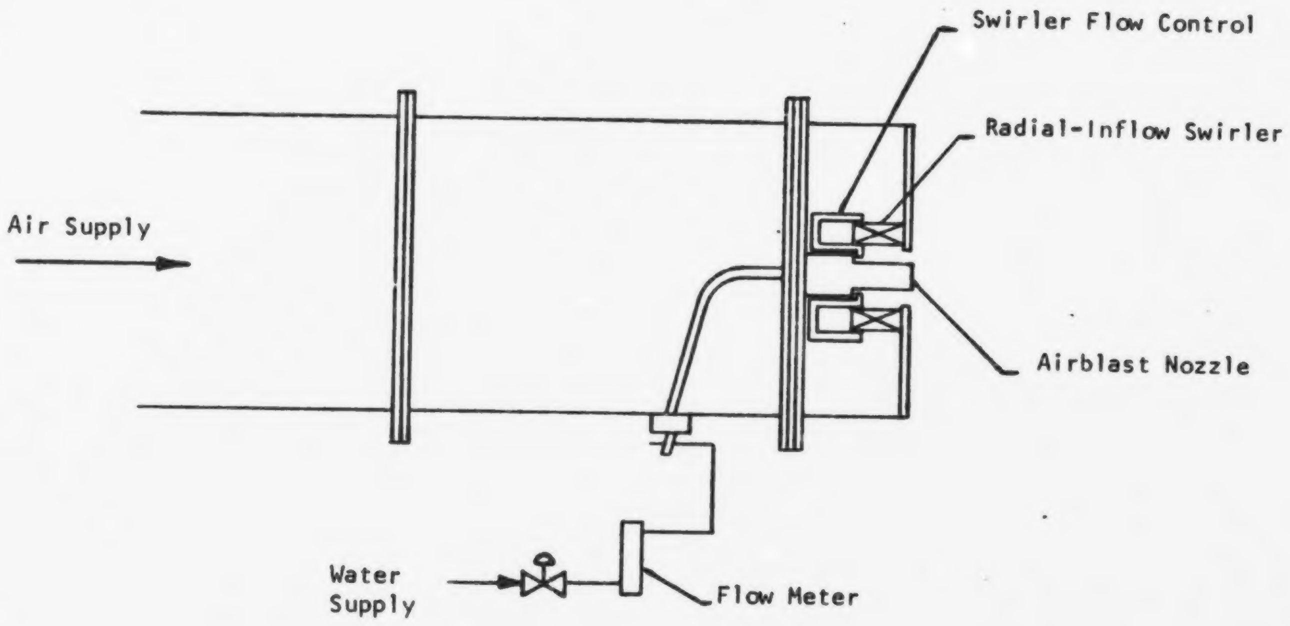
Swirler Flow Control
Radial-Inflow Swirler
Air Supply
Airblast Nozzle
Water Supply
Flow Meter

FIGURE 37 - NOZZLE MOUNTING FOR FUEL NOZZLE TESTS

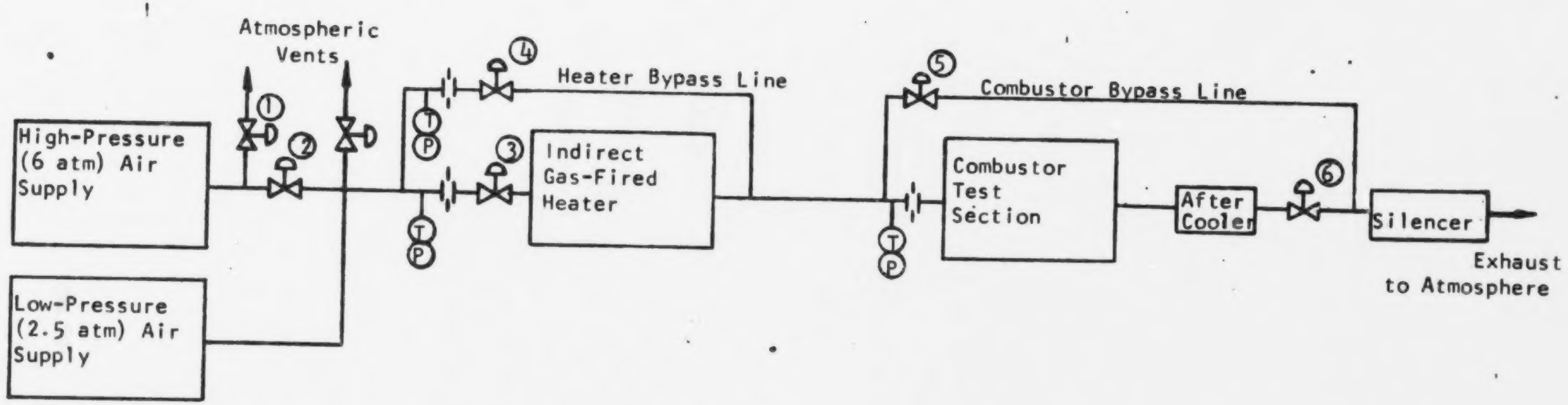
Atmospheric Vents
①
②
④
③
Heater Bypass Line
High-Pressure (6 atm) Air Supply
Low-Pressure (2.5 atm) Air Supply
T
P
T
P
Indirect Gas-Fired Heater
⑤
Combustor Bypass Line
T
P
Combustor Test Section
After Cooler
⑥
Silencer
Exhaust to Atmosphere

FIGURE 38 - AIR FLOW SCHEMATIC FOR COMBUSTION TEST RIG

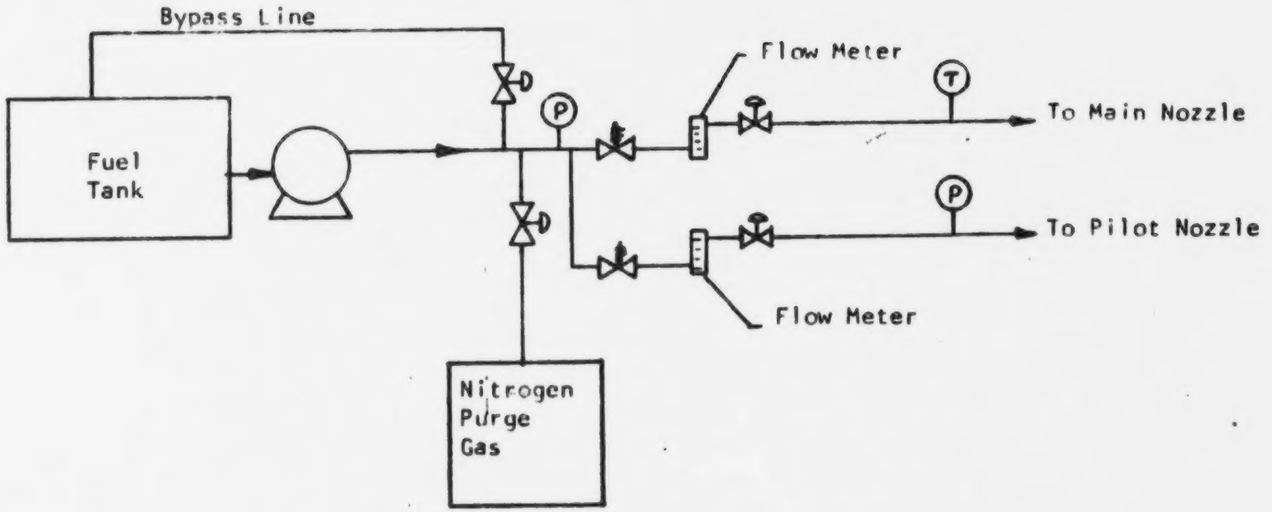
Bypass Line
Fuel Tank
Flow Meter
T
P
To Main Nozzle
P
To Pilot Nozzle
Flow Meter
Nitrogen Purge Gas

FIGURE 39 - FUEL FLOW SCHEMATIC FOR COMBUSTION TEST RIG

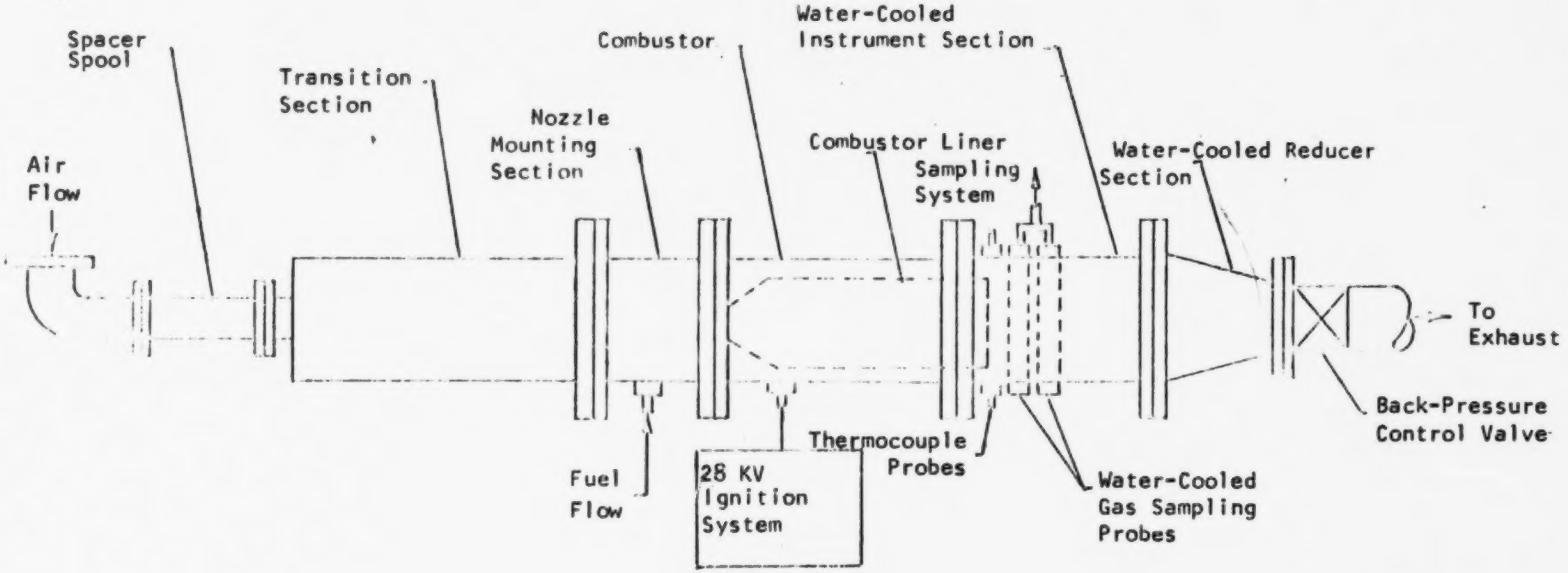
Spacer Spool
Transition Section
Combustor
Water-Cooled Instrument Section
Nozzle Mounting Section
Combustor Liner Sampling System
Water-Cooled Reducer Section
Air Flow
To Exhaust
Back-Pressure Control Valve
Thermocouple Probes
Water-Cooled Gas Sampling Probes
Fuel Flow
28 KV Ignition System

Nominal Dimensions

	Diameter in	Length in
Spacer Spool:		
Combustor A	4	17.00
Combustor B	4	23.50
Transition Section	9	19.50
Nozzle Section	9	6.25
Instrument Section	9	15.00
Reducer Section	9-6	12.00

FIGURE 40 - COMBUSTION TEST SECTION

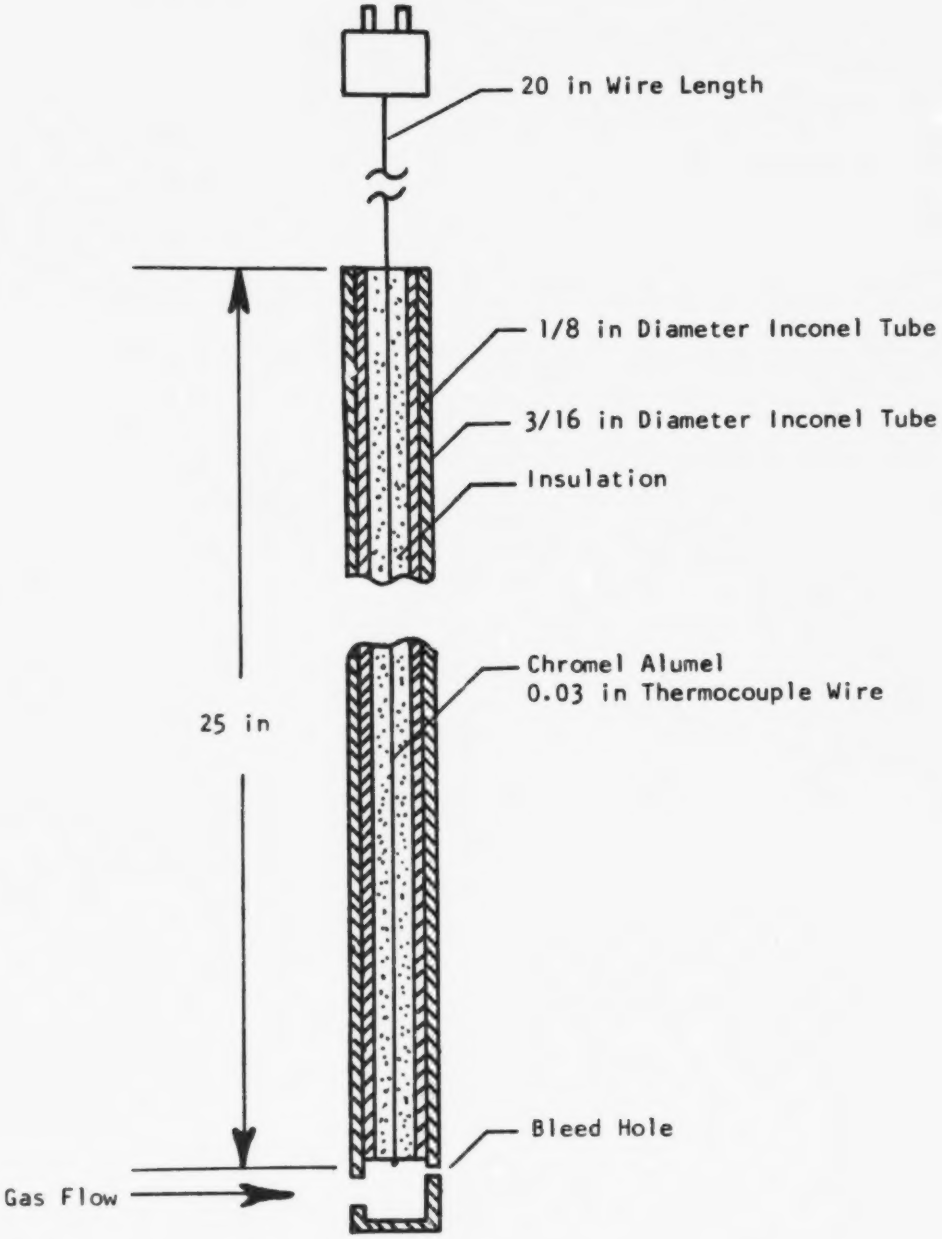
20 in Wire Length
1/8 in Diameter Inconel Tube
3/16 in Diameter Inconel Tube
Insulation
Chromel Alumel
0.03 in Thermocouple Wire
25 in
Bleed Hole
Gas Flow

FIGURE 41 - THERMOCOUPLE PROBE

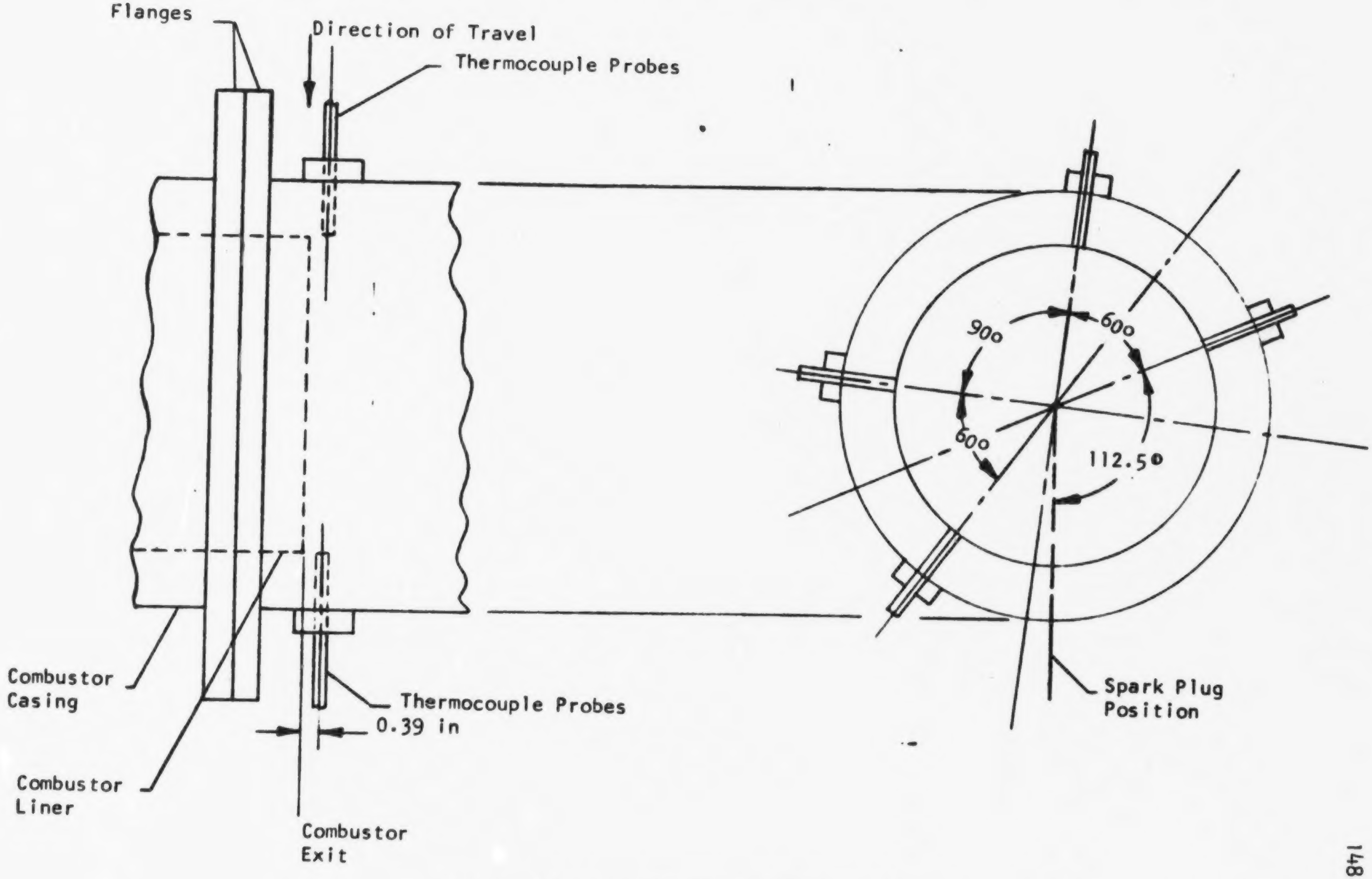
Flanges
Direction of Travel
Thermocouple Probes
90°
60°
60°
112.5°
Combustor Casing
Thermocouple Probes
0.39 in
Spark Plug Position
Combustor Liner
Combustor Exit

FIGURE 42 - SPACING OF THERMOCOUPLE PROBES

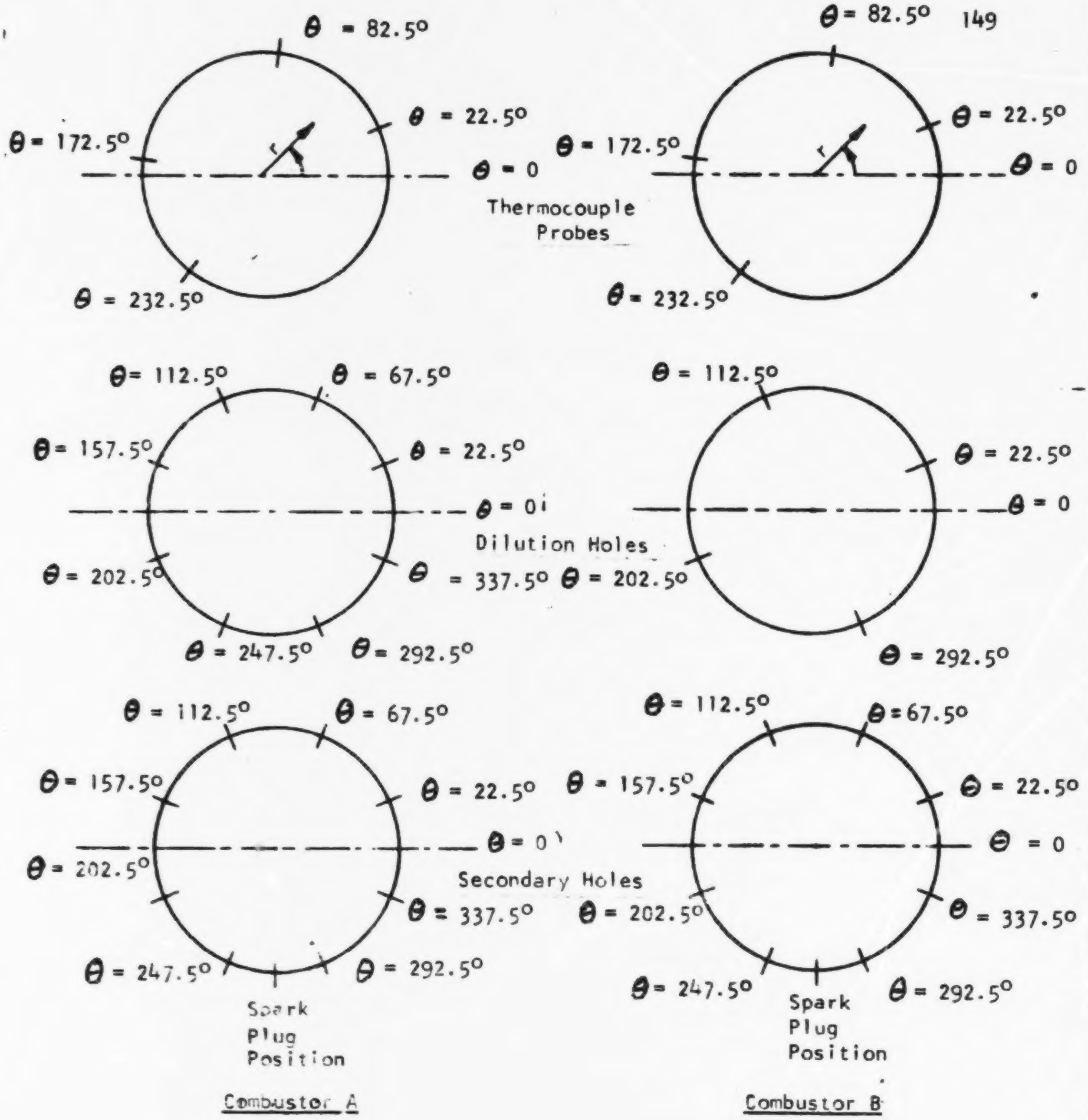
θ = 82.5°
θ = 22.5°
θ = 172.5°
θ = 0
Thermocouple Probes
θ = 232.5°
θ = 82.5°
θ = 22.5°
θ = 172.5°
θ = 0
θ = 232.5°
θ = 112.5°
θ = 67.5°
θ = 157.5°
θ = 22.5°
θ = 0
Dilution Holes
θ = 202.5°
θ = 337.5°
θ = 247.5°
θ = 292.5°
θ = 112.5°
θ = 22.5°
θ = 0
θ = 202.5°
θ = 292.5°
θ = 112.5°
θ = 67.5°
θ = 157.5°
θ = 22.5°
θ = 0
Secondary Holes
θ = 202.5°
θ = 337.5°
θ = 247.5°
θ = 292.5°
Spark Plug Position
θ = 112.5°
θ = 67.5°
θ = 157.5°
θ = 22.5°
θ = 0
θ = 202.5°
θ = 337.5°
θ = 247.5°
θ = 292.5°
Spark Plug Position
Combustor A
Combustor B

FIGURE 43 - RELATIVE CIRCUMFERENTIAL ORIENTATION OF THERMOCOUPLE PROBES

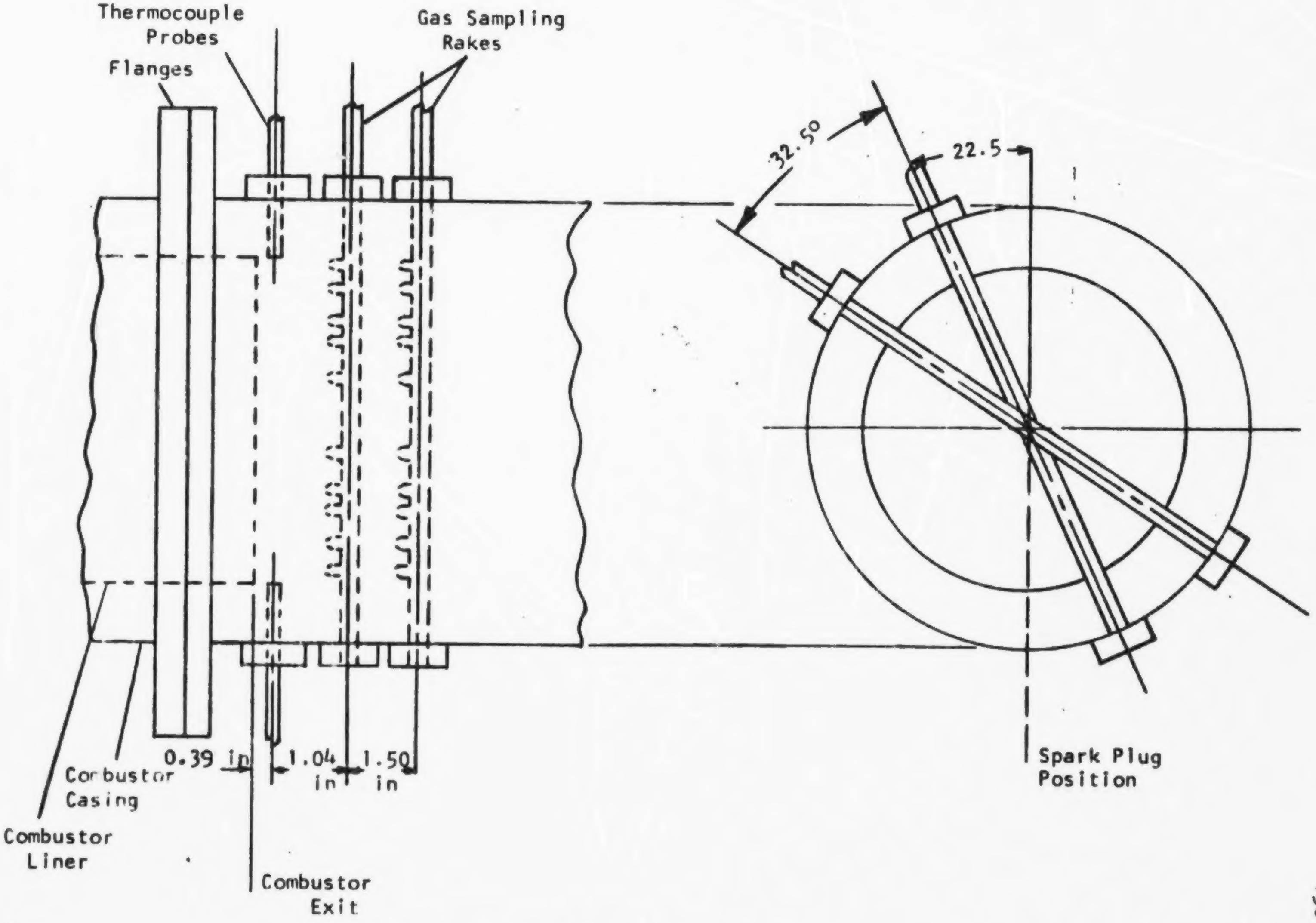
Thermocouple Probes
Flanges
Gas Sampling Rakes
32.50
22.5
0.39 in
1.04 in
1.50 in
Combustor Casing
Combustor Liner
Combustor Exit
Spark Plug Position

FIGURE 44 - SPACING OF GAS SAMPLING RAKES

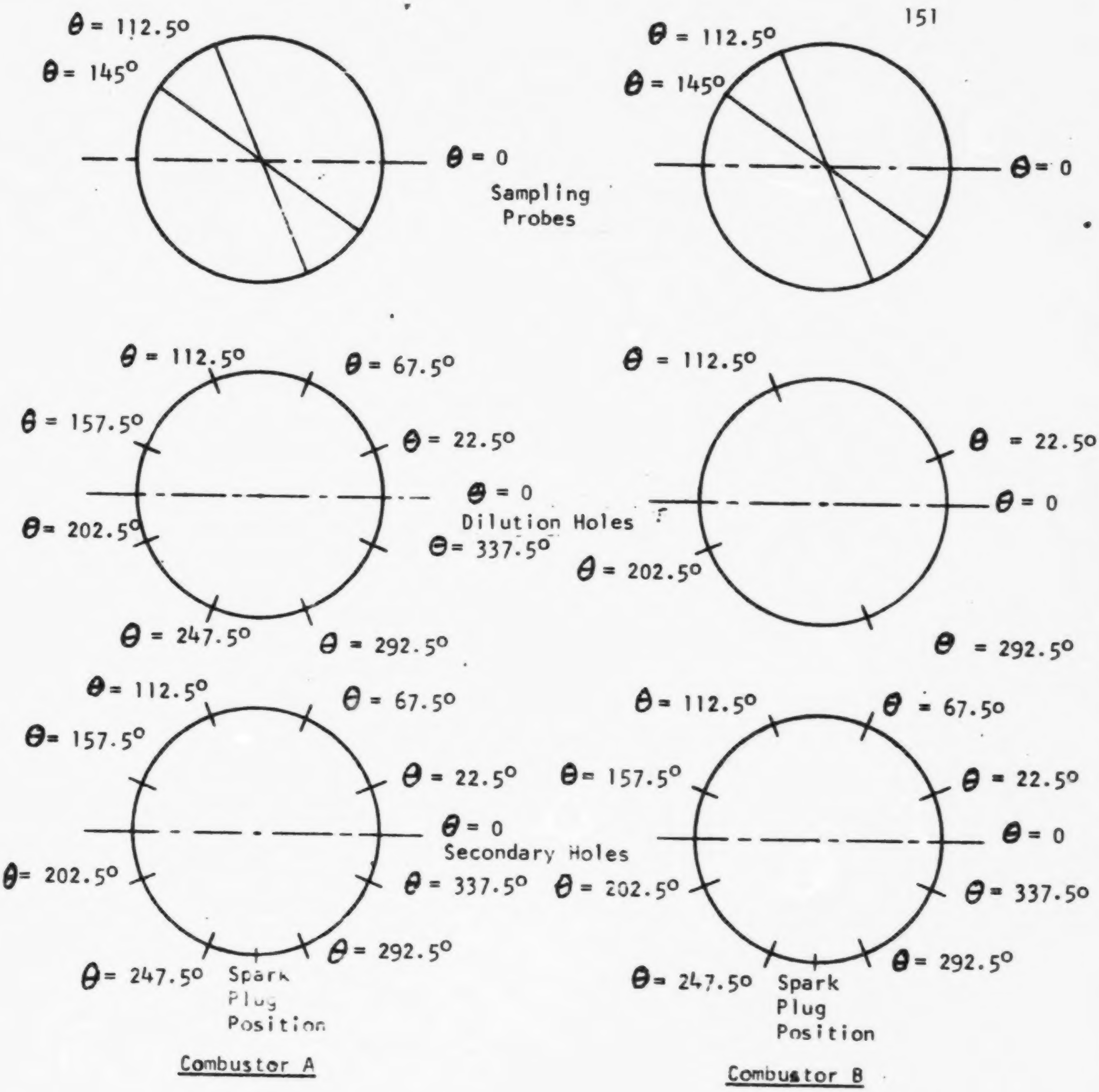
θ = 112.5°
θ = 145°
θ = 0
Sampling Probes
θ = 112.5°
θ = 145°
θ = 0
θ = 112.5°
θ = 67.5°
θ = 157.5°
θ = 22.5°
θ = 0
Dilution Holes
θ = 202.5°
θ = 337.5°
θ = 247.5°
θ = 292.5°
θ = 112.5°
θ = 22.5°
θ = 0
θ = 202.5°
θ = 292.5°
θ = 112.5°
θ = 67.5°
θ = 157.5°
θ = 22.5°
θ = 0
Secondary Holes
θ = 202.5°
θ = 337.5°
θ = 247.5°
θ = 292.5°
Spark Plug Position
θ = 112.5°
θ = 67.5°
θ = 157.5°
θ = 22.5°
θ = 0
θ = 202.5°
θ = 337.5°
θ = 247.5°
θ = 292.5°
Spark Plug Position
Combustor A
Combustor B

FIGURE 45 - RELATIVE CIRCUMFERENTIAL ORIENTATION OF GAS SAMPLING PROBES

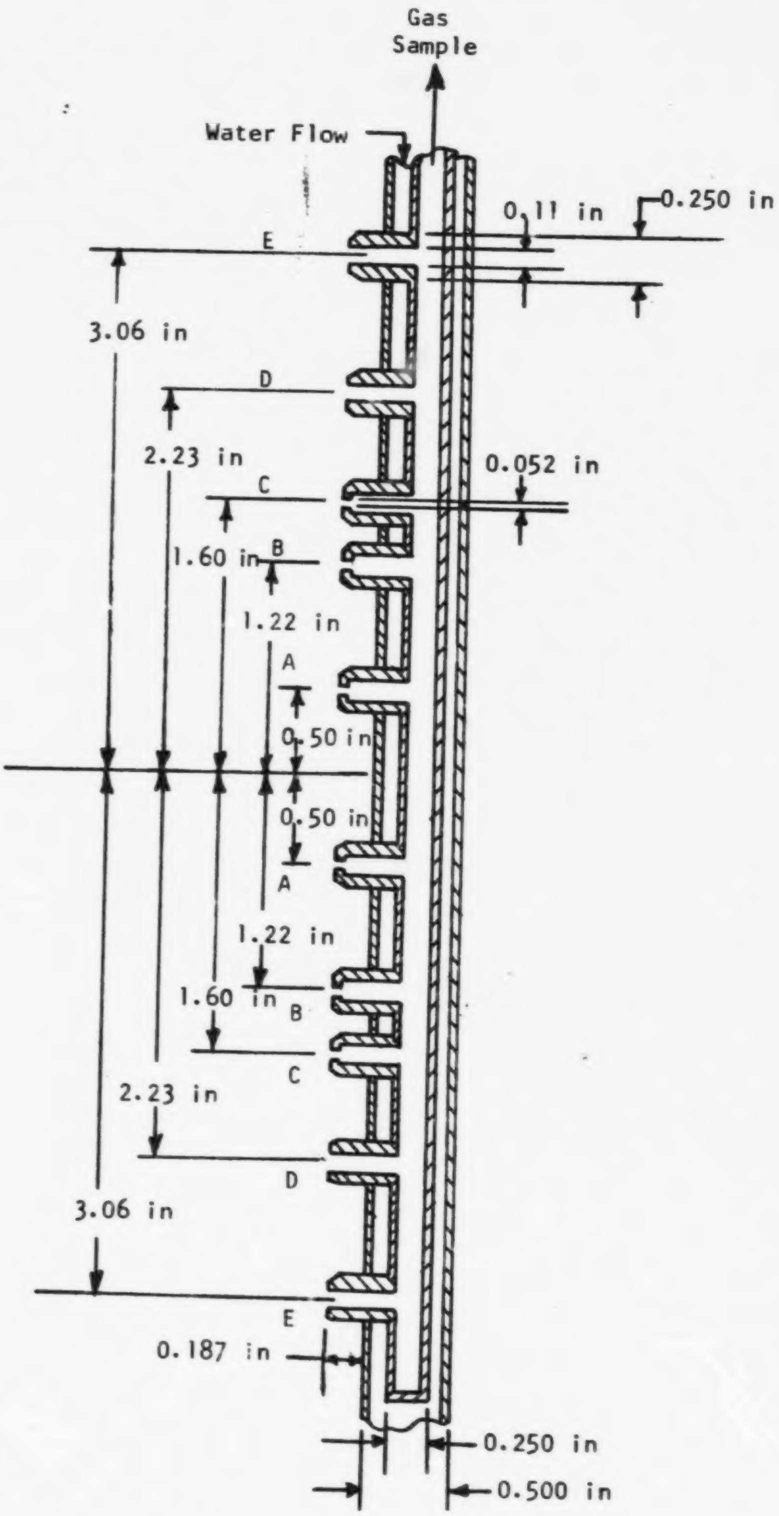
Gas
Sample
Water Flow
0.11 in
0.250 in
E
3.06 in
D
2.23 in
0.052 in
C
1.60 in
B
1.22 in
A
0.50 in
0.50 in
A
1.22 in
1.60 in
B
C
2.23 in
D
3.06 in
E
0.187 in
0.250 in
0.500 in

FIGURE 46 - DESIGN OF GAS SAMPLING RAKES

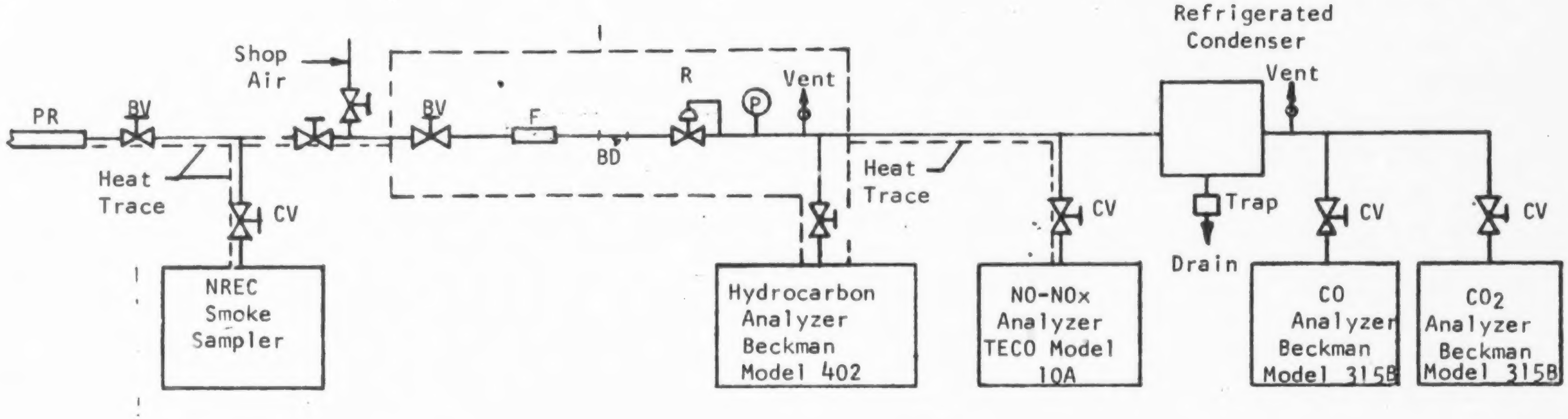
PR
BV
Heat Trace
CV
NREC Smoke Sampler
Shop Air
BV
F
BD
R
P
Vent
Hydrocarbon Analyzer Beckman Model 402
Heat Trace
CV
NO-NOx Analyzer TECO Model 10A
Refrigerated Condenser
Vent
Trap
Drain
CV
CO Analyzer Beckman Model 315B
CV
CO2 Analyzer Beckman Model 315B

PR - Probe
BV - Ball Valve
CV - Control Valve
F - Filter
BD - Blow Down
R - Regulator

FIGURE 47 - SAMPLING TRAIN OF EXISTING NREC ENGINE EXHAUST SAMPLING FACILITY

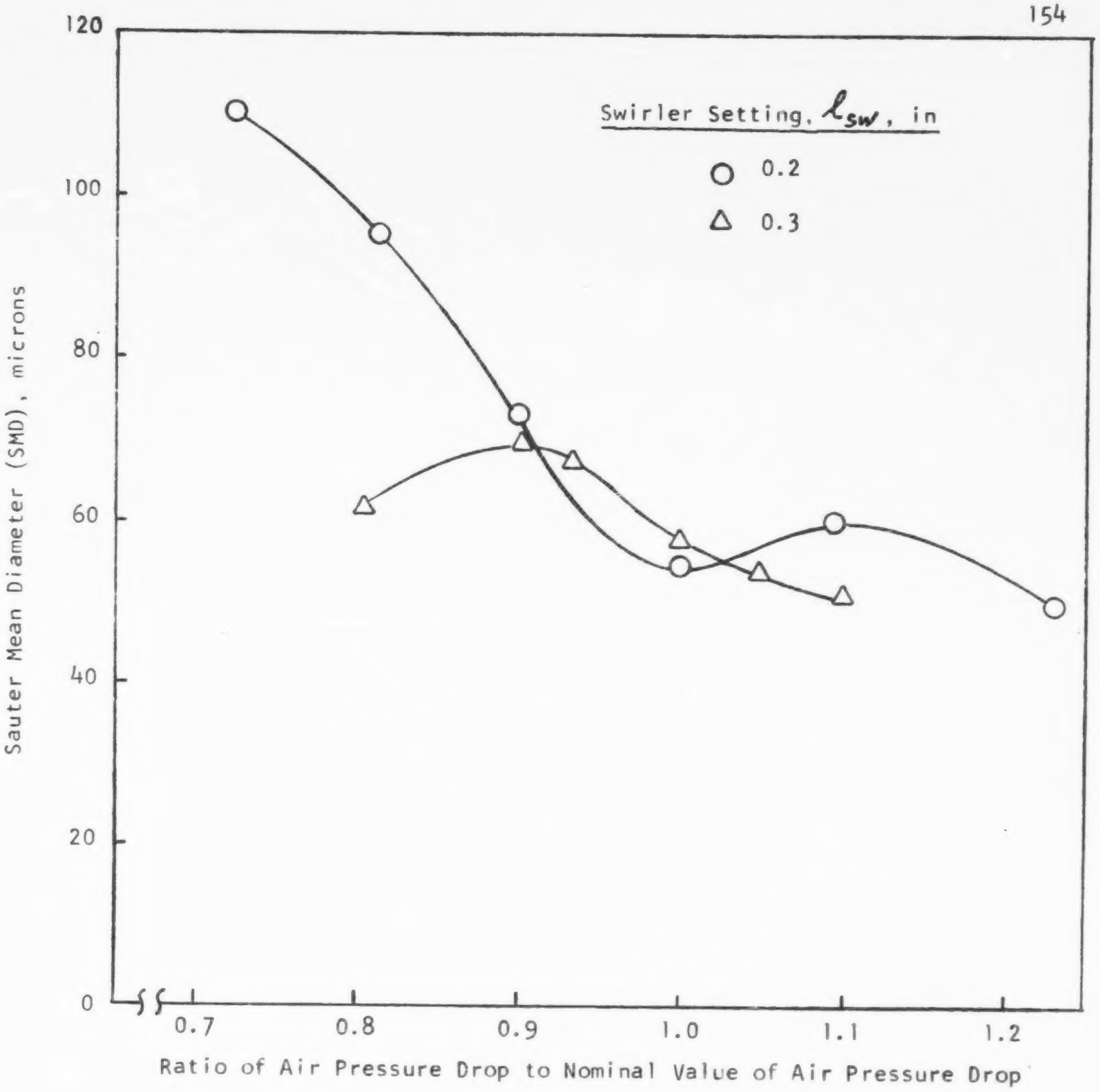

Note: Nominal test conditions correspond to simulation of hot rig conditions given in Table XXV

FIGURE 48 - EXPERIMENTALLY DETERMINED VARIATION OF MEAN DROPLET SIZE WITH AIR PRESSURE DROP FOR AIRBLAST PORTION OF NOZZLE A2.2

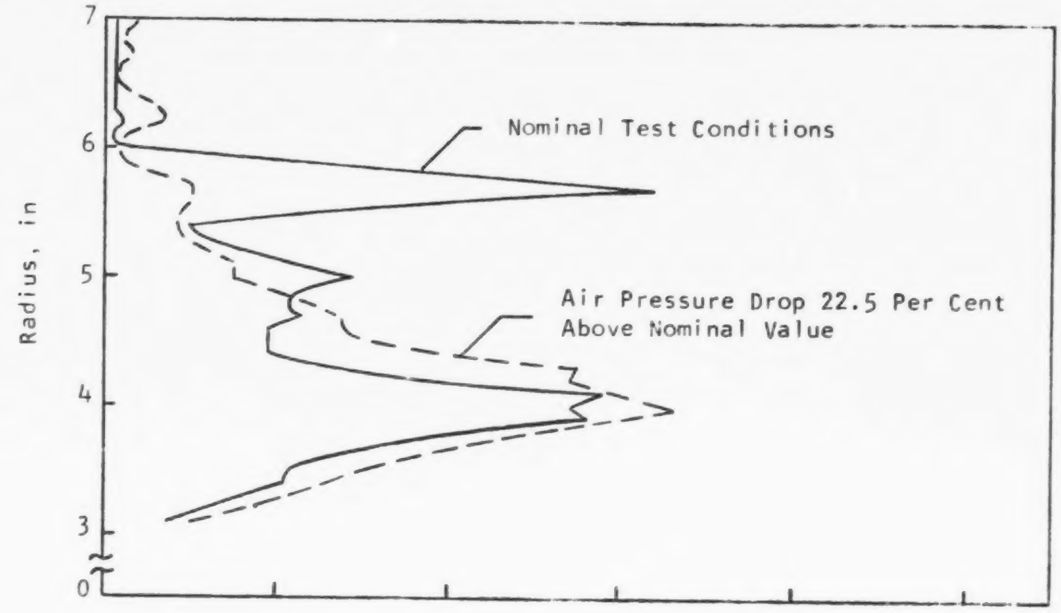

(a) ℓ_{sw} = 0.2 in

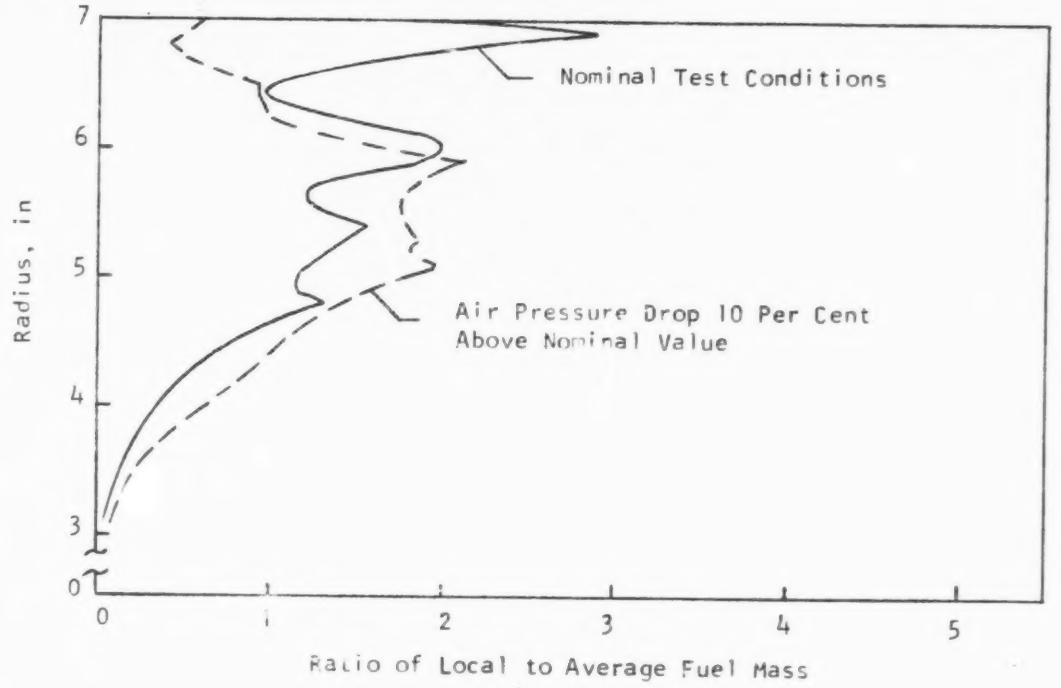

(b) ℓ_{sw} = 0.3 in

Note: Nominal test conditions correspond to simulation of hot rig conditions given in Table XXV

FIGURE 49 - EXPERIMENTALLY DETERMINED RADIAL DISTRIBUTIONS OF SPRAY FOR AIRBLAST PORTION OF NOZZLE A2.2

NOMENCLATURE

Symbols	Description	Units
A_h	Physical flow area of a single set of openings (for example, row of holes or swirler) into the combustor liner	sq ft
$A_{h,eff}$	Effective flow area ($C_d A_h$) of a single set of openings into the combustor liner	sq ft
A_{ref}	Reference flow area (casing flow area)	sq ft
A_T	Sum of effective flow areas of all openings into the combustor liner ($\Sigma A_{h,eff}$)	sq ft
b	Inlet temperature factor (see p. 170)	deg R
C_d	Discharge coefficient	--
C/H	Carbon-to-hydrogen weight ratio of the fuel	--
D_{ref}	Reference diameter (inner diameter of casing)	ft
EI	Emission index (computed as NO_2 for NOx and as C_3H_8 for HC)	mg per gm fuel
f	Mole fraction	--
g	Proportionality constant in Newton's law (32.2)	lbm ft per lbf sec^2
ℓ_{sw}	Swirler flow throttle setting (see Figure 10)	in
ℓ_{sy}	Secondary-hole flow throttle setting (see Figure 10)	in
MW	Molecular weight	lbm per lbm mole
$\dot{m}_a$	Total mass flow rate of air	lbm per sec
$\dot{m}_{bleed}$	Mass flow rate of air through bleed holes	per cent of total air flow
$\dot{m}_{cf,d}$	Mass flow rate of air through dome film cooling slot	per cent of total air flow

Symbols	Description	Units
$\dot{m}_{cf,dil}$	Mass flow rate of air through dilution zone film cooling slot	per cent of total air flow
$m_{cf,i}$	Mass flow rate of air through intermediate zone film cooling slot	per cent of total air flow
$m_{cf,p}$	Mass flow rate of air through primary zone film cooling slot	per cent of total air flow
$\dot{m}_{dil}$	Mass flow rate of air through dilution holes	per cent of total air flow
m_{FN}	Mass flow rate of air through fuel nozzle	per cent of total air flow
$\dot{m}_{fu}$	Total mass flow rate of fuel	lbm per hr
$\dot{m}_{p}$	Total mass flow rate of air through primary zone	per cent of total air flow
$\dot{m}_{p,eff}$	Effective primary-zone flow rate (portion of air flow participating in the combustion process)	per cent of total air flow
$\dot{m}_{sp}$	Mass flow rate of air through spark plug cooling holes and through clearance between spark plug and liner	per cent of total air flow
$\dot{m}_{sw}$	Mass flow rate of air through swirler	per cent of total air flow
$\dot{m}_{sy}$	Mass flow rate of air through secondary holes	per cent of total air flow
$\dot{m}_{sy,i}$	Portion of air through secondary holes flowing downstream	per cent of total air flow
$\dot{m}_{sy,p}$	Portion of air through secondary holes recirculating upstream into primary zone	per cent of total air flow
p	Total pressure	psia
ppm	Volumetric concentration of a chemical specie expressed as parts per million	ppm
q	Dynamic head	psia

Symbols	Description	Units
$q_{annulus}$	Dynamic head based on annulus flow area	psia
$q_{ref.}$	Dynamic head based on reference flow area	psia
R	Gas constant	ft lbf per lbm deg R
S_o	Degree of "mixedness" of fuel/air distribution in primary zone defined as standard deviation of mixture ratio (lbm fuel per lbm total mixture) distribution divided by mean value	--
T	Total temperature	deg F or deg R
TQ	Exit temperature traverse quality defined as difference between maximum and mean values of combustor exit temperature profile divided by temperature rise in combustor (see Appendix II)	--
x	Number of carbon atoms in one molecule of fuel (C_xH_y)	--
y	Number of hydrogen atoms in one molecule of fuel (C_xH_y)	--
Z	Air/fuel ratio (air flow rate divided by fuel flow rate)	--
ΔH_F	Lower heating value of fuel	Btu per lbm
ΔP	Pressure drop across liner	per cent of inlet pressure or psi
ΔP_{Noz}	Air pressure drop across fuel nozzle	per cent of inlet pressure or psi
$\Delta P/q_{ref}$	Pressure-loss factor	--
η_c	Combustion efficiency (see Appendix II)	--
θ	Combustion-efficiency parameter $(\theta \equiv [P_{03}^{1.75} A_{ref} D_{ref}^{0.75} \exp(T_{03}/b)]/\dot{m}_a)$	$lbf^{1.75}$ sec per lbm $ft^{0.75}$

Symbols	Description	Units
ρ	Gas density	lbm per cu ft
$\bar{\tau}_p$	Approximate primary-zone residence time calculated on basis of inlet temperature and pressure	msec
ϕ_p	Primary-zone equivalence ratio (stoichiometric air/fuel ratio divided by actual air/fuel ratio)	--

Subscript	
a	Air
CO	Carbon monoxide
CO_2	Carbon dioxide
F	Fuel
HC	Total hydrocarbons expressed as C_3H_8
NO	Nitric oxide
NOx	Total nitrogen oxides expressed as NO_2
st	Stoichiometric value
03	Combustor inlet
04	Combustor exit

APPENDICES

APPENDIX I

DESCRIPTION OF EXPERIMENTAL FACILITIES

The testing phase of the program was conducted using basically three different test rigs: a water rig for the combustor flow visualization tests, a cold-air rig for the air distribution and spray visualization tests, and a hot-test rig for the detailed combustion tests. The experimental apparatus and instrumentation used in each of these rigs are described in this appendix.

Water Rig

The flow schematic of the water rig is shown in Figure 35. The closed-loop system is connected to the main laboratory water supply and was drained and refilled at the start of each day of testing. The materials used in the water rig were selected to insure acceptable water clarity. All tanks in the system were constructed of aluminum and the water was directed through flexible rubber hoses and stainless steel piping.

The settling tank was designed to damp any turbulence generated by the pump and to straighten the flow through a set of twenty-mesh screens. The bleed valve in the settling tank was used to relieve air trapped in the tank during the filling and start-up of the system. In each test, hydrogen bubbles were used as the flow tracers. These were generated electrically by a straight-line grid of stainless steel wires located just upstream of the inlet to the combustor model. The flow patterns in the combustor were observed by illuminating a longitudinal diametrical plane in the transparent combustor model by a high-intensity slit light source. An adjustable Plexiglas duct between the combustor exit flange and the collection tank was used to compensate for the difference in length between the two combustor models tested. The water exiting from the combustor entered the open collecting tank which served to vent the hydrogen to the atmosphere.

The major measurement taken during the flow visualization tests was that of the water flow rate. This flow rate was measured by a square-edge orifice plate designed to ASME specifications. (Ref 21). The orifice size was 1.40 inches in diameter in a 4-inch pipe. The temperature upstream of the orifice was measured with a thermometer and the pressure drop across the orifice with a mercury manometer.

Cold-Air Rig

The cold-air test rig was used for both the air flow distribution tests and the spray visualization tests. The general flow schematic of the test rig in shown in Figure 36. Air was supplied by a large pressurized tank that was continuously replenished by an air compressor during operation of the rig. The test section used for the air flow distribution tests consisted of the actual metal combustors. For the spray tests the test section consisted of the specially constructed nozzle mounting section shown schematically in Figure 37. Water was used in place of the fuel, and the spray pattern was observed and photographed by illuminating with a high-intensity light source.

The air flow rate was measured using a standard ASME square edge orifice section. Orifices ranging from 0.5 inch diameter to 1.45 inch diameter in a 2-inch pipe were used for flow rates from 0.005 to 0.3 lbm/sec air. The air temperature was measured with a thermometer and the pressure drop across the orifice with a 30-inch manometer carrying 1.75 specific gravity fluid. The same type of manometer was also used to measure the static (total) pressure in the transition (or settling chamber).

Combustion Test Rig

Air Supply

A schematic of the air flow system is given in Figure 38. Air was supplied by either of two gas-turbine driven compressors. The high-pressure unit was capable of delivering up to 6.5 lbm per sec of air at 6 atm and the low-pressure unit up to 3 lbm per sec at 2.5 atm. The air from either source was heated by passing through a FECOR gas-fired indirect heater capable of heating up to 3 lbm per sec of air to 1200 degrees F. The temperature of the air leaving the heater was automatically controlled at the set point which could be adjusted to give air temperature in the range 500-1200 degrees F. The piping system consisted of 4-inch diameter pipe. Carbon steel pipe was used up to the heater inlet and well-insulated stainless steel pipe from the exit of the heater to the inlet of the combustor test section.

Fuel Supply

The fuel used in all of the combustion tests was JP-4 jet fuel (MIL-J-5624F) stored in an underground 200 gallon capacity tank. The schematic of the fuel supply system is shown in Figure 39. The fuel pump was continuously in operation during testing and was capable of delivering up to 60 gph at 600 psi. The fuel delivery pressure was adjusted manually by opening or closing the valve in the bypass line. The fuel flow to the main and pilot nozzles was controlled by needle valves contained in the flow meters.

Test Section

Figure 40 shows the major components and dimensions of the test section. The spacer spool was used to compensate for the difference in length between the two combustors tested. The transition section was designed to allow for diffusion of the incoming air entering the combustor section. It was also designed to give a plenum chamber effect for measurement of inlet total pressure. The nozzle mounting section was designed to support the fuel nozzle and provide access to the inlet end of the combustors. The instrumentation used to measure the combustor exit pressure and temperature distribution and the probes used to obtain the exhaust gas sample were mounted in the instrument section. The conical reducer section provided the transition in diameter between the instrument section and the pneumatically controlled back-pressure valve. The instrument section and the reducer section were both water-cooled.

Instrumentation

The general methods used to conduct the measurements for the combustion tests are listed in Table XXII. Specific details of the instrumentation are discussed below.

Flow Rates

The mass flow of air was measured indirectly by a 3-inch diameter square-edge orifice designed to ASME specifications. The fuel flow to the main nozzle was measured by a Brooks Instrument Company floating-ball type flow meter calibrated for JP-4 fuel and having the range 0-24 gph with 2 gph divisions. The fuel flow through the pilot was measured indirectly by the delivery pressure and directly by a similar flow meter calibrated for water and having the range of 0-9 gph of water with 1 gph divisions.

Pressures

The following pressure measurements were taken during each of the combustion tests:

1. Pressure drop across the orifice plates.
2. Pressure drop across the combustor.
3. Static (total) pressure at the combustor inlet.
4. Static pressure at the combustor exit.
5. Total pressure at the combustor exit.

Items 1 and 2 in the above list were measured with a 100-inch manometer containing 1.75 specific gravity fluid. Static and total pressures were measured with 0-100 psig range Heise gauges having 0.1 psig divisions. Inlet pressure and exit static pressure were measured by static pressure taps at the downstream end of the transition section and at the combustor exit plane in the instrument section, respectively. The combustor exit total pressure was measured using the gas sampling rakes in a no-flow mode.

All stream temperatures were measured with chromel-alumel thermocouples. Temperature measurements were taken at the following stations.

1. Upstream of the orifice plates leading to the heater inlet, the heater by-pass line, and the combustor test section.
2. Fuel temperature at the inlet to the fuel nozzle.

3. Gas sampling stream at the inlet to the gas-analysis console.
4. Combustor exit plane.

The millivolt outputs from the thermocouples were read using a digital voltmeter (DORIC Model No. DS100). The thermocouples were calibrated at two points-- 32 degrees F (ice bath) and 212 degrees F (boiling water).

The exit temperature distribution was measured by four thermocouple probes of the type shown in Figure 41. These probes were placed in remotely actuated traversing mechanisms mounted on the outside of the instrument section at the combustor exit plane. The probes were spaced in the circumferential direction such that two opposite quadrants of the combustor exit area could be traversed as shown in Figure 42 and 43. Each probe was traversed in the radial direction and readings were taken at the radial positions given in Table XXIII. These positions were selected by dividing the combustor exit into equal areas and choosing approximately the radial midpoint of the equal area rings.

Liner temperatures were measured using a number of different thermal paints each of which undergoes a phase change at a specific value of temperature. The paints were selected to provide temperature indications in the range 1400-1900 degrees F in approximately 50 degrees F intervals. The paints were applied to the outside surface of the liner in longitudinal stripes.

Exhaust Gas Composition

A list of the chemical species measured and the instruments used is given in Table XXIV. The gas sample for analysis was obtained using two water-cooled sampling rakes extending across the diameter of the instrument section as shown in Figures 44 and 45. The design of each of the two rakes is shown in Figure 46. The radial spacings of the tubes and the orifice sizes were chosen to provide equal increments in flow through each tube. The two outer tubes on both ends of each rake (D and E in Fig 46) were blocked off with a tight fitting cap when Combustor B was being tested. A sample could be obtained from either of the two rakes independently or both together. Initial tests showed that the latter approach provided a representative sample; therefore, this was the approach utilized.

A schematic of the sample handling system is given in Figure 47. The 10-foot stainless steel line from the water-cooled rakes to the temperature controlled heated box was heated with electrical tapes to an average temperature of 370 degrees F. The heated box which contained the filter and regulatory station was maintained at a temperature of 400 degrees F. The lines from the heated box to the hydrocarbon analyzer and the NO-NOx analyzer were also heated. The line to the CO and CO2 analyzers passed through a refrigerated condenser to eliminate water vapor from the sample. The sample collected at the combustor exit was divided among the various analyzers shown in Figure 47 to provide continuous and simultaneous analysis of the various pollutant species. When smoke measurements were conducted, the line to the analyzers was closed and the sample was passed through the smoke meter.

APPENDIX II

DATA REDUCTION

The equations used in computing the major performance parameters from the test data are presented in this appendix.

Fuel Properties

All of the tests were conducted using JP-4 jet fuel (MIL-J-5624F). The pertinent properties of this fuel were obtained from data given in References 8, 9, and 23. The values of these properties used in the reduction of the test data are as follows:

$\Delta H_F = 18{,}752$ Btu per lbm

$C/H = 6$

$MW_F = 112$

$Z_{st} = 14.8$

Representing the fuel by the general molecular formula CxHy and using the values of carbon-to-hydrogen weight ratio (C/H) and molecular weight (MW_F) listed above gives:

$x = 8$

$y = 16$

Air Flow Distribution

The values of air flow rate through the individual sets of openings in the combustor were computed using the data obtained in the cold-air tests. These data consisted of the variations of mass flow and pressure drop for each set of openings and the pressure and temperature of the flow. The measured values were used to compute the effective area of each set of openings by the relation,

$$\dot{m}_h = C_d A_h \left[2 g \rho \Delta P \right]^{0.5} \equiv A_{h,eff.} \left[2 g \rho \Delta P \right]^{0.5}$$

where the density, ρ , is calculated from the pressure and temperature as;

$$\rho = \frac{P}{RT}$$

The fraction of the total air flow rate through each set of openings was computed as,

$$\frac{\dot{m}_h}{m_T} = \frac{A_{h,eff}}{A_T}$$

where $\dot{m}_T$ is the total air flow rate and A_T is the sum of the values of $A_{h,eff}$ for all of the openings. The effective primary-zone flow rate was then calculated as:

$$\dot{m}_{P,eff} = \dot{m}_{FN} + \dot{m}_{SN} + 0.4\,\dot{m}_{SY}$$

Over-All Air/Fuel Ratio

The equation used to calculate the over-all air/fuel ratio (Z) was obtained by performing an atom balance assuming the reactions of the fuel were:

$$C_xH_y + \left(x + \frac{y}{4}\right) O_2 \longrightarrow x\,CO_2 + \frac{1}{2}y\,H_2O$$

$$C_xH_y + \left(\frac{x}{2} + \frac{y}{4}\right) O_2 \longrightarrow x\,CO + \frac{1}{2}y\,H_2O$$

$$C_xH_y + \frac{1}{4}\left(y - \frac{8x}{3}\right) O_2 \longrightarrow \frac{x}{3}\left(C_3H_8\right) + \frac{1}{2}\left(y - \frac{8x}{3}\right) H_2O$$

The unburned fuel (HC) is represented as C_3H_8 in the last of the reactions listed above because this is the form on which the reading from the hydrocarbon analyzer is based. The resulting equation for Z is:

$$Z = x\left(\frac{MW_a}{MW_F}\right)\frac{1 + \alpha f_{CO_2} - \left(\frac{1}{2} - \alpha\right) f_{CO} - 3(1-\alpha) f_{HC}}{f_{CO_2} + f_{CO} + 3 f_{HC}}$$

where $\alpha \equiv y/4x$ and f stands for the mole fraction of each species as determined from the emission analysis readings,

$$f_{CO_2} = ppm_{CO_2} \times 10^{-6}$$

$$f_{CO} = ppm_{CO} \times 10^{-6}$$

$$f_{HC} = ppm_{HC} \times 10^{-6}$$

Primary-Zone Equivalence Ratio

The expression used to calculate ϕ_p is

$$\phi_p = \left(\frac{100}{\dot{m}_{p,eff}}\right) \frac{Z_{st}}{Z}$$

where $\dot{m}_{p,eff}$ is the effective primary-zone air flow rate expressed as percentage of total air flow rate.

Emission Index

The values of the emission index in mg per gm fuel for each of the pollutant species were computed from the following general relation:

$$EI_i = f_i \left(\frac{MW_i}{MW_a}\right) (Z+1) \times 10^3$$

where the subscript "i" stands for each of the species, NO, NOx (expressed as NO_2), CO, and HC (expressed as C_3H_8).

Combustion Efficiency

The combustion efficiency was computed from the measured emissions of hydrocarbons and carbon monoxide with the relation

$$\eta_c = 1 - \frac{3}{x}\left(\frac{MW_F}{MW_{HC}}\right)\left(EI_{HC} \times 10^{-3}\right) - \left(\frac{\Delta H_{CO}}{\Delta H_F}\right)\left(EI_{CO} \times 10^{-3}\right)$$

where ΔH_{CO} is the heat of combustion of carbon monoxide, 4,348 Btu per lbm CO (Ref 24).

Exit Temperature Traverse Quality

The traverse quality was calculated from the measured exhaust gas temperature distribution as

$$TQ = \frac{T_{c4,max} - \bar{\bar{T}}_{c4}}{\bar{\bar{T}}_{c4} - T_{03}}$$

where

$T_{04,max}$ = maximum measured value of exhaust gas temperature

$\bar{\bar{T}}_{04}$ = average exhaust gas temperature

T_{03} = inlet gas temperature

Combustion Efficiency Parameter

The combustion efficiency parameter used in correlating the blow-out data was calculated as

$$\theta = \frac{P_{03}^{1.75} A_{ref} D_{ref}^{0.75} \exp\left(T_{03}/b\right)}{\dot{m}_a}$$

where b, the inlet temperature factor (Refs 8 and 9) was approximated by the linear equation

$$b = 596\ \phi_p \text{ deg R}$$

and evaluated at the design value of ϕ_p for each combustor.

APPENDIX III

NOZZLE SPRAY ANALYSIS TESTS

At the conclusion of the combustion testing portion of the program, a series of tests was conducted to determine the spray performance of the airblast portion of the nozzle designated as A2.2 (see Table V). The results obtained for this specific nozzle should be fairly typical, since all of the nozzles examined in this program are essentially of the same general design. The spray analysis tests were performed by the Accessories Division of Parker Hannifin Corporation using a high-speed spray analyzer (Ref 25) which has the capability of providing detailed information on droplet size and distribution. The tests and results obtained are described in detail in Reference 26 and are summarized in this appendix.

Description of Tests

The nozzle was tested at two swirler settings ("closed" and "part open") under cold-flow conditions (essentially ambient air temperature and pressure) selected so as to model hot-rig operation at the two sets of conditions given in Table XXV. These swirler settings and hot-rig flow conditions correspond approximately to idle and 50 per cent power operation. In addition to these tests, the effect of air pressure drop on spray performance was examined by varying the air flow rate about the nominal value for each of the two swirler settings.

Results

At the nominal flow conditions corresponding to simulation of the hot-rig conditions, the distributions of droplet size and mean values are as given in Table XXVI for each of the two swirler settings. The variations of SMD with air pressure drop are shown in Figure 48. The general trends of the data indicate that atomization improves (that is, the mean droplet size decreases) as the air pressure drop is increased.

The radial distribution of the fuel spray was measured at an axial distance 4 in downstream of the nozzle. The distributions obtained at the nominal test conditions for the two swirler settings are shown in Figure 49. As can be seen, both distributions are relatively nonuniform exhibiting a number of sharp peaks. The effect of increasing the air pressure drop on the spray distribution is also shown in Figure 49. In general, the uniformity of the spray improves as the air pressure drop is increased.

Visual examination of the atomizer assembly both during and after testing led to the following observations:

1. The nozzle contains eight fuel ports and eight swirler vanes.
2. Eight corrosion patches were present on the I. D. of the nozzle indicating that combustion had occurred previously within the confines of the prefilming cylinder of the nozzle.
3. At high values of air pressure drop, eight separate and distinct fuel streaks were observed.
4. At low values of air pressure drop, the eight streaks coalesced into three oscillating streaks. As the air pressure drop was reduced to even lower values, the oscillation became more severe and fuel could be observed in puddles on the O. D. of the prefilming cylinder.

Conclusions

The nozzle as tested under modeled hot-rig conditions exhibited poor atomization quality which can be reasonably attributed to fuel streaking. Although the specific causes of the fuel streaking cannot be determined precisely, it is likely that the observed corrosion patches and possible inefficiency of the radial inflow swirler are contributing factors.